

November 2015

Inkjet Printing for Biosensing and Security Applications

Brian Creran
University of Massachusetts - Amherst

Follow this and additional works at: https://scholarworks.umass.edu/dissertations_2

 Part of the [Analytical Chemistry Commons](#), [Materials Chemistry Commons](#), and the [Organic Chemistry Commons](#)

Recommended Citation

Creran, Brian, "Inkjet Printing for Biosensing and Security Applications" (2015). *Doctoral Dissertations*. 517.
<https://doi.org/10.7275/7531257.0> https://scholarworks.umass.edu/dissertations_2/517

This Open Access Dissertation is brought to you for free and open access by the Dissertations and Theses at ScholarWorks@UMass Amherst. It has been accepted for inclusion in Doctoral Dissertations by an authorized administrator of ScholarWorks@UMass Amherst. For more information, please contact scholarworks@library.umass.edu.

Inkjet Printing for Biosensing and Security Applications

A Dissertation Presented

by

Brian Creran

Submitted to the Graduate School of the
University of Massachusetts Amherst in partial fulfillment

of the requirements for the degree of

DOCTOR OF PHILOSOPHY

September 2015

Department of Chemistry

© Copyright by Brian Creran 2015

All Rights Reserved

Inkjet Printing for Biosensing and Security Applications

A Dissertation Presented

by

BRIAN CRERAN

Approved as to style and content by:

Vincent M. Rotello, Chair

Matthew A. Holden, Member

Dhandapani Venkataraman, Member

Kenneth R. Carter, Member

Craig T. Martin, Department Head

Department of Chemistry

DEDICATION

To Jackie and Dad

ACKNOWLEDGMENTS

First, I would like to thank my committee members, Profs. Holden, Vekataraman, and Carter, for all of your input throughout my doctoral studies. Many of the experiments you suggested during our meetings were done and included in this work, significantly improving its overall quality and impact on the scientific community. More importantly, I want to thank each of you for the visits we had outside of the scheduled meetings to better myself professionally. My sincerest thanks.

This work could not have been done without the help of the entire Rotello Group, both past and present. It has been a privilege and honor to work with each and every one of you, whether it was for just a quick experiment or for many years of research. One of the true strengths of the Rotello Group that leads to such success in our research is the people working in it. Of particular note, my many thanks go out to Myoung Hwan Park, Xiaoning Li, Bradley Duncan, Bo Yan, Ryan Landis, Vikas Nandwana, Li-Sheng Wang, Oscar R. Miranda and Chandra Subramani as you all went above and beyond to ensure our research was a success. I would also like to take a moment to thank all of my collaborators around the world including Shazia Mumtaz and Timon Schwaebel for their gracious help with our projects.

In most acknowledgements, we tend to forget those who really keep our research going smoothly and without much fanfare. Thank you Carrie, Anne, Kris, Vicki, MaryAnne, Chris, Kay, jms, Marv, Ryan, and Bob for all of your hard work over my time here. Of special note, I would like to thank Carol Greene, our group accountant, for everything you do to keep the entire group going. Your contributions are not lost on us graduate students!

Last, but by far not least here at UMass, I would like to thank my advisor Vincent M. Rotello for the last 6 and half years. Thank you for the sage-like wisdom and constant encouragement to make my work exceptional. It was an honor to work for you.

One does not consist totally at graduate school. Thank you Kirk, P.J., Shawn, and Frank for ensuring that I saw the outside world occasionally.

Personally, I would like to thank both my wife and father for everything they have done for me so that I could make it to writing a thesis. Jackie, thank you for being there when times were tough and sticking with me. I know living with a PhD student is not the easiest. You are an amazing wife. I am lucky to have you in my life. Finally, Dad, thank you for everything. I know it is very easy to say but you have done so much for me that it would take a document this long to list each and everything. Thanks for telling me to keep going to school (even though I wanted to stop!) and really believing in me. I hope I made you proud.

ABSTRACT

INKJET PRINTING FOR BIOSENSING AND SECURITY APPLICATIONS

SEPTEMBER 2015

BRIAN CRERAN, A.B. COLLEGE OF THE HOLY CROSS

Ph.D., UNIVERSITY OF MASSACHUSETTS AMHERST

Directed by: Professor Vincent M. Rotello

The adaptation of inkjet printing technology has recently been used to create controlled high throughput micro- and nano-scaled structures. Coupling this technique with gold nanoparticles in our research has produced new platforms for biosensors, chemical patterning, and anti-counterfeiting applications. In this presentation, we will highlight promising fabrication strategies including the development of test strips for the determination of bacteria in drinking water as well as the use of patterned nanoparticles for security applications.

TABLE OF CONTENTS

	Page
ACKNOWLEDGMENTS.....	v
LIST OF TABLES.....	xi
LIST OF FIGURES.....	xii
CHAPTER	
1. INTEGRATION OF INKJET PRINTING FOR BIOLOGICAL AND MATERIALS ASSEMBLY	1
Introduction	1
Technology Overview	1
Droplet formation.....	2
Ink Properties Effect Droplet Creation.....	4
Applications of Inkjet Printing for Biosensing.....	5
Nanoparticles Influence on Sensing.....	7
Applications of Inkjet Printing for Materials Applications	10
Dissertation Overview.....	11
2. LASER DESORPTION IONIZATION MASS SPECTROMETRIC IMAGING OF MASS BARCODED GOLD NANOPARTICLES FOR SECURITY APPLICATIONS.....	14
Introduction	14
Results and Discussion.....	16
Materials and Methods.....	20
Conclusions	22
3. DETECTION OF BACTERIA USING INKJET-PRINTED ENZYMATIC TEST STRIPS.....	24
Introduction	24

Results and Discussion	27
Materials and Methods.....	45
Test Strip Procedure	46
Sensor Construction and Storage	46
Profile Image Analysis	47
CPRG Leaching Analysis	47
Bacteria Culturing	48
Conclusions	48
4. COLORIMETRIC PROTEIN SENSING USING CATALYTICALLY AMPLIFIED SENSOR ARRAYS.....	52
Introduction	52
Results and Discussion	54
Materials and Methods.....	60
Conclusions	64
5. DETECTION OF BACTERIA IN DRINKING WATER BY STABLE INKJET PRINTED TEST STRIPS USING ARTIFICIAL ENZYMES	67
Introduction	67
Results and Discussion	69
Materials and Methods.....	76
High Temperature Iron Oxide Nanoparticle Creation	76
Low Temperature Fe_3O_4 , MnFe_2O_4 , and CoFe_2O_4 , Nanoparticles Synthesis.....	76
Bacteria Creation	77
Solution Testing	77
Inkjet Printing.....	78
Inkjet Printing of the Chlorine Sensor.....	78
Conclusions	78

APPENDIX: SCIENTIFIC OPERATION OF AN ARTISAN 50 PRINTER FOR A LABORATORY ENVIRONMENT	81
BIBLIOGRAPHY	122

LIST OF TABLES

Table	Page
Table 1 - Absorbance values of the analyte solution after incubating with the sensor	32
Table 2 - Cyan average percentages along with the standard deviation of 6 chosen spots taken from the scanned image of each test strip versus concentration of bacteria.....	39
Table 3 - Magenta average percentages along with the standard deviation of 6 chosen spots taken from the scanned image of each test strip versus concentration of bacteria.....	40
Table 4 - Yellow average percentages along with the standard deviation of 6 chosen spots taken from the scanned image of each test strip versus concentration of bacteria.....	41
Table 5 - Cyan average percentages along with the standard deviation of 6 chosen spots taken from the scanned image of each test strip versus salt concentration.	43
Table 6 - Magenta average percentages along with the standard deviation of 6 chosen spots taken from the scanned image of each test strip versus salt concentration.	44
Table 7 - Yellow average percentages along with the standard deviation of 6 chosen spots taken from the scanned image of each test strip versus salt concentration.	44
Table 8 - Concentrations at which the test strips respond to several common water contaminants as well as the current water regulations for that. Note that the maximum sodium dodecyl sulfate level is for all foaming agents in water and is not specific for this chemical.	45
Table 9 - Physical properties of protein analytes.	56
Table 10 - Identification of 80 unknown protein samples with LDA using Fe ₃ O ₄ NP sensor array.	60

LIST OF FIGURES

Figure	Page
Figure 1 - (a) Schematic diagram of a piezoelectric inkjet print head. (b) Schematic representation of wave propagation and reflection in a piezoelectric tubular actuator. Reproduced from Reference 1.....	3
Figure 2 - Inkjet printing of glucose biosensor prototype. Reproduced from Reference 7.....	6
Figure 3 - A schematic representation of a sensor element in the sensor comprised of β -galactosidase (β -Gal) and cationic AuNPs and differentiation of proteins in 3-D. a) As shown, β -gal is displaced from the β -Gal/AuNP complex by protein analytes, restoring the catalytic activity of β -Gal towards the fluorogenic substrate 4-methylumbelliferyl- β -D-galactopyranoside, resulting in an amplified signal for detection. b) Differential protein pattern of the nine proteins at 1 nM. c) Canonical score plot of the first three factors of fluorescence response patterns obtained through β -Gal/AuNP sensor array against nine target proteins in 1 nM concentration. Reproduced from Reference 14.....	9
Figure 4 - Anti-counterfeiting mass barcoding strategy	16
Figure 5 - Mass spectra of the four nanoparticles used in this study, with the m/z value used for scanning highlighted	17
Figure 6 - a) The Au^+ signal determined by scanning the ITO coated glass surface b) the Au_2^+ signal and c) the NP 1 ligand signal (detected ions: Au^+ $m/z = 197$, Au_2^+ $m/z = 394$, NP 1 ligand $m/z = 422$)	18
Figure 7 - Ligand LDI-IMS signals for the various ligands tinted different colors for viewing. a.) NP 1 b.) NP 3 c.) NP 2 and d.) NP 4 e.) all 4 signals combined showing the completed pattern	19
Figure 8 - Overlapped two channel printing. MSI of overlapped printing gold NPs, detected ions: blue letters AMHERST (NP 4 $m/z = 548$), green letters UMASS (NP 1 $m/z = 422$), red pattern (Au^+ , $m/z = 197$)	20
Figure 9 – Screen capture of the pattern to be printed on the substrate.....	21
Figure 10 - Chemical basis and inkjet printing scheme for the test strips used in these studies.....	27

Figure 11 - a) Before and b) after printing β -gal onto a piece of paper that was preprinted with CPRG by using inkjet printing.....	28
Figure 12 - Representative patterned strips before immersion.	29
Figure 13 - Colorimetric response of the patterned test strip after immersion in water	30
Figure 14 - Change in color response of the 12 sensor patterns after immersion.	30
Figure 15 - Variance in the color change of the 12 sensor designs.	31
Figure 16 - Checkboard pattern used in Microsoft PowerPoint to generate the test strip functionality.....	31
Figure 17 - Motility experiments of both substrate and enzyme along the paper substrate.	32
Figure 18 - Optimization matrix for the β -galactosidase and CPRG substrate components after 30 seconds of immersion in MilliQ water and 5 minutes of development time.	33
Figure 19 - Magenta response of the scanned test strips against the ratio of enzyme to printed CPRG. Error bars represent 6 measurements of each test strip.....	34
Figure 20 - NP-free test strip response against pH buffered MilliQ water solutions.	35
Figure 21 - NP-free test strip response against pH buffered drinking water solutions at relevant pH levels.....	35
Figure 22 - Ratios of AuNP/ β -gal to test the inhibition concentration for the test strips after 30 seconds of immersion in MilliQ water and 5 minutes of development time.	36
Figure 23 - Magenta response against the amount of AuNPs equivalents needed to inhibit the enzyme. Error bars represent 6 measurements of each test strip.....	37
Figure 24 - Test-strip sensitivity in cfu against a) <i>E. coli</i> XL1 and b) <i>Bacillus subtilius</i> . The average magenta component values of the strips are plotted in c). Error bars represent 6 measurements of each test strip.	38
Figure 25 - Visual comparison of test strips where β -gal was not printed between a strip immersed in MilliQ water (Left) and concentrated <i>E. coli</i> XL1 bacteria (Right)	41
Figure 26 - a) Visual and b) graphical response of our test strips to various concentrations of sodium chloride in water. Error bars represent 6 measurements of each test strip. ...	42

Figure 27 - a. Illustration of the Fe ₃ O ₄ NP enzyme mimetic amplified colorimetric sensing of proteins. b. Structures of Dop-Fe ₃ O ₄ and TMA-Fe ₃ O ₄ . c. Hydrodynamic diameter and zeta potential of Fe ₃ O ₄ NPs in 5 mM CH ₃ COONa buffer at pH 5.0.	53
Figure 28 - Normalized OD at 420 nm upon protein addition with fixed NPs concentration (25 µg/mL). a. Concentration dependent OD curve of lipase. Inset is the hydrodynamic diameter of functionalized Fe ₃ O ₄ NPs and lipase-NP complexes. b. Normalized OD curve of lysozyme with modest permutation. Inset: hydrodynamic diameter of functionalized Fe ₃ O ₄ NPs and lysozyme-NP complexes. Results are average of three measurements and error bars are standard deviation. The NP concentration used in the size measurement is 250 µg/mL and the protein is at a concentration of 500 nM.	55
Figure 29 - Array-based sensing of ten proteins. a. Photograph of the color change upon addition of protein solutions at 50 nM. b. OD response (OD/OD ₀ at 420 nm) patterns in the presence of proteins at 50 nM (responses are an average of five measurements and the error bars are the standard deviation). c. Canonical score plot for the OD response patterns as obtained from LDA with 95% confidence ellipses.	58
Figure 30 - Sensing strategy used for bacteria determination in this work.....	69
Figure 31 – Chemical Structures of the Particles used in the Study	70
Figure 32 - Colorimetric Responses to Bacteria Based on the Chemical Functionality of the Particle	70
Figure 33 - Proposed Inkjet Printed Test Strip Fabrication	71
Figure 34 - The components printed separately as well as together.	72
Figure 35 - Solution-based testing using the developed particles against concentrations of E. coli DH5α bacteria	73
Figure 36 - Colorimetric response of our test strips to various concentrations of E. coli DH5α bacteria	73
Figure 37 - Colorimetric response in both solution (a) and on a test strip (b) using various concentrations of E. coli XL1 bacteria.....	74
Figure 38 – Chlorine Sensor on a Test Strip Format	75
Appendix Figure 39 - A comparison of a cartridge containing a sponge (left) versus a high quality spongeless cartridge (right). Note that the left cartridge is not for an Epson Artisan 50 cartridge and is used as a demonstration only.....	83

Appendix Figure 40 - Computer chip located on the cartridge.	84
Appendix Figure 41 - A 50%/50% mix of the cyan and yellow channels.	106
Appendix Figure 42- A Powerpoint sheet that has the different combinations of cyan and yellow channels	107
Appendix Figure 43 - Proper paper lining on the CD tray	108
Appendix Figure 44 - Some pattern examples from our work.	109

CHAPTER 1

INTEGRATION OF INKJET PRINTING FOR BIOLOGICAL AND MATERIALS ASSEMBLY

Introduction

Inkjet printing is a versatile technique that has been widely used for the creation of two-dimensional patterns onto surfaces. The mild conditions attained by inkjet printing make it particularly suited for handling a wide range of materials especially fragile biological samples. Another attractive advantage of inkjet printing is the placement of predetermined quantities of material that can be performed without the need for additional patterning steps, reducing waste. In short, inkjet printing uses electrical actuators to 10-20 pL of liquid from micron-sized apertures out towards a substrate to create the pattern of interest. This technology has become a reliable technique for rapid large scale fabrication as well as a tool for basic research. While the most ubiquitous use of inkjet printing is for creating paper documents, it has seen use in organic solar cell creation, chemical synthesis, combinatorial chemistry, and sensor fabrication.

Technology Overview

As a general technique, inkjet printing can be divided into two main categories: drop-on-demand and continuous inkjet. Historically, early inkjet printers operated on a continuous basis using electrostatic plates to deflect the emitted drops to the paper or to a collection basin for reuse later. These types of printers, while still used for high speed printing on industrial scales, has been largely overtaken by drop-on-demand printing strategies. These have largely been superseded by drop-on-demand systems. One such strategy, developed by both Canon and Hewlett-Packard, where a heated metal plate creates a vapor bubble inside the ink chamber,

causing a droplet of ink to be pushed out of the nozzle. This heating only lasts a few milliseconds, raising the temperature to approximately 300°C. While this thermal method of printing is relatively simple, the heat of bubble formation may impact the ink used as well as been known to clog the printing nozzles over time. Piezoelectric drop on demand printing, developed by Seiko-Epson, uses a glass tube that has been encased in a layer of piezoelectric ceramic. For proper printing, a pulse is generated causing the walls of the tube to compress, ejecting the droplet out of the nozzle and onto the substrate. As expected, this system is more delicate on the printed solution, especially if the material is heat sensitive, but piezoelectric systems tend to be more costly and also have clogging issues. Generally, both piezoelectric and thermal printing have nozzle sizes on the range of 20-30 μm , but the constant drive to generate smaller droplets to increase pattern resolution continues to reduce nozzle size.

Droplet formation

A typical inkjet printhead is shown schematically in Figure 1.¹ As our work in this document is done using a piezoelectric inkjet system, we will discuss how it works rather than thermal inkjet printing. How the printhead works can be summarized as such: a voltage difference is applied to the piezoelectric actuator by the system causing the volume of the chamber to shrink. Pressure waves are created by this change that are dispersed throughout the capillary. When the positive pressure wave hits the nozzle opening, the ink is pushed out of the nozzle. An ink droplet is pushed out if the kinetic energy transferred outward is larger than the surface energy needed for creation of the droplet. How fast the droplet is ejected depends again on the kinetic energy, which needs to be at least a few meters per second to overcome the effect of air that will decelerate the droplet.^{2,3}

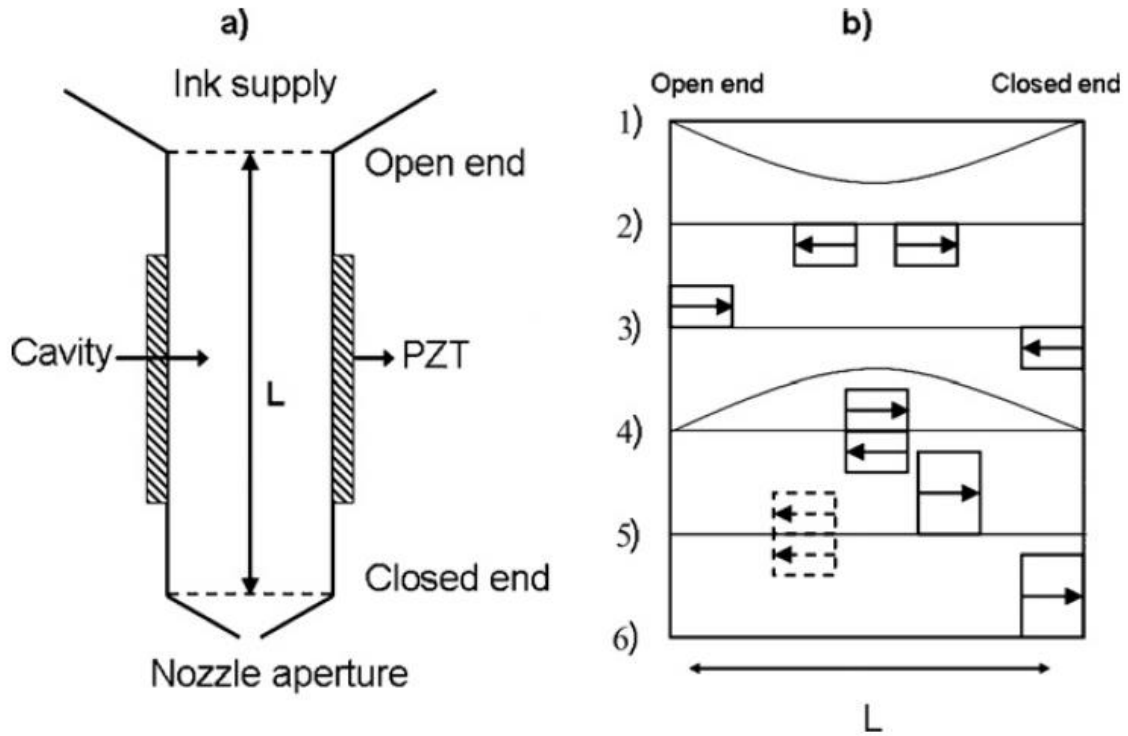


Figure 1 - (a) Schematic diagram of a piezoelectric inkjet print head. (b) Schematic representation of wave propagation and reflection in a piezoelectric tubular actuator. Reproduced from Reference 1.

How the created pressure waves interact after being generated is important for proper jetting. When the initial increase in voltage causes the piezo actuator to move outwards (Figure 1b), a negative pressure wave is generated in the chamber. This wave splits up with the resulting waves going in opposite directions with half amplitude. According to acoustic wave theory, the nozzle opening is considered closed as it is much smaller than the cross-section of the capillary, while the reservoir side is considered an open side as the feed tube is much larger than the capillary. This setup leads to the wave sent towards the nozzle side to be reflected without changing its phase, but the wave sent toward the reservoir end is reflected back with a changed phase. As the two waves come back to the center, the voltage across the piezoelectric element drops, causing the actuator to move inward to generate positive pressure in the vessel. The

newly created positively charged wave then interacts with the reflected waves made previously, destroying the negative pressure wave and doubling the positive wave that then interacts with the nozzle.^{2,3,4}

From an ink development side, how the waves decay depends on the ink that the waves go through and therefore how reliable jetting occurs. Inducing the piezoelectric printhead system at high frequency yields sporadic printing as the waves have not had enough time to decay completely and would then interact with the following pressure wave instead. On the other hand, slower frequencies mean slower droplet ejection lowering overall printing efficiency. Controlling the overall decay time can be optimized by the composition of the ink fluid.¹ For example, Antohe et al. found that waves decay slower in ethylene glycol than if they were generated in water, which they claim is due to the higher viscosity of ethylene glycol that dampens the decay effect.⁵

Ink Properties Effect Droplet Creation

As expected, the chemical composition of the ink has a large impact on whether droplets are formed. To attempt to quantitate the printability of ink components, Fromm developed the Z number grouping of fluid properties that simply is the inverse of the Ohnesorge number (Oh), for dimensionless drop formation analysis in DOD print heads:

$$Z = (d\rho\gamma)^{1/2}/\eta = Oh^{-1} \quad (1)$$

where η , ρ , and γ are the viscosity, density, and surface tension of the liquid, respectively, and d is the diameter of the nozzle.³ From this equation, Fromm inferred that droplet could only be formed when $Z > 2$ and that if you use the same pressure pulse and increase the value of Z , the droplet volume increases. This theoretical work was then tested experimentally by Derby et al.

who used concentrated alumina wax suspensions to show that printing can occur when Z is between 1 and 10.⁴ The upper limit of Z is determined to be the highest value that does not generate small satellite drops during printing rather than one cohesive drop whereas the lower limit represents the suspensions ability to dissipate the pressure wave. Derby and colleagues also confirmed Fromm's theory that droplet volumes do increase as the Z values increase over a range of Z values from 1 to 14. One could potentially print inks that are have Z values higher than 10 as long as the satellite drops all merge with the main droplet. Schubert et al. tested a wide range of common industrial solvents with low viscosities from 0.4 to 2 mPas and surface tensions ranging from 23 to 73 mN m⁻¹.⁶ These materials could be successfully printed, which seemed to contradict earlier reports as these solvents had Z values from 21 to 91. Schubert and colleagues hypothesized that printability might be more affected by the vapor pressure of the ink component, where poor droplet formation was seen with solvents higher than 100 mmHg.

Applications of Inkjet Printing for Biosensing

One of the earliest usage of inkjet printing outside of the document creation field was in the realm of sensing, especially biosensors. From a commercial aspect, portable diagnostics that can be used at the point of care such as glucose monitoring are of increasing medical need. While screen printing and other means of materials deposition have been shown to create biosensors, the use of expensive enzymes that need to be portioned onto the sensor with high reproducibility tends to not be amenable to these techniques. One of the first reports of an inkjet printed glucose sensor was reported in 1988 where a solution of glucose oxidase (GOD) is mixed with the conductive polymer poly(3,4-ethylenedioxythiophene/polystyrene sulfonic acid) (PEDOT/PSS) and printed onto a conductive indium tin oxide conductive surface (Figure 2).⁷ The printed surface is then encapsulated by a membrane of cellulose acetate. Based on the enzyme

catalyzed reaction of glucose that produces a readable amperometric signal, it was shown that inkjet printed biosensors could be potentially useful diagnostics.

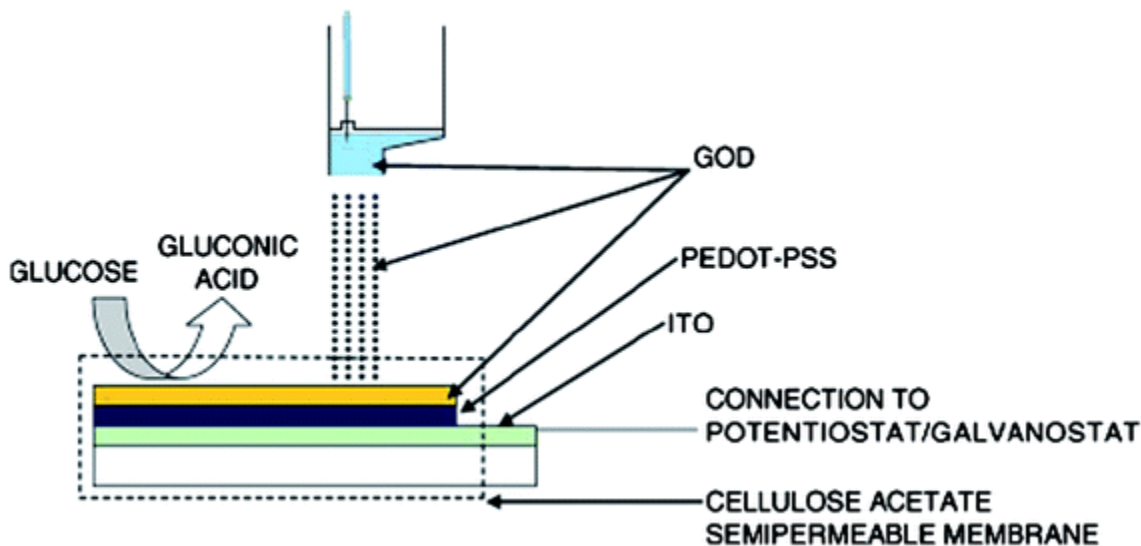


Figure 2 - Inkjet printing of glucose biosensor prototype. Reproduced from Reference 7.

Since the creation of the printed glucose sensor, many inkjet printed sensors based on electrical potential have been created using inkjet technology. For example, many amperometric and potentiometric enzymes that have been screen printed into working biosensors have been subsequently manufactured using inkjet technology, mainly to reduce the cost and waste of screen printing these sensors. Inkjet printed sensors have been made to detect the overall protein concentration in aqueous solutions as well as for the detection of specific amino acids (L-lactate) that is relevant to the dairy industry.⁸ More complex biosensing involving the detection of specific bacteria strains have been investigated using inkjet printed sensors. Using a combination of bacteriophages and redox enzymes, this methodology can detect down to very low concentrations of specific bacteria (10 Bacillus anthracis bacteria/mL) in solution.⁹ In brief, this system works by loading the sensor with a pathogen-specific phage for the bacteria of interest. If it is found, the bacteria is infected by phage, causing the bacteria to lyse and release

the contents of the bacteria out into the analyte mixture. Through the use of a β -galactosidase electrochemical assay that can sense the presence of the sugars that were released, the signal is generated that can be easily analyzed. Given how the sensor works, it is not only specific for the bacteria of interest but only to live bacteria.

One of the key features of inkjet printing is the ability to deposit multiple inks onto a surface to make sensor arrays for multiple analyte detection. Recently, Ligler and colleagues created a sandwich-type immunoassay by depositing antibodies via piezoelectric inkjet printing.¹⁰ In their work, the sensor was able to detect simultaneously both proteins and bacteria – a reported first for a single immunoassay test. Even more interestingly, the test detected harmful bacteria such as *Bacillus globigii* and *Vibrio cholerae* and toxins such as ricin and staphylococcal enterotoxin B. The U.S Naval Research Laboratory reported in 2003 creating a prototype of this type of sensor that also included detection of *Salmonella* for food safety concerns.

Nanoparticles Influence on Sensing

Nanoparticles (NPs) have become particularly interesting in the creation of biological sensors due to their unique physicochemical properties that are absent from their macroscale counterparts. In fact, nanomaterials such as metal nanoparticles, quantum dots, micelles, and carbon nanotubes have been incorporated into many promising sensor designs.¹¹ Gold nanoparticles (AuNPs) are the most stable metal nanoparticles that are readily available through either chemical reduction of gold salts or physical treatment of bulk gold. Besides the large surface-to-volume ratio that is common for all nanomaterials, AuNPs possess unique optical and electronic properties and excellent biocompatibility.¹² Iron oxide nanoparticles have also been used in sensor applications also due to their electronic and magnetic properties as well as their inexpensive cost for production.¹³

As an example of nanoparticles being used in biosensing strategies, Rotello et al. explored recently the use of enzymes to provide array-based sensors with enhanced sensitivity.¹⁴ The increased sensitivity required for many diagnostic uses presents a challenging goal for array-based sensors due to the fact that the detection process generally relies on fluorescence responses that are restricted by the inherent emissivity of the fluorophores used. Cationic AuNPs electrostatically bind the anionic β -Galactosidase (β -Gal), inhibiting the enzyme without denaturation. In this enzyme-amplified array sensing approach, the sensitivity of the array is amplified through an enzymatic reaction (Figure 3a). This system couples the signal amplification process of ELISA with the versatility of the “chemical nose” approach as it is able to sense and identify a range of biomedically relevant proteins at nanomolar concentrations in both buffer and desalted human urine. Displacement of the particle by analyte proteins restores β -Gal activity, generating a fluorescent readout signal that is amplified through enzymatic catalysis with a limit of detection of 1 nM in both buffer as well as in biofluid solutions (Figure 3b).

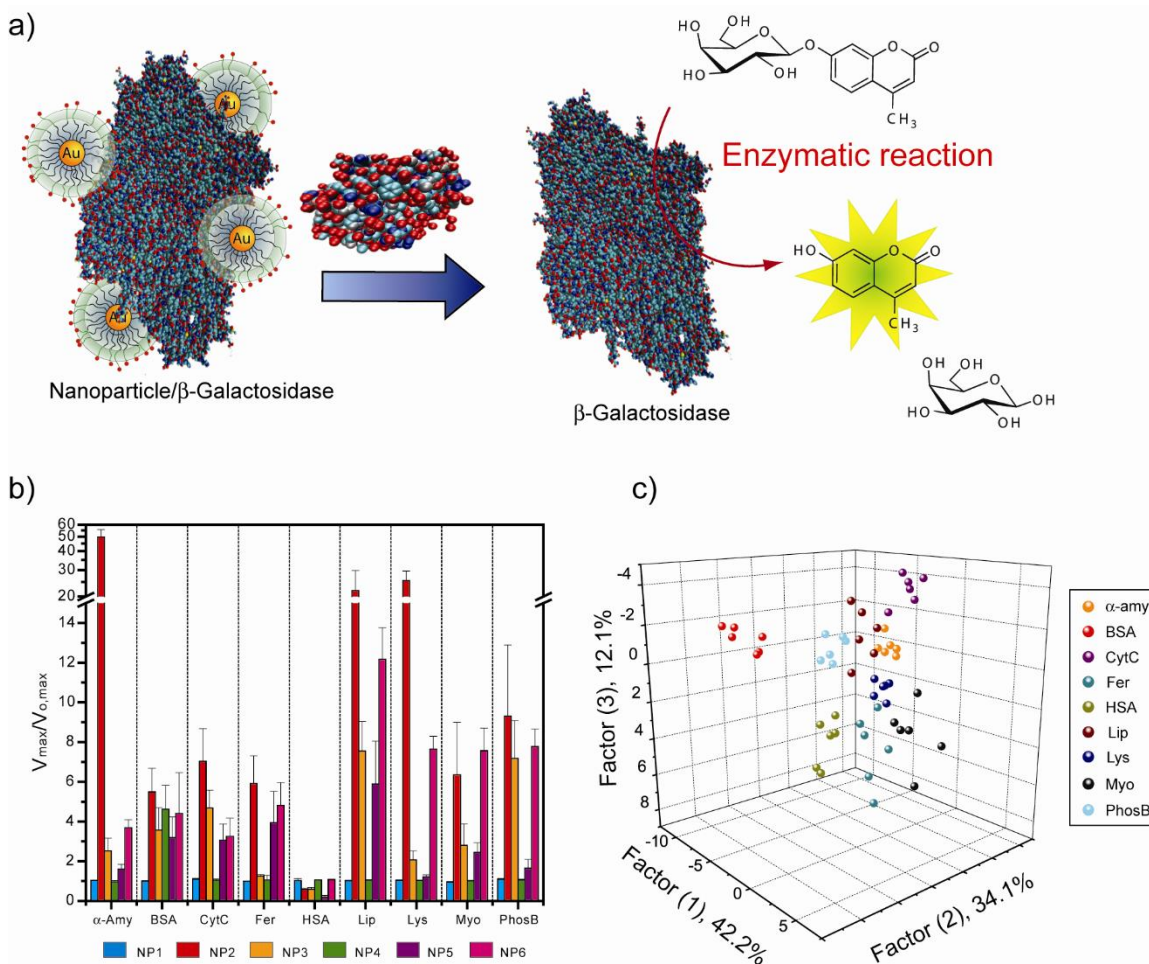


Figure 3 - A schematic representation of a sensor element in the sensor comprised of β -galactosidase (β -Gal) and cationic AuNPs and differentiation of proteins in 3-D. a) As shown, β -gal is displaced from the β -Gal/AuNP complex by protein analytes, restoring the catalytic activity of β -Gal towards the fluorogenic substrate 4-methylumbelliferyl- β -D-galactopyranoside, resulting in an amplified signal for detection. b) Differential protein pattern of the nine proteins at 1 nM. c) Canonical score plot of the first three factors of fluorescence response patterns obtained through β -Gal/AuNP sensor array against nine target proteins in 1 nM concentration.

Reproduced from Reference 14.

Applications of Inkjet Printing for Materials Applications

As inkjet printing can reliably deposit low viscosity inks onto a surface, depositing metal solder onto a surface to create conductive patterns without generating waste has been extensively researched. Boldman and colleagues first published work in 1992 showing this could be done, patterning 100 μm droplets onto a surface reliably.¹⁵ From that work, other research groups have investigated using other metals or metal precursors that could not only be quickly printed but later heated to form conductive areas. For example, silver metal inks with organic dispersants are significantly used in industrial applications as they can be converted to conductive lines after annealing at temperatures of approximately 300°C. By alternating between printing one layer then annealing then printing more material on top of the previous print, Vest and colleagues were able to create conductive lines with resistivity of 1 Ω .¹⁶

Devices have been also created using inkjet printing. While larger reviews have been published outlining current work in this field, it is important to note that inkjet printing has been used to create devices such as organic field transistors and solar cells and components such as conductive polymer strands and ceramic structures¹⁷. As discussed previously, however, inks that can be reliably ejected out of the nozzle tend to be dilute solutions requiring multiple printing passes to allow enough material to be deposited for proper device fabrication. While these drawbacks can be dealt with in small scale production, larger commercialization of this technology has been slow to occur. Furthermore, the resolution of droplet size of approximately 50 μm can be too large for small device fabrication.

There is much interest in conventional inkjet printing with NP inks given their unique electronic and optical properties.¹⁸ As stated before, creating conductive patterns using NP inks seems obvious, however, there is only a few reports outlining research in this field.¹⁹ The method has

also been applied to printing electrodes for photovoltaic cells.¹⁷ One of the more investigated usage of NP inks in the form of magnetic inks for security printing on financial documents.²⁰ In these methods, the particles must be small enough and not cluster together to exist in a superparamagnetic state in the ink formulation, but must later dry into a densely packed layer to create a magnetic layer. Multiple examples of this type of printing have been described in literature so far but recent reports still discuss difficulty creating magnetic alignment in the films.²¹

Dissertation Overview

This dissertation is focused on inkjet printing nanoparticles for applications in both security applications and biosensing. Through the use of both gold and iron oxide nanoparticles, I have been able to generate a new system for both depositing and visualizing printed material on surfaces as well as making new diagnostics for bacteria detection. Specifically, Chapter 2 reports on incorporating functionalized gold nanoparticles into an ink and printing them onto surfaces using straightforward inkjet printing.²² These particles act as a 'barcode' can be detected in an ambient and non-destructive manner by laser desorption ionization mass spectrometry imaging. Chapter 3 builds on the gold nanoparticle printing, incorporating enzymes into our inkjet printing to develop a paper based diagnostic for bacteria concentration in water.²³ To correct the stability of the test strips produced, Chapter 4 examines the use of iron oxide nanoparticles as sensing components, using charged proteins as a test bed for detection.²⁴ Finally, Chapter 5 puts all of our work together to begin the optimization of more stable test strips.

Notes

[1] Tenkin, E.; Smith, P.J.; Shubert, U.S. *Soft Matter*, **2008**, *4*, 703.

[2] Dijkstra, J. F. *J. Fluid Mech.*, **1984**, *139*, 173.

- [3] Fromm, J. E. *IBM J. Res. Dev.*, **1984**, 28, 322.
- [4] Reis, N.; Ainsley, C.; Derby, B. *J. Appl. Phys.*, **2005**, 97, 094903
- [5] Antohe, B. V.; Wallace, D. B. *J. Imaging Sci. Technol.*, **2002**, 46, 409.
- [6] de Gans, B.-J.; Kazancioglu, E.; Meyer, W.; Schubert, U. S. *Macromol. Rapid Commun.*, **2004**, 25, 292.
- [7] Kimura, Y. K. T. K. *J. Biosensors*, **1988**, 4, 41.
- [8] Newman, J. D.; White, S. F.; Tothill, I. E.; Turner, A. P. F. *Anal. Chem.*, **1995**, 67, 4594.
- [9] Neufeld, T.; Schwartz-Mittelmann, A.; Biran, D.; Ron, E. Z.; Rishpon, J. *Anal. Chem.*, **2003**, 75, 580.
- [10] Delehanty, J. B.; Ligler, F. S. *Anal. Chem.*, **2002**, 74, 5681.
- [11] Miranda, O. R.; Creran, B.; Rotello, V. M. *Curr. Opin. Chem. Biol.*, **2010**, 14, 728.
- [12] Yeh, Y.-C.; Creran, B.; Rotello, V. M. *Nanoscale*, **2012**, 4, 1871.
- [13] Wu, W.; He, Q.; Jiang, C. *Nanoscale Res. Lett.*, **2008**, 3, 397.
- [14] Miranda, O. R.; Chen, H.-T.; You, C.-C.; Mortenson, D. E.; Yang, X.-C.; Bunz, U. H. F.; Rotello, V. M. *J. Am. Chem. Soc.*, **2010**, 132, 5285.
- [15] Hayes, D. J.; Wallace, D. B.; Boldman, M. T. *Proc. SPIE-Int. Soc. Opt. Eng.*, **1992**, 1847, 316.
- [16] Vest, R. W.; Tweedell, E. P.; Buchanan, R. C. *Int. J. Hybrid Microelectron.*, **1983**, 6, 261.
- [17] Singh, M.; Haverinen, H. M.; Dhagat, P.; Jabbour, G. E. *Adv. Mater.*, **2010**, 22, 673.
- [18] Bermel, A. D.; Bugner, D. E. *J. Imaging Sci. Technol.*, **1999**, 43, 320.
- [19] Calvert, P. *Chem. Mater.*, **2001**, 13, 3299.
- [20] Sirringhaus, H.; Shimoda, T. *MRS Bulletin*, **2003**, 28, 802.
- [21] Song, H.; Spencer, J.; Jander, A.; Nielsen, J.; Stasiak, J.; Kasperchik, V., & Dhagat, P. *J. Appl. Phys.*, **2014**, 115(17), 17E308.
- [22] Creran, B.; Yan, B.; Moyano, D. F.; Gilbert, M. M.; Vachet, R. W.; Rotello, V. M. *Chem. Commun.* **2012**, 48, 4543.

[23] Creran, B.; Li, X.; Duncan, B.; Kim, C. S.; Moyano, D. F.; Rotello, V. M. *ACS Appl. Mater. Interfaces* **2014**, *6*, 19525.

[24] Li, X.; Wen, F.; Creran, B.; Jeong, Y.; Zhang, X.; Rotello, V. M. *Small* **2012**, *8*, 3589.

CHAPTER 2

LASER DESORPTION IONIZATION MASS SPECTROMETRIC IMAGING OF MASS BARCODED GOLD NANOPARTICLES FOR SECURITY APPLICATIONS

Introduction

Counterfeit materials are a rapidly increasing global issue. It is estimated that illegally produced materials cost between 5 and 7% of the total annual revenue of governments and businesses.¹ More troubling is the prevalence of fraudulent drugs and vaccines that endanger human health, as up to 25% of all drugs available in developing countries are counterfeit in packages created to appear as legitimate product.² These threats are exacerbated by technological advances in image capturing and printing techniques that give criminals new tools to produce high quality copies of drug packaging, currency, and security documents.

While overt protection strategies based on physical or visual inspection remains an important part of verifying authenticity, covert methods using specialized materials and detection schemes have been devised for high value goods including currency³ and pharmaceuticals.⁴ Forensic methods requiring laboratory analysis for authentication are of particular interest, as the overall complexity of observation serves as a counterfeiting deterrent. Destructive chemical analysis of the material by thin layer chromatography,⁵ liquid chromatography,⁶ and gas chromatography⁷ can identify the inks and pigments used in the material; these methods are however unattractive where sample preservation is needed. Furthermore, the solvent needed for analysis can often alter the integrity of the response providing unreliable results. Ambient, non-destructive analysis techniques such as infrared reflectance,⁸ microscope ATR-infrared spectroscopy,⁹ and Raman spectroscopy¹⁰ have been

used to verify authenticity, although the broader use of these methods is limited due to the lack of specific chemical information, limiting the output diversity.

Imaging mass spectrometry (IMS) has recently been used in security applications since it produces non-destructive visual representations of mass profiles that can be compared to samples known to be genuine.^{11,12} For example, Cooke *et al.* used ambient IMS to analyze valid currencies against known counterfeit bills by ink analysis as a proof-of-concept verification technique.¹³ However, the use of solvent complicates the analysis procedure. Designing a system where a manufacturer can incorporate a specific chemical signature into their security inks whose pattern can be visualized only through IMS provides a significant challenge for the counterfeiter.

In our current research, we have demonstrated that functionalized gold nanoparticles (NPs) can be engineered for accurate detection by laser desorption/ionization MS (LDI-MS).^{14,15} Recent work by our groups has shown that surface ligands attached to gold NPs are ionized far more efficiently than the ligand alone due to the particle's strong absorbance at wavelengths (i.e. 337 nm and 355 nm) commonly used in commercially available mass spectrometers.¹⁶ We report here the use of surface ligands with unique structures and mass fingerprints as "mass barcodes" to identify gold NPs. These ligands can be altered through a wide range of synthetic means, providing flexible and tunable masses for detection by LDI-IMS. Moreover, different ligands can be employed to provide multiple channels for higher security as well as higher density of information reporting. In these studies, gold NPs were patterned onto a surface by inkjet printing. The correct pattern was visible only when the surface was scanned for the correct mass signature of the gold NPs (Figure 4).

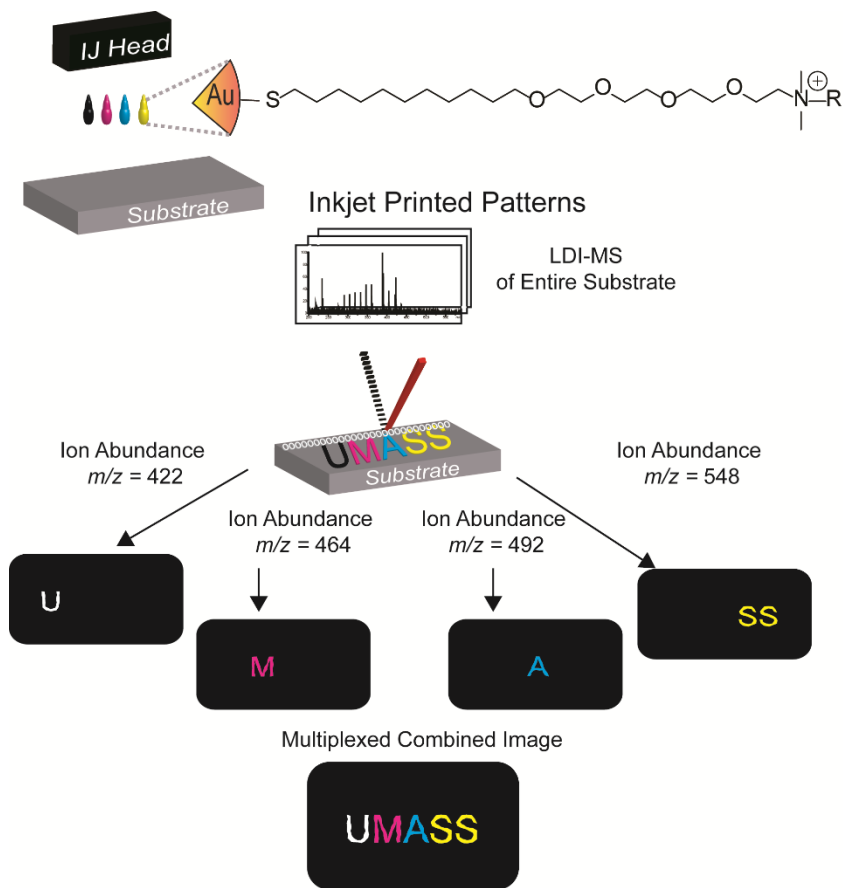


Figure 4 - Anti-counterfeiting mass barcoding strategy

Results and Discussion

The ligands for our study were chosen to achieve distinct mass fragmentation signals. The ligands featured a thiol bonding group for the gold nanoparticles, an alkane chain to stabilize the ligand shell, an oligo(ethylene) glycol to aid water solubility, and a variable ammonium group with a flexible mass head group to provide distinctive mass signatures. The chemical structures of the particles and the corresponding MS spectra are shown in Figure 5. Gold NPs synthesis, place exchange, and inkjet ink formulation can be found in the Materials and Methods section.

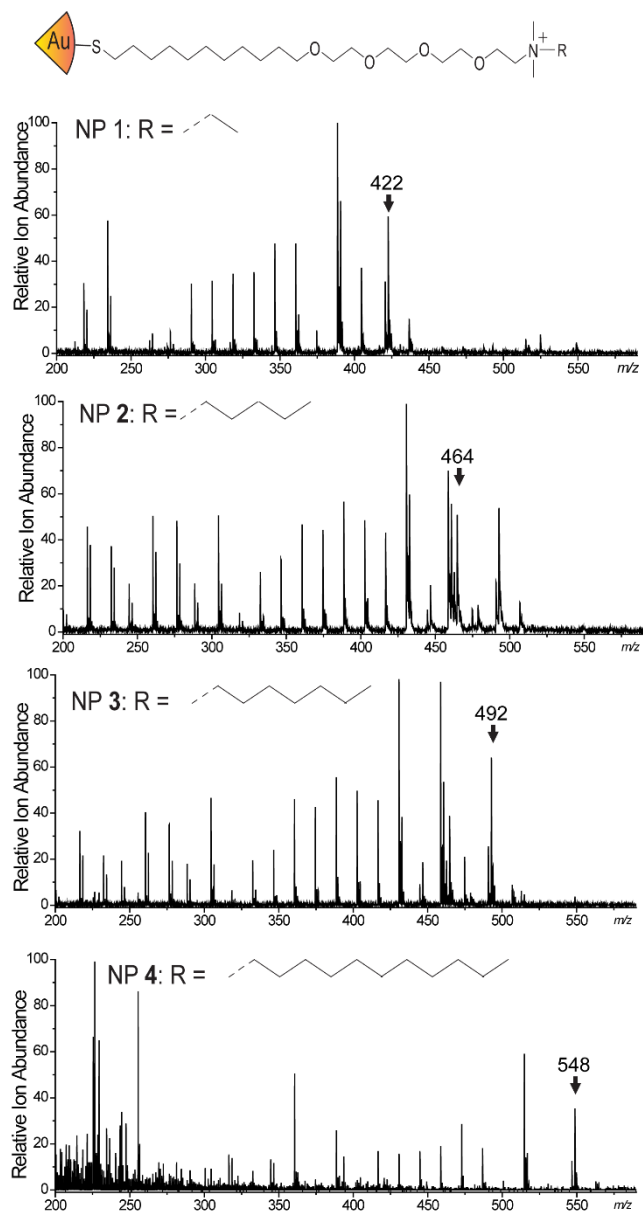


Figure 5 - Mass spectra of the four nanoparticles used in this study, with the m/z value used for scanning highlighted

To validate our system, we first deposited gold NP 1 onto indium tin oxide (ITO) coated glass slides, commonly used in IMS.^{12,16,17} The ions from the gold core as well as ions from the surface ligands were successfully detected. In Figure 6, we show the successful patterning of our gold nanoparticles inks as the specified pattern can be seen when analyzed for the Au^+ signal.

Scanning for both the Au_2^+ signal and the NP 1 ligand also provided the correct image as seen in Figure 6b and Figure 6c, respectively.

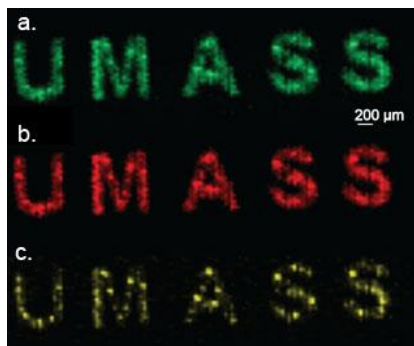


Figure 6 - a) The Au^+ signal determined by scanning the ITO coated glass surface b) the Au_2^+ signal and c) the NP 1 ligand signal (detected ions: Au^+ $m/z = 197$, Au_2^+ $m/z = 394$, NP 1 ligand $m/z = 422$)

To further investigate the capability of this inkjet printing technique, we printed separate inks in one printing cycle. A commercially available Nano Assisted Laser Desorption Ionization (NALDITM) surface was employed in the following experiments.¹⁷ Use of the NALDI surface demonstrated the breadth of this printing technique on different surfaces. Moreover, it creates the possibility of new potential applications of this technique because a NALDI surface is capable of facilitating the ionization process of small molecules not attached onto a NP surface.^{18,19} For our study, we deposited four different gold NP inks onto the NALDI substrate to investigate their use as an anti-counterfeiting technique. Figure 7a shows a LDI-IMS searching for just the mass barcode for NP 1, indicating no visible response from the other printed gold NP inks. Figure 7b-d also show minimal response from the other mass barcodes, however, combining all of these scans provides us with the image of interest (Figure 7e). This image can only be obtained by analyzing for each of the four mass barcodes, greatly reducing the ability of the counterfeiter to visualize the image.

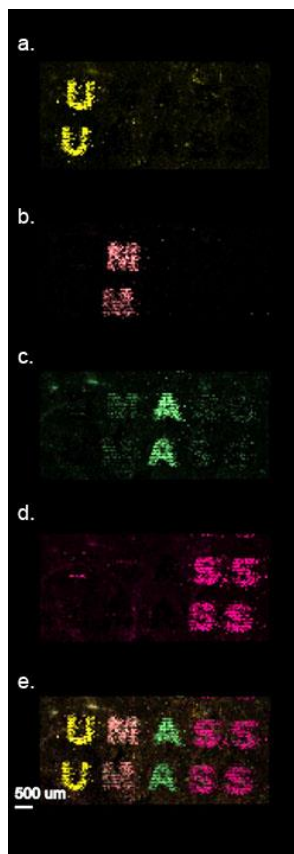


Figure 7 - Ligand LDI-IMS signals for the various ligands tinted different colors for viewing. a.) NP 1 b.) NP 3 c.) NP 2 and d.) NP 4 e.) all 4 signals combined showing the completed pattern

Since the pattern above could in theory be determined simply by scanning for Au^+ or Au_2^+ , we printed two different patterns superimposed on each other on the same NALDI substrate area. In Figure 8, we saw no significant visible pattern on the substrate. However, when scanning for the NP 1 ligand ($m/z = 422$), a clear pattern is detected on the surface. When scanning for the NP 4 ligand (Figure 8c), we saw the second pattern on the substrate that was not previously visible. This demonstrates the ability of inkjet printing to deposit multiple nanoparticle patterns onto the same portion of a substrate, providing unique and sophisticated mass signatures.

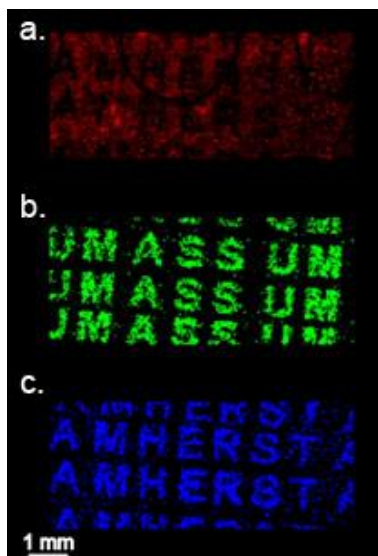


Figure 8 - Overlapped two channel printing. MSI of overlapped printing gold NPs, detected ions: blue letters AMHERST (NP 4 $m/z = 548$), green letters UMASS (NP 1 $m/z = 422$), red pattern (Au^+ , $m/z = 197$)

Materials and Methods

Gold nanoparticles with the attached ligand were synthesized in a two-step method. This entailed the preparation of pentanethiol stabilized nanoparticles of approximate 2.5 nm size using the Brust method followed by a ligand exchange reaction.²⁰ Ligands were synthesized according to previous methods.²¹ After purification, the nanoparticles were diluted to a concentration of $1\mu\text{M}$ with water, filtered through a $.2\mu\text{m}$ polypropylene membrane (Puradisc 25AS, Whatman), and syringed into a virgin aftermarket Epson inkjet cartridge for printing (MIS Associates, Auburn Hills, MI USA).

Printing was done using an Epson Artisan 50 inkjet printer (Long Beach, CA USA) which was used as packaged. The substrate was loaded into the printer by taping the bottom of the substrate to the included CD tray. For our work, patterning was done by using the Print CD software

provided with the Epson printer. The text was written in Arial font in Bold letters at a font size of 2 for appropriate detection. In order to print only the channel of interest, the color of the letter has to match the channel printed. To print only the magenta channel, the RGB value must be set to (255,0,255); The cyan channel, (0,255,255); the yellow channel, (255,255,0). A representative screen capture of the printed is shown in Figure 9. The ICM color management also must be turned off in the Advanced tab of the printer properties to ensure no mixing of the channels occurs. Before printing, the printheads were cleaned two times using the “Head Cleaning” function in the Maintenance tab of the printer properties to ensure that the channels were filled.

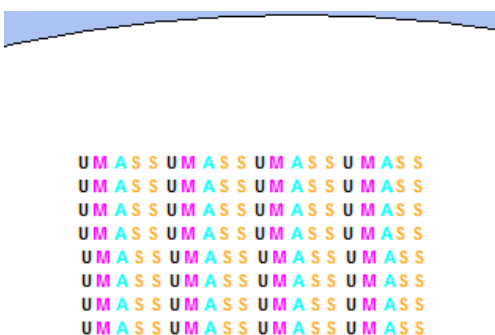


Figure 9 – Screen capture of the pattern to be printed on the substrate.

The LDI-MS image analysis was carried out on a Bruker Autoflex III MALDI-TOF mass spectrometer (Bruker Daltonics, Bremen, Germany) (Autoflex III). The Autoflex III is equipped with a Smartbeam-laser and with the FlexImaging 2.1 software package (Bruker Daltonics, Bremen, Germany). LDI measurements were done in operating conditions as follows: ion source 1 = 19.00 kV, ion source 2 = 16.60 kV, lens voltage = 8.44 kV, reflector voltage = 20.00 kV, reflector voltage 2 = 9.69 kV, pulsed ion extraction time = 10 ns, suppression = 180 Da, and positive reflectron mode in a mass range of 100–1200 Da. The mass spectrometric imaging sequence was generated by FlexImaging 2.1 software. Imaging was performed by continuously

scanning the surface in the x-direction and y-direction. The lateral resolution for the LDI-MS imaging was set to 50 μm . A total of 50 laser shots were measured per position. In general, \sim 400,000 laser shots were fired on a \sim 20 mm^2 area. The data analysis and image generation were performed in FlexImaging 2.1. The indium tin oxide (ITO) glass slides and the NALDITM substrate were obtained from Bruker Daltonics (Billerica, MA USA) and Nanosys (Palo Alto, CA USA) respectively.

Conclusions

In summary, we have developed an efficient security strategy using the mass signature barcode of functionalized gold nanoparticles to provide discernible patterns through LDI-IMS. By using inkjet printing, we can create surfaces that can be quickly altered either by modifying the physical pattern or by changing the functional gold NPs used. The diversity of mass options coupled with the efficiency of the “read” process makes this strategy promising for a wide variety of covert anti-counterfeiting applications. This technique also gives shows that we can reliably print gold nanoparticles out of our printer for further studies.

Notes

- [1] Staake, T.; Thiesse, F. Fleisch, E. *Eur J Market*, **2009**, *43*, 320.
- [2] Fernandez, F. M.; Green, M. D.; Newton, P. N. *Ind. Eng. Chem. Res.*, **2008**, *47*, 585.
- [3] Lancaster, I. M.; Mitchell, A. *Proceedings of SPIE 5310*, **2004**, *5310*, 34.
- [4] Aldhous, P. *Nature*, **2005**, *434*, 132.
- [5] Neumann, C.; Ramotowski, R.; Genessay, T. *J. Chromatogr. A*, **2011**, *1218*, 2793.
- [6] Causin, V.; Casamassima, R.; Marega, C.; Maida, P.; Schiavone, S.; Marigo, A.; Villari, A. *J. Forensic Sci.*, **2008**, *53*, 1468.
- [7] Liu, Y.-Z.; Yu, J.; Xie, M.-X.; Liu, Y.; Han, J.; Jing, T.-T. *J. Chromatogr. A*, **2006**, *1135*, 57.

- [8] Bügler, J. H.; Buchner, H.; Dallmayer A. *J. Forensic Sci.*, **2008**, *53*, 982.
- [9] Trafela, T.; Strlic, M.; Kolar, J.; Lichtblau, D. A.; Anders, M.; Mencigar, D. P.; Pihlar, B. *Anal. Chem.*, **2007**, *79*, 6319.
- [10] Geiman, I.; Leona, M.; Lombardi, J. R. *J. Forensic Sci.*, **2009**, *54*, 947.
- [11] Tang, H.-W.; Wong, M. Y.-M.; Chan, S. L.-F.; Che, C.-M.; Ng, K.-M. *Anal. Chem.*, **2011**, *83*, 453.
- [12] McDonnell, L. A.; Heeren, R. M. A. *Mass Spectrom. Rev.*, **2007**, 606.
- [13] Ifa, D. R.; Gumaelius, L. M.; Eberlin, L. S.; Manicke, N. E.; Cooks, R. G. *Analyst*, **2007**, *132*, 461.
- [14] Zhu, Z.-J.; Ghosh, P. S.; Miranda, O. R.; Vachet, R. W.; Rotello, V. M. *J. Am. Chem. Soc.*, **2008**, *130*, 14139.
- [15] Yan, B.; Zhu, Z.-J.; Miranda, O. R.; Chomposor, A.; Rotello, V. M.; Vachet, R. W. *Bioanal. Chem.*, **2010**, *396*, 1025.
- [16] Chughtai, K.; Heeren, R. M. *Chem. Rev.*, **2010**, *110*, 3237.
- [17] Cornett, D. S.; Reyzer, M. L.; Chaurand, P.; Caprioli, R. M. *Nat. Methods*, **2007**, *4*, 828.
- [18] Northen, T. R.; Yanes, O.; Northen, M. T.; Marrinucci, D.; Uritboonthai, W.; Apon, J.; Golledge, S. L.; Nordström, A.; Siuzdak, G. *Nature*, **2007**, *449*, 1033.
- [19] Taira, S.; Sugiura, Y.; Moritake, S.; Shimma, S.; Ichiyangi, Y.; Setou, M.; *Anal. Chem.*, **2008**, *80*, 4761.
- [20] Brust, M.; Walker, Bethell, D.; Schiffrin, D. J.; Whyman, R. *J. Chem. Soc., Chem.*, **1994**, 801.
- [21] Hostetler, M. J.; Templeton, A. C.; Murray, R. W. *Langmuir*, **1999**, *15*, 3782.

CHAPTER 3

DETECTION OF BACTERIA USING INKJET-PRINTED ENZYMATIC TEST STRIPS

Introduction

Detection of bacteria in drinking water is critical for global public safety and health. According to the World Health Organization, ~1.7 million people are killed every year by bacteria-related diseases such as infectious diarrhea and cholera.¹ Several methodologies have been developed for bacterial detection based on techniques such as culturing,² chemiluminescence,³ bioluminescence,⁴ and mass spectrometry.⁵ Each of these systems has its advantages; however the utility of these methods is generally limited by the high cost of analysis, the need for trained personnel, and the overall stability of the sensor. Furthermore, all of these strategies are laboratory-based, limiting their utility for bacterial analysis at the water source.

Nanotechnology has significantly enhanced sensing strategies for detecting bacteria through the use of nanoparticles, using unique physicochemical properties that are absent from their macroscale counterparts.⁶ For example, Weissleder et al. reported the use of magneto-DNA probes specific to bacteria strains capable of rapid and specific profiling directly in clinical samples.⁷ Functionalized gold nanoparticles (AuNPs) have also been shown to aid detection in systems for sensing proteins,⁸ cells,⁹ and viruses.¹⁰ In our research, we have developed an array-based sensing system based on noncovalent conjugates of AuNPs and a fluorescent polymer that allow the detection and classification of a wide range of bacteria within minutes in a laboratory setting.¹¹

Developing nanoparticle-based sensors that are portable and highly sensitive yet inexpensive is extremely challenging. While sensors exist with low limits of detection that do not require

instruments for readouts,¹² most do not have the robustness to be used for on-site detection, nor can they be manufactured economically. Point of use utility is critical as most off-site testing takes 24 h or longer for proper analysis. As water conditions can change rapidly due to fecal contaminates,¹³ the results obtained with these methods do not provide up to date water safety information. Rapid testing for bacteria, ideally performed at the water source on a low-cost strip platform, would be ideal given the inherent advantages of these platforms such as efficiency and portability.¹⁴

Signal amplification is generally required to maintain high sensitivity in rapid-detection visual sensors.¹⁵ In laboratories, enzymatic amplification has been widely employed in enzyme-linked immunosorbent assays.¹⁶ This strategy has great potential for visual instrument-free detection due to the wide range of fluorescent and colorimetric enzyme substrates available. However, effective implementation of enzymatic amplification to low-cost platforms is challenging. Lateral flow approaches have shown success in performing enzyme immunoassays in a test-strip format,¹⁷ where enzymes pre-conjugated or labeled with antibodies are separated from enzyme substrates in different zones of the strip during fabrication.¹⁸ Recently, our group developed an enzyme–AuNP conjugate system for the colorimetric detection of bacteria.¹⁹ However, this system still requires the use of solution-based methods for both fabrication and analysis that are difficult to use outside of the laboratory.

Inkjet printing is an attractive non-contact material deposition method as it is low cost, simple, fast, and reproducible, and generates a low amount of waste during printing.²⁰ These attributes have made this strategy highly promising for patterning both synthetic and biological systems.^{21,22,23,24} Previous reports have investigated the use of inkjet printed enzymes to create horseradish peroxidase²⁵ and glucose²⁶ electrochemical biosensors as well as for fabricating

colorimetric sensors for the detection of neurotoxins²⁷ and pesticides using a lateral flow format.²⁸

Rapid response time and simplicity of use are important for point of use systems. To achieve rapid response times and simple 'dip and use' utility, the enzyme and a colorimetric substrate were spatially printed from different cartridges to prevent mixing before immersion. The close proximity of enzyme and substrate provides a rapid sensing platform. To create the colorimetric response needed for visual detection of bacteria, we adapted a sensing construct that uses β -galactosidase (β -gal) and surface-functionalized AuNPs (Figure 10).¹⁹ In brief, cationic AuNPs were electrostatically bound to the anionic β -gal, causing reversible inhibition of the enzyme. When incubated with a colorimetric substrate (chlorophenol red- β -D-galactopyranoside (CPRG)), the color of the sensor remains pale yellow. When negatively charged bacteria are present, a competitive equilibrium is formed between the bacteria and the enzyme for the nanoparticles. This displacement restores enzymatic activity to the β -gal, which then cleaves the colorimetric substrate to produce a deep purple color.

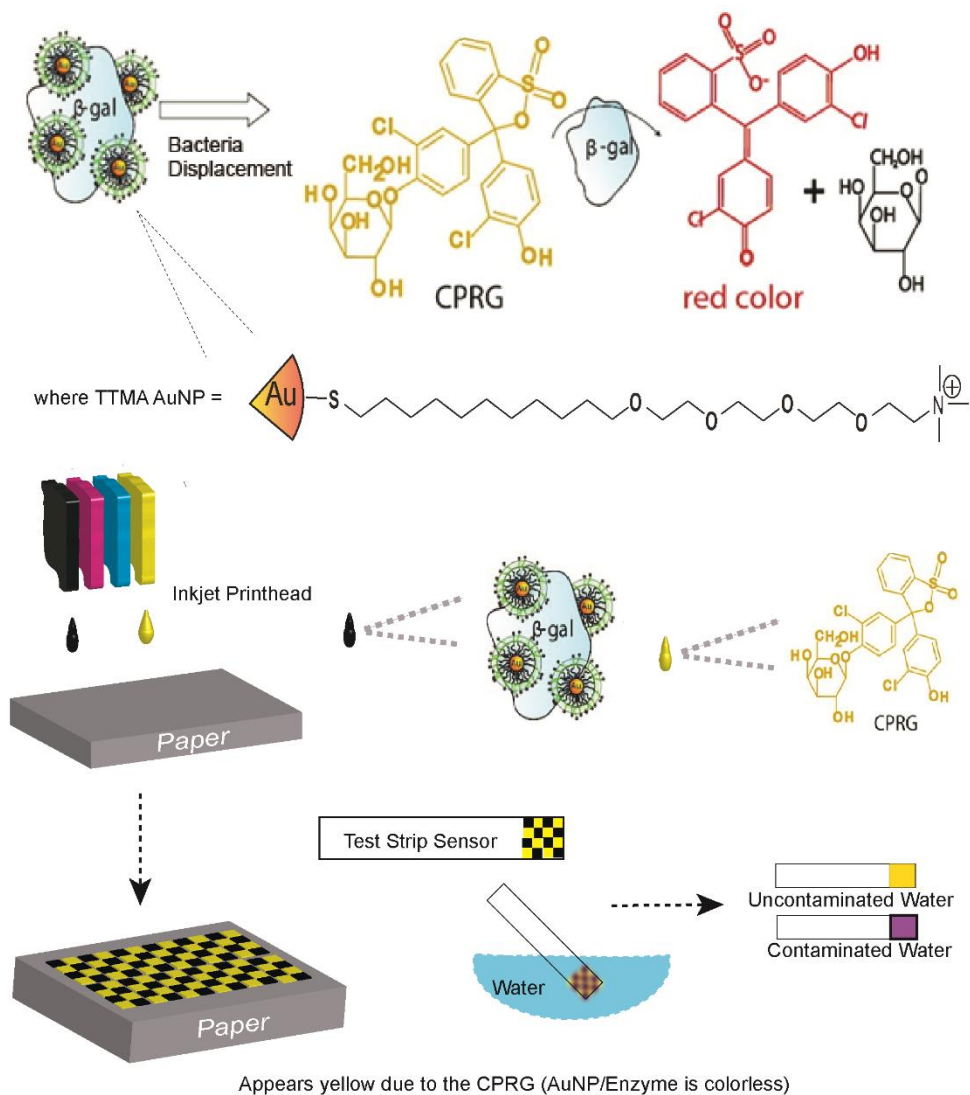


Figure 10 - Chemical basis and inkjet printing scheme for the test strips used in these studies.

Results and Discussion

Enzymes can easily be damaged during the inkjet printing process.²⁹ To minimize the impact of the printing process piezoelectric printing was used, avoiding the harsh $\sim 300^\circ\text{C}$ used in thermal inkjet printing.²⁰ In Figure 11a, we show a piece of paper printed solely with a 2.5 mM CPRG solution in MilliQ water that shows the pale yellow color of the material. We then printed a

solution of 500 nM β -gal in MilliQ water directly onto the same paper. In Figure 11b, we show that the enzyme does in fact survive the printing process as the paper changes color from yellow to purple as patterned. This result indicates that the enzyme survives the inkjet printing process and therefore can be incorporated as a component of the sensor.

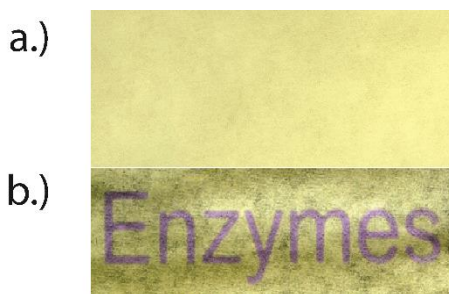


Figure 11 - a) Before and b) after printing β -gal onto a piece of paper that was preprinted with CPRG by using inkjet printing.

Precise patterning of the material is needed to produce a large uniform color change as well as ensure that the materials do not mix before immersion in the water. By creating different patterns such as spheres, checkerboards, and waves (Figure 12) but keeping both the CPRG and β -gal solution concentrations constant, we created 12 different test strips to optimize our design. To quantify the strip response, each sensor was digitally scanned using a Canon LiDE 210 desktop scanner to produce average CMY component values. As seen in Figure 13, multiple patterns showed a deep purple color when immersed, however, the small checker response showed the most consistent and highest response across the test strip surface. This visual interpretation is confirmed by graphing the color change measurements of a cross-section of each of the 12 strips both before and after immersion into water (Figure 14 and Figure 15). Therefore, we chose the small checker pattern for test strip construction (Figure 16). To better quantitate the mobility of the sensor components, we printed a simple line of both CPRG or

enzyme and immersed the strip into a solution of the opposite material. As shown in Figure 17, the CPRG substrate moves approximately 1 mm along the strip in both directions, but the printed enzyme does not move from where it was printed. This indicates that the sensor operates by the substrate moving over the enzyme complex. Given that the sensor works through the use of a water-soluble substrate, testing to ensure that the substrate does not leach out into the analyte solution. Even after leaving the sensor in an analyte solution for 5 minutes, very little substrate was seen photometrically coming off of the strip (Table 1).

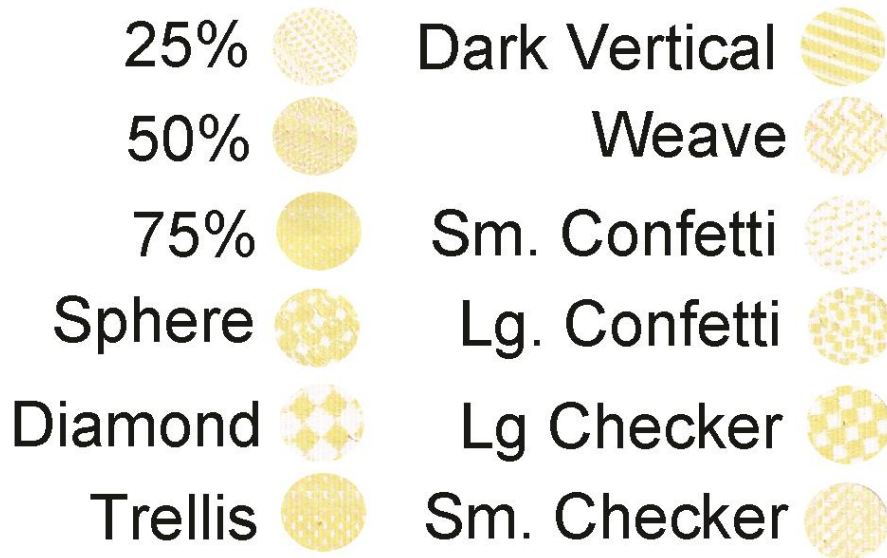


Figure 12 - Representative patterned strips before immersion.

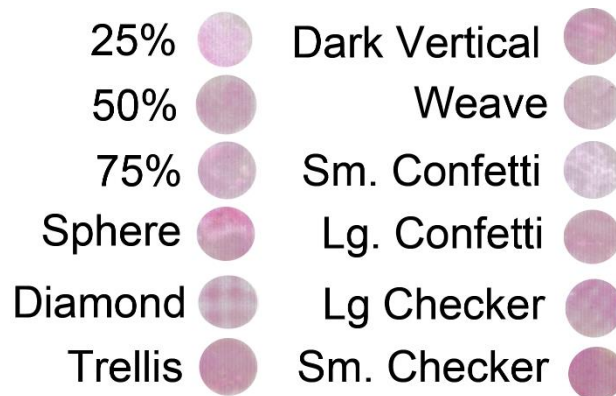


Figure 13 - Colorimetric response of the patterned test strip after immersion in water

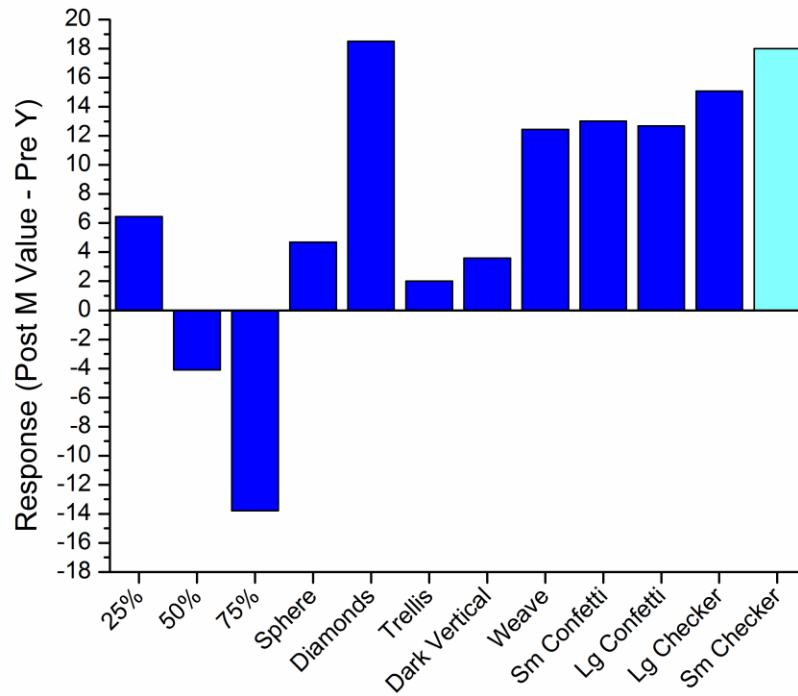


Figure 14 - Change in color response of the 12 sensor patterns after immersion.

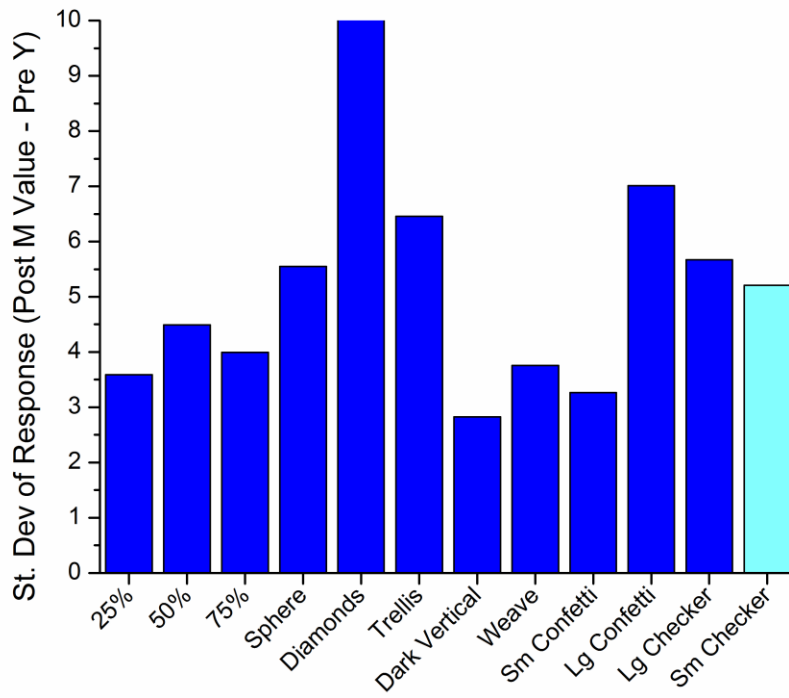


Figure 15 - Variance in the color change of the 12 sensor designs.



Figure 16 - Checkboard pattern used in Microsoft PowerPoint to generate the test strip functionality

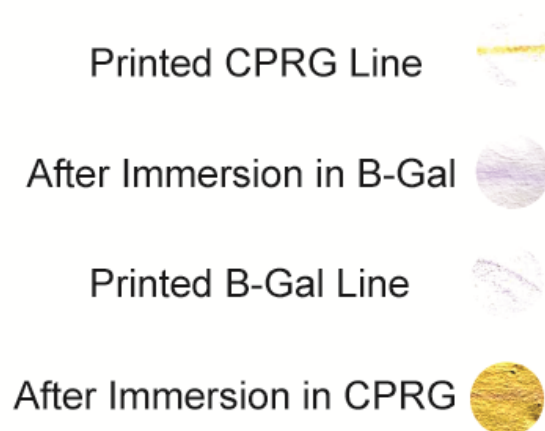


Figure 17 - Motility experiments of both substrate and enzyme along the paper substrate.

<u>Solution</u>	<u>Absorbance at 595 nm</u>
Control (No Strip)	.07±.01
Strip Incubated Water	.08±.01

Table 1 - Absorbance values of the analyte solution after incubating with the sensor

The quantities of β -gal, AuNP, and CPRG were optimized to produce vivid sensor responses when incubated with bacteria. As the colorimetric response is based on how much of the substrate is processed by the enzyme, we first determined the response generated by varying quantities of β -gal and substrate. The solutions were inkjet printed in an alternating ~2 mm square checkerboard pattern to provide close proximity without intermixing. In

Figure 18, we show images of the various concentrations of substrate and enzyme printed onto W.B Mason Flagship paper and immersed in MilliQ water for 30 seconds. As the concentration of CPRG increases, the color change from yellow to purple is significantly enhanced. However,

this effect lessens at higher concentrations of CPRG, possibly due to enzyme aggregation. This visual interpretation can also be seen graphically by plotting the magenta response as shown in Figure 19. Given these results, we chose 500 nM β -gal and 2.5 mM CPRG as our testing amount as it provided the greatest color change within a reasonable 5 min time period.

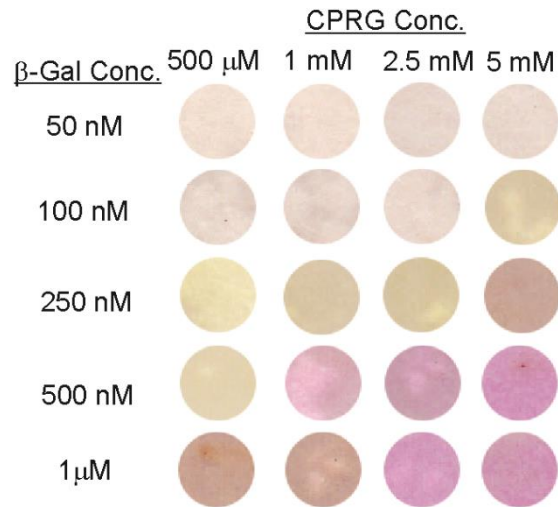


Figure 18 - Optimization matrix for the β -galactosidase and CPRG substrate components after 30 seconds of immersion in MilliQ water and 5 minutes of development time.

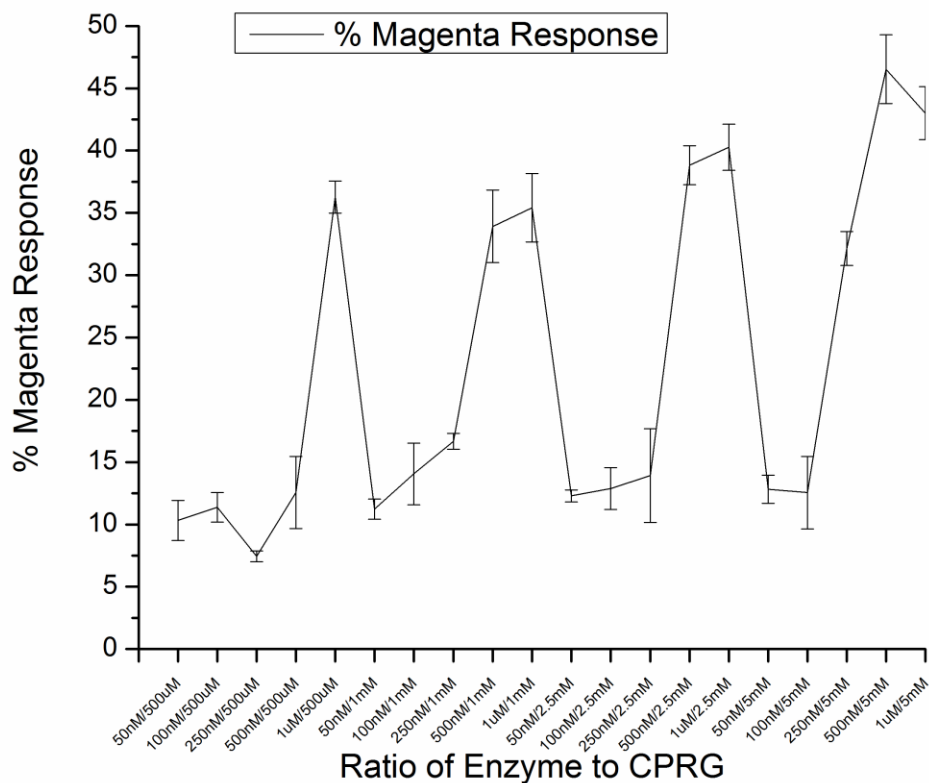


Figure 19 - Magenta response of the scanned test strips against the ratio of enzyme to printed CPRG. Error bars represent 6 measurements of each test strip.

Given the sensor depends on enzymes that can be altered by pH, we tested our NP-free strips to ensure durability against real world samples. To investigate, we dipped the strips into a range of MilliQ water buffered to a range of pH values to see at what level will the enzyme degrade, producing no colorimetric response. In Figure 20, the strips showed that the enzymes on the strip operate best between pH 5 and 7. To investigate further the range between pH 6.5 and 8.5 whose range is acceptable for drinking water, we used pH adjusted bottled water to more closely probe the response of the strip (Figure 21). These strips only showed a lower response

where the pH was above 8. This result indicates that while most water will be suitable for our sensor system, water with a high pH value will need pre-treatment for analysis.



Figure 20 - NP-free test strip response against pH buffered MilliQ water solutions.



Figure 21 - NP-free test strip response against pH buffered drinking water solutions at relevant pH levels.

The proper ratio of AuNP to β -gal was determined next. The β -gal enzyme must be properly inhibited before testing for bacteria, as uninhibited β -gal will process the substrate as if bacteria are present, providing a false positive. Premixed β -gal/AuNP solutions were inkjet printed alongside the 2.5 mM CPRG substrate. The strips were then tested in MilliQ water to see if any change in color was apparent. As shown in

Figure 22, ratios below 1:8 enzyme to particle showed incomplete inhibition of the particle generating a purple color. While the 1:8 enzyme to particle test strip had only a slight color change when immersed into water, the 1:10 ratio showed no visible change at all and therefore was selected for further use in this study. This result is quantitatively shown by graphing the magenta response against AuNP equivalents, showing a plateau of response around 10 equivalents of AuNPs (Figure 23).

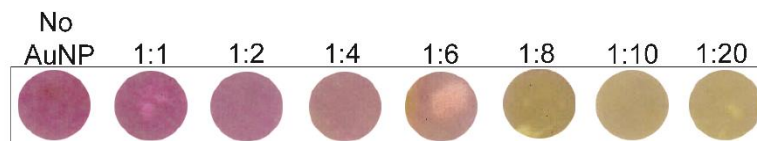


Figure 22 - Ratios of AuNP/ β -gal to test the inhibition concentration for the test strips after 30 seconds of immersion in MilliQ water and 5 minutes of development time.

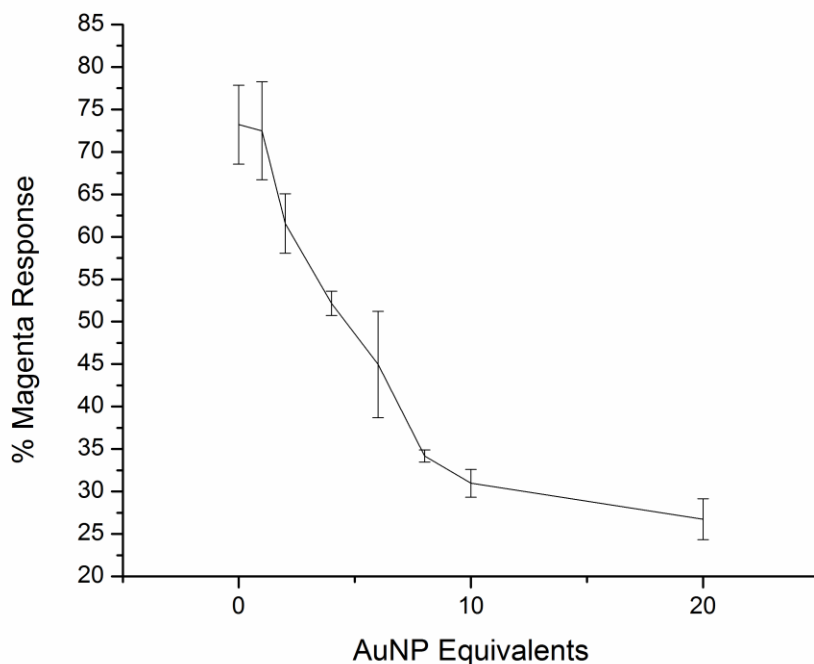


Figure 23 - Magenta response against the amount of AuNPs equivalents needed to inhibit the enzyme. Error bars represent 6 measurements of each test strip.

We immersed the printed strips into various concentrations of both Gram-negative (*E. coli* XL1) and Gram-positive (*Bacillus subtilis*) bacteria to test the sensitivity of the printed strips. As seen in Figure 24a from data from Table 2, Table 3, and Table 4, visible changes in color were observed for *E. coli* XL1 down to 10^2 bacteria mL^{-1} (cfu) 5 min after dipping. Similar behavior was seen in test strips immersed in the *Bacillus subtilis* (*B. subtilis*) bacteria). As seen in Figure 24b from data from Table 2, Table 3, and Table 4, plotting the magenta component value against bacteria concentrations clearly indicates that the strip used in the water contaminated with 10^3 cfu does show a color change similar to that seen at higher concentrations. These results indicate that these strips can detect bulk concentrations of bacteria whose output can be

determined visually. By adding a portable low-cost scanner, we have also shown that we can lower the limit of bacterial detection by analyzing the sensor response.

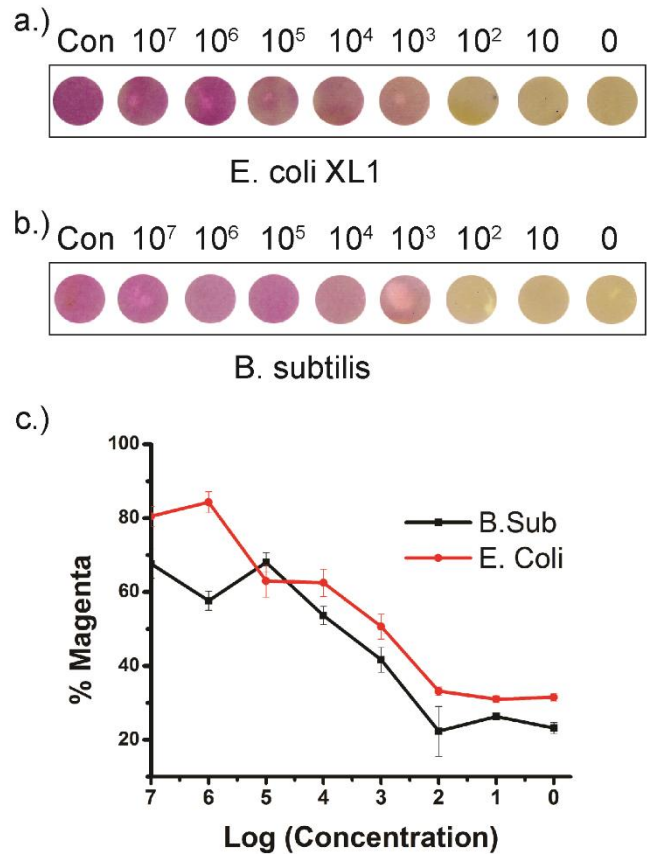


Figure 24 - Test-strip sensitivity in cfu against a) *E. coli* XL1 and b) *Bacillus subtilis*. The average magenta component values of the strips are plotted in c). Error bars represent 6 measurements of each test strip.

<u>Log</u> <u>(Concentration)</u>	<u>B. Sub</u>	<u>St Dev</u>	<u>E. Coli</u>	<u>St Dev</u>
7	28.5	1.64317	38.5	5.95819
6	25.6667	2.87518	35.8333	7.19491
5	27.5	0.83666	33.3333	3.26599
4	26.3333	1.50555	34.1667	1.94079
3	14.3333	8.4538	30	1.67332
2	19.1667	3.0605	30.6667	1.8619
1	23	1.26491	29.1667	0.75277
0	22.3333	1.63299	28.6667	1.63299

Table 2 - Cyan average percentages along with the standard deviation of 6 chosen spots taken from the scanned image of each test strip versus concentration of bacteria.

<u>Log</u> <u>(Concentration)</u>	<u>B. Sub</u>	<u>St Dev</u>	<u>E. Coli</u>	<u>St Dev</u>
7	67.6667	3.9833	80.5	2.73861
6	57.6667	2.58199	84.3333	2.80476
5	68	2.68328	63	4.38178

4	53.6667	2.50333	62.5	3.67423
3	41.6667	3.38625	50.6667	3.38625
2	22.3333	6.7429	33.1667	1.16905
1	26.3333	1.0328	31	0.89443
0	23.1667	1.47196	31.5	1.04881

Table 3 - Magenta average percentages along with the standard deviation of 6 chosen spots taken from the scanned image of each test strip versus concentration of bacteria.

<u>Log (Concentration)</u>	<u>B. Sub</u>	<u>St Dev</u>	<u>E. Coli</u>	<u>St Dev</u>
7	9.66667	2.50333	23.3333	3.32666
6	11.5	4.03733	14.1667	9.9482
5	9.5	3.44964	35.1667	4.70815
4	24.5	2.16795	38.6667	1.50555
3	26	8.31865	46.1667	1.47196
2	50.8333	1.94079	63	7.58947
1	51.3333	2.87518	63.5	2.25832
0	58.1667	2.99444	63.6667	3.26599

Table 4 - Yellow average percentages along with the standard deviation of 6 chosen spots taken from the scanned image of each test strip versus concentration of bacteria.

As bacteria can inherently generate β -gal,³⁰ a control experiment was done to investigate whether the native enzyme will impact test strip response. To test this impact, we incubated a test strip containing CPRG but no printed β -gal into both a clean MilliQ water solution and a concentrated (10^8 bacteria/mL) *E. coli* XL1 solution and scanned each for visual determination. As seen in Figure 25, the strip showed no colorimetric response after 30 seconds of immersion in the bacteria indicating that the native bacteria does not produce enough β -gal to interfere with sensor operation. However, it is important to note that other strains of bacteria do produce β -gal, so further sensor testing to determine total as well as fecal coliforms against a wider range of bacteria will be needed to address regulatory requirements.



Figure 25 - Visual comparison of test strips where β -gal was not printed between a strip immersed in MilliQ water (Left) and concentrated *E. coli* XL1 bacteria (Right)

Drinking water can also be contaminated with other materials that could affect the sensitivity of the paper based sensor. As drinking water can contain levels of sodium chloride as high as 5 mM that can interfere with the electrostatic behavior of our sensor system, we first tested our sensor system against varying levels of salt. In Figure 26 from data from Table 5, Table 6, and Table 7, we show that at concentrations above 150 mM the sensor generates a strong visual false positive for high concentrations of bacteria. By scanning these test strips, we were able to graphically show in Figure 26 that the salt affects the response at concentrations >25 mM, a

level five times higher than the highest acceptable salt standard for drinking water as well as higher than 10mM that can be detected by human taste.³¹ Therefore, these strips will not be affected by the ionic strength of normal drinking water.

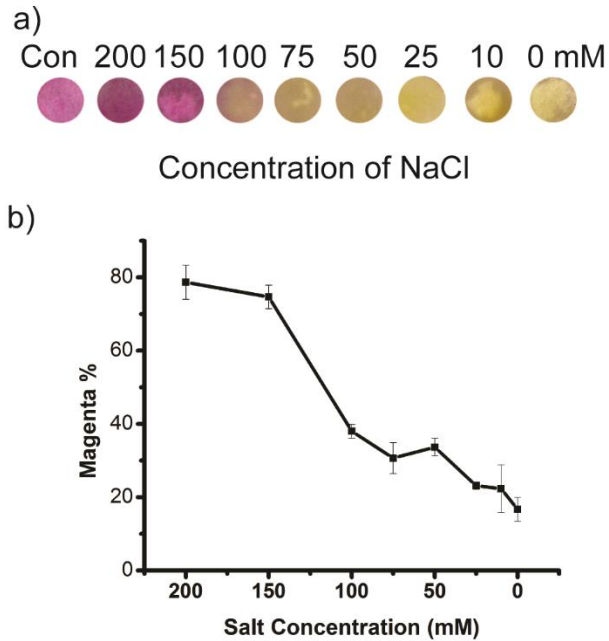


Figure 26 - a) Visual and b) graphical response of our test strips to various concentrations of sodium chloride in water. Error bars represent 6 measurements of each test strip.

<u>Concentration</u>	<u>% Cyan</u>	<u>St Dev</u>
200	40.1667	0.98319
150	26.3333	5.20256
100	27.6667	1.21106
75	26.8333	2.99444

50	28.5	1.51658
25	21.1666	1.329
10	21.6667	6.121
0	14.3333	2.80476

Table 5 - Cyan average percentages along with the standard deviation of 6 chosen spots taken from the scanned image of each test strip versus salt concentration.

<u>Concentration</u>	<u>% Magenta</u>	<u>St Dev</u>
200	78.6667	4.67618
150	74.6667	3.20416
100	38	1.89737
75	30.6667	4.2269
50	33.6667	2.42212
25	23.1667	.983192
10	22.3333	6.53197
0	16.6667	3.26599

Table 6 - Magenta average percentages along with the standard deviation of 6 chosen spots taken from the scanned image of each test strip versus salt concentration.

<u>Concentration</u>	<u>%</u>	
	<u>Yellow</u>	<u>St Dev</u>
200	28.6667	3.55903
150	16	8.50882
100	53.5	4.72229
75	63	5.32917
50	61.3333	4.17931
25	65.5	6.156
10	78.6667	9.75021
0	53.5	3.61939

Table 7 - Yellow average percentages along with the standard deviation of 6 chosen spots taken from the scanned image of each test strip versus salt concentration.

We also investigated the effect of 6 different chemicals found in heavily contaminated water that have been shown to inhibit the β -gal enzyme (Table 8). In these cases, high concentrations of contaminants will not allow the strip to change color, showing a clean water result when the sample is anything but safe. To test the impact of contaminants on the strip, water containing high concentrations of bacteria was spiked with water containing cadmium, lead, copper, zinc,

sulfate, and sodium dodecyl sulfate and allowed to mix. After 5 minutes, the strips were immersed to note the visible change between water contaminated with simply bacteria and samples contaminated with metal and bacteria. As seen in Table 8, only cadmium and copper showed any degradation due to the added metal. Furthermore, the amounts of these contaminants needed to cause changes to the strip far exceed the highest acceptable values for drinking water.³²

<u>Metal Used</u>	<u>Inhibition Concentration</u>	<u>Maximum Acceptable Concentration for Drinking Water</u>
Copper	5 mg/mL	1.3 mg/mL
Lead	>20000 ppb	15 ppb
Zinc	>20000 ppm	20 ppm
Cadmium	5 mg/mL	.005 mg/mL
Sulfate	>1 g/L	250 mg/L
Sodium Dodecyl Sulfate	>4 mg/L	1.0 mg/L

Table 8 - Concentrations at which the test strips respond to several common water contaminants as well as the current water regulations for that. Note that the maximum sodium dodecyl sulfate level is for all foaming agents in water and is not specific for this chemical.

Materials and Methods

The β -galactosidase was purchased from Sigma Aldrich and used without purification. The CPRG substrate was purchased from Roche Analytical and used as purchased. Sodium chloride (NaCl), lead, cadmium, copper, zinc, sodium sulfate, and sodium dodecyl sulfate were purchased from Fisher Scientific. Gold nanoparticles with the attached ligand were synthesized in a two-step method. This entailed the preparation of pentanethiol stabilized nanoparticles with a core size of approximately 2.5 nm using the Brust method followed by a ligand exchange reaction.^{33,34} The

TTMA ligand was synthesized according to previous methods.⁸ Before printing, the nanoparticles, CPRG, and enzymes were filtered through a 0.2 μm polypropylene membrane (Puradisc 25AS, Whatman) and syringed into a virgin aftermarket Epson inkjet cartridge for printing (MIS Associates, Auburn Hills, MI USA). Inkjet printing was done using an Epson Artisan 50 inkjet printer.

Test Strip Procedure

Paper test strips were immersed into the analyte solution for 30 seconds and removed for drying. In the case of the drinking water studies, Poland Springs bottled water was used and adjusted as needed. After 5 minutes, the strips were evaluated both visually and by use of a scanner. 6 CMYK values for each test strip were obtained from the scanned images through the use of Adobe Photoshop and averaged to generate the colorimetric response. The K value was shown to be negligible in all readings and therefore is not reported.

Sensor Construction and Storage

The paper substrate was placed into the standard paper feed of the printer. For our work, patterning was done through the use of Microsoft PowerPoint software. A large checkerboard square pattern with two alternating materials was created to maximize the amount of sensors printed on each paper. In order to print only the channel of interest, the color of the letter has to match the channel printed. To print only the magenta channel, the RGB value must be set to (255,0,255). For cyan channel printing, (0,255,255) must be used and for yellow channel (255,255,0) must be used. The image color management (ICM) also must be turned off in the Advanced tab of the printer properties to ensure no mixing of the channels occurs. Before printing, the print heads were cleaned two times using the “Head Cleaning” function in the

Maintenance tab of the printer properties to ensure that the channels were filled. After printing, the sensor sheet was cut into small circles through the use of a standard hole punch and glued onto a 1 cm by 4 cm strip of card stock paper to provide rigidity to the sensor. Completed strips were kept refrigerated for up to week before being used in our study.

Profile Image Analysis

To quantitatively investigate the change in color across the sensor strip, one scanned strip image per pattern was analyzed using ImageJ software. By taking a representative 70 pixels of the image, a RGB Profile Plot was generated whose RGB values were converted to CMY color space. To compare the color response from pattern to pattern, we took the average yellow response of the strip before immersion and subtracted it from the average magenta response after dipping. Figure 14 shows that the small checker is as good as the diamond pattern but better than any of the other sensor designs. To quantify heterogeneity, we graphed the standard deviation of responses across the sensor surface. Figure 15 shows that the diamond pattern has by far the highest variation across the surface of all patterned surfaces. Taking these two graphs together indicates that the small checker pattern is the best to use for our system.

CPRG Leaching Analysis

To quantitate the amount of CPRG that could possibly leach out into the analyte mixture, we incubated a completed test strip with 50 μ L of MilliQ water. After five minutes, the strip was removed and 50 μ L of a 0.5 nM β -galactosidase solution was added to the solution. The solution was incubated for 5 minutes and the color change was assessed at the 595 nm wavelength similar to our previous work¹. A control solution was also analyzed containing enzyme and

MilliQ water. Visually, both solutions appeared clear and no significant difference was seen in the absorbance values.

Bacteria Culturing

Strains of both Escherichia coli (E. coli XL1 Blue; Gram-negative) and Bacillus subtilis (B. subtilis; Gram-positive) bacteria were cultured in lysogeny broth (LB) growth medium and successively washed via centrifugation with 5 mM PBS (pH 7.4). Both samples of each bacteria were adjusted to an OD of 1.0 at the 600nm wavelength, which relates to $\sim 10^8$ bacteria/mL. These bacteria were used within 48 hours after purification to ensure a viable sample.

Conclusions

In summary, we have created a printable paper-based sensor for the rapid determination of concentration/presence of bacteria in water. By using inkjet printing, we can create inexpensive water monitors that can be read and interpreted by untrained people simply by visual inspection. Further real world testing of these strips, especially using contaminated water sources will, however, be required for implementation of this strategy. Furthermore, this system shows the potential for creating other enzyme/substrate systems by co-printing the components using inkjet printing, with potential impacts in environmental, laboratory, and biomedical science as a whole. However, the stability of these systems has to be addressed as one week of stability in a refrigerated environment is not useful for out of laboratory usage. We will look into the use of artificial enzymes in Chapter 4, albeit for protein sensing.

Notes

[1] Kindhauser, M. K. Communicable Diseases 2002. World Health Organization, Geneva, **2003**.

[2] Kim, J. H.; Grant, S. B. *Environ. Sci. Technol.* **2004**, *38*, 2497.

- [3] Oleniaz, W. S.; Pisano, M. A.; Rosenfeld, M. H.; Elgart, R. L. *Environ. Sci. Technol.* **1968**, *2*, 1030.
- [4] Frischer, M. E.; Danforth, J. M.; Foy, T. F.; Juraske, R. J. *Environ. Qual.* **2005**, *34*, 1328.
- [5] Pineda, F. J.; Lin, J. S.; Fenselau, C.; Demirev, P. A. *Anal. Chem.* **2000**, *72*, 3739.
- [6] Yeh, Y.-C.; Creran, B.; Rotello, V. M. *Nanoscale*, **2012**, *4*, 1871.
- [7] Chung, H. J.; Castro, C. M.; Im, H.; Lee, H.; Weissleder, R. *Nat. Nanotechnol.* **2013**, *8*, 369.
- [8] You, C. C.; Miranda, O. R.; Gider, B.; Ghosh, P. S.; Kim, I. B.; Erdogan, B.; Krovi, S. A.; Bunz, U. H. F.; Rotello, V. M. *Nat. Nanotechnol.* **2007**, *2*, 318.
- [9] Bajaj, A.; Miranda, O. R.; Kim, I. B.; Phillips, R. L.; Jerry, D. J.; Bunz, U. H. F.; Rotello, V. M. *Proc. Natl. Acad. Sci. U. S. A.* **2009**, *106*, 10912.
- [10] Shawky, S. M.; Bald, D.; Azzazy, H. M. E. *Clin. Biochem.* **2010**, *43*, 1163.
- [11] Phillips, R. L.; Miranda, O. R.; You, C. C.; Rotello, V. M.; Bunz, U. H. F. *Angew. Chem.* **2008**, *120*, 2628.
- [12] Zhao, W.; Brook, M. A.; Li, Y. F. *ChemBioChem* **2008**, *9*, 2363.
- [13] Halkos, G. E.; Tzeremes, N. G. *Annu. Rev. Microbiol.* **2001**, *55*, 201.
- [14] Yetisen, A. K.; Akram, M. S.; Lowe, C. R. *Lab Chip*, **2013**, *13*, 2210.
- [15] Cao, X. D.; Ye, Y. K.; Liu, S. Q. *Anal. Biochem.* **2011**, *417*, 1.

- [16] Baldrich, E.; Vignes, N.; Mas, J.; Munoz, F. X. *Anal. Biochem.* **2008**, *383*, 68.
- [17] Then, W. L.; Garnier, G. *Rev. Anal. Chem.*, **2013**, *32*, 269.
- [18] Parolo, C.; de la Escosura-Muniz, C. A.; Merkoci, A. *Biosens. Bioelectron.* **2012**, *40*, 412.
- [19] Miranda, O. R.; Li, X.; Garcia-Gonzalez, L.; Zhu, Z.-J.; Yan, B.; Bunz, U. H. F.; Rotello, V. M. *J. Am. Chem. Soc.* **2011**, *133*, 9650.
- [20] Komuro, N.; Takaki, S.; Suzuki, K.; Citterio, D. *Anal. Bioanal. Chem.* **2013**, *405*, 5785.
- [21] de Gans, B. J.; Duineveld, P. C.; Schubert, U. S. *Adv. Mater.* **2004**, *16*, 203.
- [22] Tekin, E.; Smith, P. J.; Schubert, U. S. *Soft Matter* **2008**, *4*, 703.
- [23] Derby, B. J. *Mater. Chem.* **2008**, *18*, 5717-5721.
- [24] Creran, B.; Yan, B.; Moyano, D. F.; Gilbert, M. M.; Vachet, R. W.; Rotello, V. M. *Chem. Commun.* **2012**, *48*, 4543.
- [25] Setti, L.; Fraleoni-Morgera, A.; Mencarelli, I.; Filippini, A.; Ballarin, B.; Di Biase, M. *Sens Actuators B* **2007**, *126*, 252.
- [26] Setti, L.; Fraleoni-Morgera, A.; Ballarin, B.; Filippini, A.; Frascaro, D.; Piana, C. *Biosens. Bioelectron.* **2005**, *20*, 2019.
- [27] Hossain, S. M. Z.; Luckham, R. E.; Smith, A. M.; Lebert, J. M.; Davies, L. M.; Pelton, R. H.; Filipe, C.D.M.; Brennan, J.D. *Anal. Chem.* **2009**, *81*, 5474.

- [28] Hossain, S. M. Z.; Luckham, R. E.; McFadden, M. J.; Brennan, J. D. *Anal. Chem.* **2009**, *81*, 9055.
- [29] Nishioka, G. M.; Markey, A. A.; Holloway, C. K. *J. Chem. Soc., Chem.* **2004**, *126*, 16320-16321.
- [30] Griffith, K. L.; Wolf, R.E. *Biochem. Biophys. Res. Commun.* **2002**, *290*, 397.
- [31] Rabin, M.; Poli de Figueiredo, C. E.; Wagner, M. B.; Antonello, I. C. *Appetite* **2009**, *52*, 609.
- [32] Drinking Water Contaminates <http://water.epa.gov/drink/contaminants/> (Accessed 6/24/14).
- [33] Brust, M.; Walker, Bethell, D.; Schiffrin, D. J.; Whyman, R. *J. Chem. Soc., Chem.*, **1994**, 801.
- [34] Hostetler, M. J.; Templeton, A. C.; Murray, R. W. *Langmuir*, **1999**, *15*, 3782-3789.

CHAPTER 4

COLORIMETRIC PROTEIN SENSING USING CATALYTICALLY AMPLIFIED SENSOR ARRAYS

Introduction

The detection of proteins at low concentrations is of critical importance in allergy testing,^{1, 2} clinical treatment,^{3, 4} and early diagnosis of many diseases,^{5, 6} requiring development of fast, sensitive, and cost-effective protein sensors aimed at point-of-care applications. Among these sensors, colorimetric methods provide both enhanced instrumental transduction as well as the potential for direct visual readout.⁷ For example, the clearly distinguished color shifts resulting from controllable aggregation of gold nanoparticles have facilitated simple color readout for biosensor applications.⁸

Array-based sensing uses differential binding interactions with an array of selective receptors, providing an alternative to small molecule⁹/biomarker¹⁰ detection. Colorimetric implementation of this methodology has created highly effective small molecule sensors that have been applied to a variety of important analytes.¹¹ Application of colorimetric methods to array-based sensing of biomolecules is challenging, however, due to the low concentrations of these materials relative to the amount of signal required for colorimetric transduction.¹² In recent studies we have used enzyme amplification for colorimetric detection of bacteria.¹³ While enzyme-based amplification processes are attractive, protein stability under transport and storage conditions limits the application of this strategy to highly controlled environments.¹⁴

Synthetic enzyme mimics¹⁵ such as macromolecular complexes,¹⁶ iron oxide nanoparticles,¹⁷ and cerium oxide nanoparticles^{18,19} feature higher stability than enzymes over a wide range of pH levels and temperatures. The ability of these mimics to catalytically amplify responses has made them useful for biosensing. For instance, Fe₃O₄ NPs that mimic horseradish peroxidase (HRP)

activity have been used to replace HRP in traditional immunoassay techniques^{17, 20} and to achieve label-free detection of nucleic acids.²¹ We report here the extension of this approach to array-based sensing of proteins, with Fe₃O₄ NPs serving as both recognition and recognition elements for highly sensitive (50 nM) detection and identification of proteins.

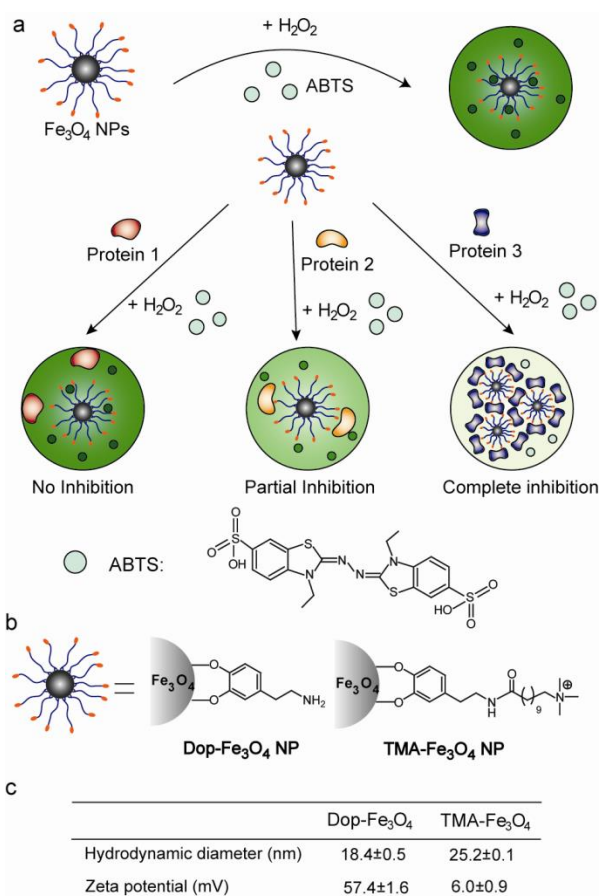


Figure 27 - a. Illustration of the Fe₃O₄ NP enzyme mimetic amplified colorimetric sensing of proteins. b. Structures of Dop-Fe₃O₄ and TMA-Fe₃O₄. c. Hydrodynamic diameter and zeta potential of Fe₃O₄ NPs in 5 mM CH₃COONa buffer at pH 5.0.

Results and Discussion

For our sensing studies, dopamine functionalized Fe_3O_4 NP (Dop- Fe_3O_4 NP) and trimethylammonium functionalized Fe_3O_4 NP (TMA- Fe_3O_4 NP) were fabricated (Figure 27b-c). Profile generation with these particles arises from differential interactions of these particles with analyte proteins with concomitant alteration in catalytic efficiency (Figure 27a). Signal generation was provided by the Fe_3O_4 NP-catalyzed oxidation of colorless 2,2'-azino-bis(3-ethylbenzothiazoline-6-sulfonic acid) (ABTS), to a green product in the presence of hydrogen peroxide (H_2O_2).

Initial studies focused on optimizing the sensor response. An effective chromogenic response was observed using 25 $\mu\text{g}/\text{mL}$ Fe_3O_4 NP with 2.5 mM H_2O_2 and 1 mM ABTS in 5 mM sodium acetate (CH_3COONa) buffer (pH 5.0). Changes in NP activity were then determined using two model proteins, lipase and lysozyme (Figure 28). In the case of lipase, a dramatic drop in reaction rate was observed, with complete inhibition observed at higher concentrations (50 nM, Figure 28). By contrast, lysozyme did not significantly affect the colorimetric reaction up to a concentration of 100 nM (Figure 28b). The mechanism for protein differentiation was probed by dynamic light scattering (DLS) measurements of the protein-NP complexes using 10-fold higher concentration of particle and protein to provide reliable DLS signals. Lipase-NP complexes formed large aggregates with both Fe_3O_4 NPs (Figure 28a inset), consistent with the large change in activity observed. In contrast, no significant changes in particle size were observed after incubation with lysozyme (Figure 28b inset).

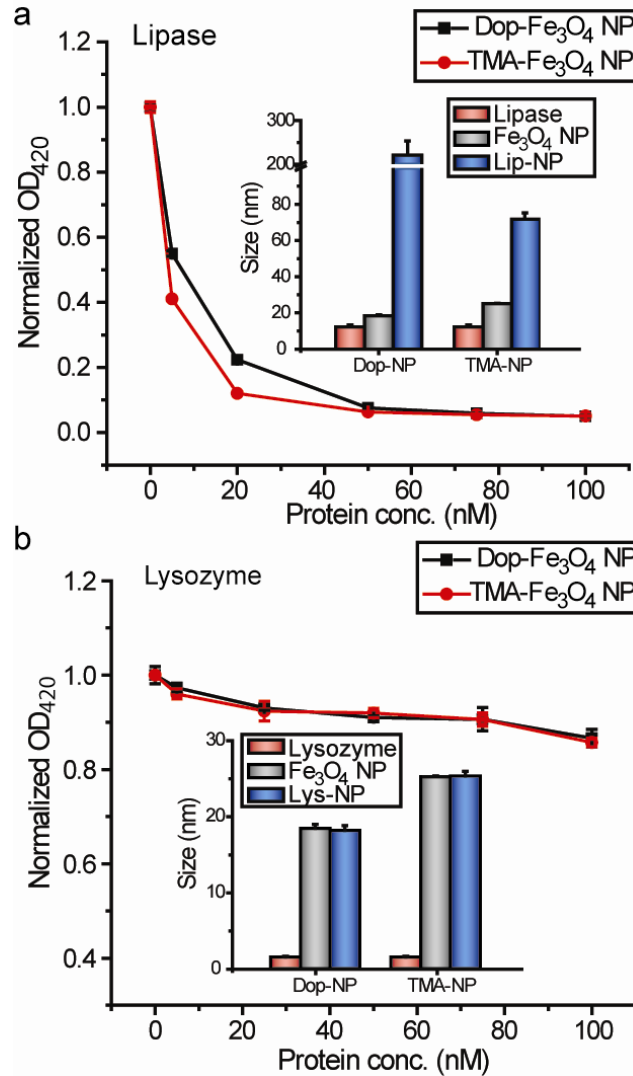


Figure 28 - Normalized OD at 420 nm upon protein addition with fixed NPs concentration (25 µg/mL). a. Concentration dependent OD curve of lipase. Inset is the hydrodynamic diameter of functionalized Fe₃O₄ NPs and lipase-NP complexes. b. Normalized OD curve of lysozyme with modest permutation. Inset: hydrodynamic diameter of functionalized Fe₃O₄ NPs and lysozyme-NP complexes. Results are average of three measurements and error bars are standard deviation. The NP concentration used in the size measurement is 250 µg/mL and the protein is at a concentration of 500 nM.

Protein	MW (kDa)	pI
α -amylase (α -Am)	50	5.0
bovine serum albumin (BSA)	66.3	4.8
α -chymotrypsin (ChT)	25	8.7
cytochrome c (CytC)	12.3	10.7
transferrin (Tf)	76	5.9
human serum albumin (HSA)	69.4	5.2
lipase (Lip)	58	5.6
lysozyme (Lys)	14.4	11.0
myoglobin (Myo)	17	7.2
alkaline phosphatase (PhosB)	140	5.7

Table 9 - Physical properties of protein analytes.

Sensing of individual analytes in isolation provides a testbed for array-based sensors, providing insight into their ability to detect small changes in analyte structure. The ability of our sensor to discriminate proteins was tested using ten proteins featuring varying size and charge (Table 9). In the procedure, each protein solution was first mixed with NP (25 μ g/mL) to a final protein concentration of 50 nM and incubated at room temperature for 30 minutes followed by the addition of H₂O₂ (2.5 mM) and ABTS (1 mM). After 15 minutes of incubation at room

temperature, OD responses (OD/OD_0 , where OD_0 is a control without addition of protein) at 420 nm were monitored.

As displayed in Figure 29b, the two particle sensor array generated a range of outputs.²² As a general trend, proteins possessing lower pIs (α -Am, BSA, HSA, Lip) exhibited relatively stronger inhibition of the NP activity than those with higher pIs (Lys, CytC, ChT, Myo), indicating surface charge plays an important role in discrimination. Proteins with similar pIs also gave different signal patterns, however, indicating that protein size and surface hydrophobicity also play a role in protein-NP interactions. Each protein can be reproducibly discerned by the OD response patterns. The pattern differences among analytes can be easily detected even by the naked eye (Figure 29a).

Linear discriminant analysis (LDA) was employed to quantitatively differentiate the OD response patterns of the Fe_3O_4 NPs with proteins. All five replicates of the ten proteins are grouped with 100% accuracy according to the jackknifed classification matrix, and scores of the two factors are plotted with 95% confidence ellipses (Figure 29c). In the canonical score plot, the distribution of analyte clusters along the factor 1 axis primarily reflects the OD/OD_0 value. The individual response from each of the elements provides reasonable differentiation: TMA- Fe_3O_4 NP itself can differentiate the ten proteins with 90% accuracy and Dop- Fe_3O_4 NP with 78%. It is noteworthy that by the use of only two modified Fe_3O_4 NPs, the sensor can detect and identify ten proteins rapidly and effectively. The detection efficiency was further validated by the identification of unknown samples using the training set in Figure 29 with 95% accuracy (76 of 80) (Table 10).

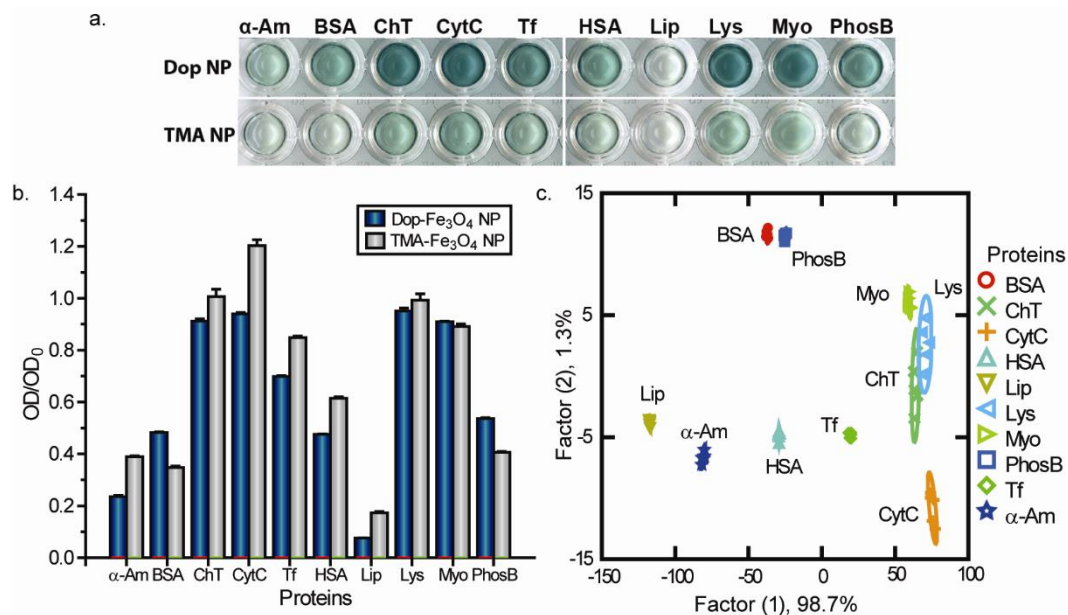


Figure 29 - Array-based sensing of ten proteins. **a.** Photograph of the color change upon addition of protein solutions at 50 nM. **b.** OD response (OD/OD₀ at 420 nm) patterns in the presence of proteins at 50 nM (responses are an average of five measurements and the error bars are the standard deviation). **c.** Canonical score plot for the OD response patterns as obtained from LDA with 95% confidence ellipses.

Entry	Absorbance response pattern (OD/OD ₀)		Identification	Accuracy
	Dop-NP	TMA-NP		
1	0.21	0.40	α -Am	Yes
2	0.48	0.62	HSA	Yes
3	0.46	0.32	BSA	Yes
4	0.95	1.06	Lys	Yes
5	0.92	1.26	CytC	Yes
6	0.93	1.36	CytC	NO
7	0.90	1.06	ChT	Yes
8	0.54	0.44	PhosB	Yes
9	0.08	0.18	Lip	Yes
10	0.71	0.87	Tf	Yes
11	0.55	0.43	PhosB	Yes
12	0.89	1.04	ChT	Yes
13	0.91	0.84	Myo	Yes
14	0.70	0.91	Tf	Yes
15	0.22	0.39	α -Am	Yes
16	0.48	0.63	HSA	Yes

17	0.97	1.05	Lys	Yes
18	0.46	0.33	BSA	Yes
19	0.95	1.28	CytC	Yes
20	0.08	0.17	Lip	Yes
21	0.97	1.36	CytC	Yes
22	0.08	0.17	Lip	Yes
23	0.47	0.37	BSA	Yes
24	0.53	0.43	PhosB	Yes
25	0.88	1.01	ChT	Yes
26	0.68	0.87	Tf	Yes
27	0.21	0.40	α -Am	Yes
28	0.46	0.61	HSA	Yes
29	0.86	0.82	Myo	Yes
30	0.93	1.04	ChT	NO
31	0.70	0.87	Tf	Yes
32	0.97	0.97	Lys	Yes
33	0.47	0.63	HSA	Yes
34	0.86	1.03	ChT	Yes
35	0.91	1.27	CytC	Yes
36	0.47	0.34	BSA	Yes
37	0.90	0.89	Myo	Yes
38	0.08	0.17	Lip	Yes
39	0.21	0.38	α -Am	Yes
40	0.52	0.42	PhosB	Yes
41	0.21	0.39	α -Am	Yes
42	0.92	0.86	Myo	Yes
43	0.08	0.17	Lip	Yes
44	0.70	0.85	Tf	Yes
45	0.95	1.02	Lys	Yes
46	0.43	0.63	HSA	Yes
47	0.94	1.25	CytC	Yes
48	0.49	0.41	BSA	NO
49	0.46	0.38	BSA	Yes
50	0.86	1.00	ChT	Yes
51	0.08	0.17	Lip	Yes
52	0.94	1.04	Lys	Yes
53	0.21	0.37	α -Am	Yes
54	0.53	0.41	PhosB	Yes
55	0.45	0.36	BSA	Yes
56	0.89	1.01	ChT	Yes
57	0.91	0.82	Myo	Yes
58	0.67	0.85	Tf	Yes

59	0.91	1.25	CytC	Yes
60	0.46	0.61	HSA	Yes
61	0.48	0.61	HSA	Yes
62	0.41	0.31	BSA	Yes
63	0.91	0.85	Myo	Yes
64	0.68	0.85	Tf	Yes
65	0.89	0.99	ChT	Yes
66	0.52	0.42	PhosB	Yes
67	0.21	0.38	α -Am	Yes
68	0.07	0.17	Lip	Yes
69	0.92	1.03	ChT	NO
70	0.92	1.24	CytC	Yes
71	0.99	1.26	CytC	Yes
72	0.86	0.84	Myo	Yes
73	0.21	0.38	α -Am	Yes
74	0.48	0.62	HSA	Yes
75	0.92	1.04	ChT	Yes
76	0.07	0.18	Lip	Yes
77	0.54	0.43	PhosB	Yes
78	0.46	0.36	BSA	Yes
79	0.68	0.85	Tf	Yes
80	0.95	1.07	Lys	Yes

Table 10 - Identification of 80 unknown protein samples with LDA using Fe₃O₄ NP sensor array.

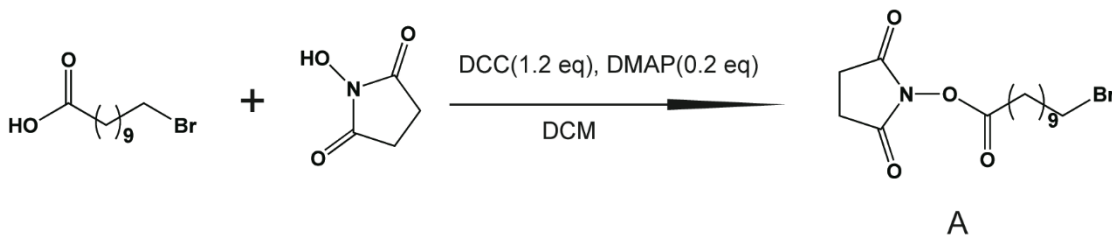
Materials and Methods

Synthesis of dopamine functionalized Fe₃O₄ NP (Dop-Fe₃O₄ NP). Water-dispersible Dop-Fe₃O₄ NPs were synthesized and purified according to literature.²³ In the general process, FeCl₂•4H₂O (99.4 mg, 0.5 mmol), FeCl₃•6H₂O (270.3 mg, 1mmol), and 20 g of diethylene glycol (DEG) were added to a nitrogen-protected three-necked flask. A solution of NaOH (160 mg, 4 mmol) in 20 g DEG was then added to the flask. The mixture was heated for 2 h at 220 °C. At the end of heating, a mixture of 3-hydroxytyramine hydrochloride (189 mg, 1 mmol) in 400 μ L of H₂O and 5 g of DEG was injected into the flask. After cooling to room temperature (r.t.), the solid product

was isolated by centrifugation and washed five times with ethanol and finally redispersed in water.

Synthesis of dopamine trimethyl ammonium (DTMA) ligand.

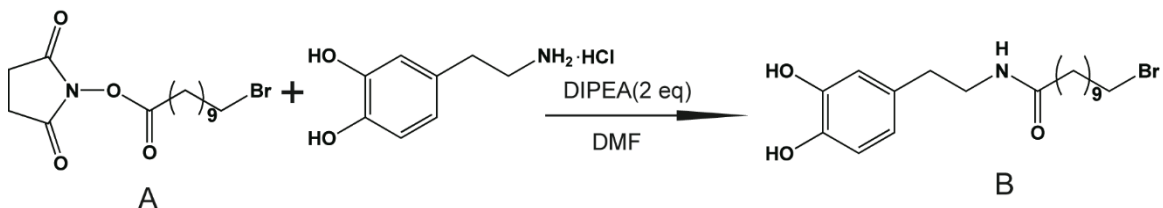
Step 1.



1-Bromoundecanoic acid (500 mg, 1.88 mmol) was dissolved in dry DCM. To this solution N-hydroxysuccinimide (216 mg, 1.88 mmol) was added followed by a solution of DCC (456 mg, 2.26 mmol) in 5 mL of dry DCM at 0 °C. The mixture was stirred for 15 min, and then DMAP (46 mg, 0.38 mmol) was added. After 1 h the reaction was allowed to reach r.t.. A white precipitate formed indicating the advancement of the reaction. The reaction was continued for 24 h. The white precipitate was filtered and the solvent was removed from the filtrate to give a residue that was then re-dissolved in DCM and washed with water. The organic layer was dried over Na₂SO₄, filtered and evaporated and the crude product obtained was purified by flash chromatography with 3:1 hexanes:EtOAc as eluent to give the activated acid in 90 % yield.

¹H NMR (400 MHz, CDCl₃): 1.24-1.42 (m, 12H, CH₂); 1.56 (m, 2H, CH₂); 1.77 (m, 2H, CH₂); 2.25 (t, 2H, CH₂); 2.72 (t, 4H, CH₂); 3.31(t, 2H, CH₂)

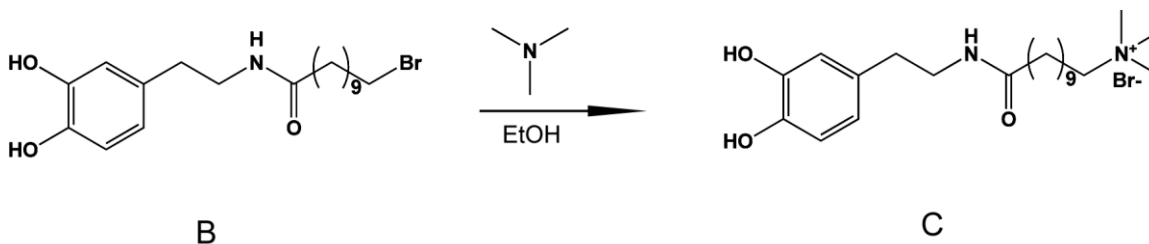
Step 2.



3-Hydroxytyramine hydrochloride (356mg, 1.88mmol) was dissolved in dry DMF and the solution was purged for 10 min with nitrogen gas. DIPEA (507mg, 3.76 mmol) was slowly added to the reaction mixture. The mixture was stirred for another 5 min and then compound A (670mg, 1.18 mmol) was added to the reaction mixture. The mixture was stirred at r.t. for 64 h. After that the DMF was evaporated under reduced pressure. The residue was dissolved in ethyl acetate. The soluble part was taken out and washed with 1M HCl and brine water. The organic component was dried over Na_2SO_4 and evaporated to get the crude product. The crude product obtained was purified by flash chromatography with 3:1 EtOAc:hexanes as eluent to give the activated acid in 55 % yield.

$^1\text{H NMR}$ (400 MHz, CDCl_3): 1.24-1.42 (m, 12H, CH_2); 1.56 (m, 2H, CH_2); 1.81 (m, 2H, CH_2); 2.18 (t, 2H, CH_2); 2.65 (t, 2H, CH_2); 3.31 (t, 2H, CH_2); 3.55 (t, 2H, CH_2); 6.42 (d, 1H, H_{arom}); 6.66-6.74 (m, 2H, H_{arom})

Step 3.



Compound B (230 mg, 0.59 mmol) and trimethylamine (696 mg, 11.8 mmol) were dissolved in 1 mL of EtOH. The solution was degassed with nitrogen gas. The reaction mixture was stirred at r.t. for 64 h and then the solvent was evaporated under vacuum. The residue was purified by washing with hexane and ether several times to obtain C in 99% yield.

$^1\text{H NMR}$ (400 MHz, MeOD): 1.24-1.42 (m, 12H, CH_2); 1.56 (m, 2H, CH_2); 1.81 (m, 2H, CH_2); 2.18 (t, 2H, CH_2); 2.78 (t, 2H, CH_2); 3.19 (s, 9H, CH_3); 3.31 (t, 2H, CH_2); 3.55 (t, 2H, CH_2); 6.42 (d, 1H, H_{arom}); 6.66-6.74 (m, 2H, H_{arom})

Synthesis of trimethyl ammonium functionalized Fe_3O_4 NP (TMA- Fe_3O_4 NP). Sun's method²⁴ was used to obtain 4-nm Fe_3O_4 NPs. $\text{Fe}(\text{acac})_3$ (2 mmol) was mixed in phenyl ether (20 mL) with 1,2-hexadecanediol (10 mmol), oleic acid (6 mmol), and oleylamine (6 mmol) under nitrogen and was heated to reflux for 30 min. After cooled to room temperature, the dark-brown mixture was treated with ethanol under air, and a dark-brown material was precipitated from the solution. The product was dissolved in hexane in the presence of oleic acid and oleylamine and reprecipitated with ethanol to give 4-nm Fe_3O_4 nanoparticles. A place-exchange reaction²⁵ of DTMA dissolved in DCM with the obtained 4-nm Fe_3O_4 NPs was carried out for 2 days at 40 °C.

DCM was then evaporated under reduced pressure. The residue was dissolved in a small amount of distilled water and dialyzed (membrane MWCO = 10,000) to remove excess ligands.

Conclusions

In summary, we have developed a new platform for sensitive, fast, and effective colorimetric identification of proteins that uses a catalytically active particle for both recognition and signal transduction/amplification. By tuning the surface functionalities, The Fe₃O₄ NPs were able to differentiate ten proteins at a concentration of 50 nM, substantially lower concentrations than prior array-based protein sensors (1–350 μM).¹¹ Furthermore, these particles that interact electrostatically may be able to sense other negatively charged species such as bacteria and will be investigated in Chapter 5.

Notes

- [1] Mullenix, M. C.; Wiltshire, S.; Shao, W. P.; Kitos, G.; Schweitzer, B. *Clin. Chem.* **2001**, *47*, 1926.
- [2] Kingsmore, S. F.; Patel, D. D. *Curr. Opin. Biotechnol.* **2003**, *14*, 74.
- [3] Okuno, J.; Maehashi, K.; Kerman, K.; Takamura, Y.; Matsumoto, K.; Tamiya, E. *Biosens. Bioelectron.* **2007**, *22*, 2377.
- [4] Anderson, N. L.; Anderson, N. G. *Mol. Cell. Proteomics* **2002**, *1*, 845.
- [5] Hartwell, L.; Mankoff, D.; Paulovich, A.; Ramsey, S.; Swisher, E. *Nat. Biotechnol.* **2006**, *24*, 905.
- [6] Larsson, A.; Johansson, M. E.; Wangefjord, S.; Gaber, A.; Nodin, B.; Kucharzewska, P.; Welinder, C.; Belting, M.; Eberhard, J.; Johnsson A.; Uhlen, M.; Jirstrom K. *Br. J. Cancer* **2011**, *105*, 666.
- [7] (a) Charych, D. H.; Nagy, J. O.; Spevak, W.; Bednarski, M. D. *Science* **1993**, *261*, 585. (b) Thanh, N. T. K.; Rosenzweig, Z. *Anal. Chem.* **2002**, *74*, 1624. (c) Sastry, M.; Lala, N.; Patil, V.;

Chavan, S. P.; Chittiboyina, A. G. *Langmuir* **1998**, *14*, 4138. (d) Ho, H. A.; Najari, A.; Leclerc, M. *Acc. Chem. Res.* **2008**, *41*, 168.

[8] (a) Elghanian, R.; Storhoff, J. J.; Mucic, R. C.; Letsinger, R. L.; Mirkin, C. A. *Science* **1997**, *277*, 1078. (b) Storhoff, J. J.; Elghanian, R.; Mucic, R. C.; Mirkin, C. A.; Letsinger, R. L. *J. Am. Chem. Soc.* **1998**, *120*, 1959. (c) Aili, D.; Selegard, R.; Baltzer, L.; Enander, K.; Liedberg B. *Small*, **2009**, *5*, 2445. (d) Huang, C. C.; Huang, Y. F.; Cao, Z. H.; Tan, W. H.; Chang, H. T. *Anal. Chem.* **2005**, *77*, 5735.

[9] (a) Rakow, N. A.; Suslick, K. S. *Nature* **2000**, *406*, 710. (b) Lavigne, J. J.; Savoy, S. M.; Clevenger, M. B.; Ritchie, J. E.; McDoniel, B.; Yoo, S. J.; Anslyn, E. V.; McDevitt, J. T.; Shear, J. B.; and Neikirk, D. P. *J. Am. Chem. Soc.* **1998**, *120*, 6429.

[10] (a) You, C. C.; Miranda, O. R.; Gider, B.; Ghosh, P. S.; Kim, I. B.; Erdogan, B.; Krovi, S. A.; Bunz, U. H. F.; Rotello, V. M. *Nat. Nanotech.* **2007**, *2*, 318. (b) De, M.; Rana, S.; Akpınar, H.; Miranda, O. R.; Arvizo, R. R.; Bunz, U. H. F.; Rotello, V. M. *Nat. Chem.* **2009**, *1*, 461. (c) Albert, K. J.; Lewis, N. S.; Schauer, C. L.; Sotzing, G.A.; Stitzel, S. E.; Vaid, T. P.; Walt, D. R. *Chem. Rev.* **2000**, *100*, 2595.

[11] (a) Folmer-Andersen, J. F.; Kitamura, M.; Anslyn, E. V. *J. Am. Chem. Soc.* **2006**, *128*, 5652. (b) Greene, N. T. and Shimizu, K. D. *J. Am. Chem. Soc.* **2005**, *15*, 5695. (c) Zhang, C.; Suslick, K. S. *J. Am. Chem. Soc.* **2005**, *127*, 11548. (d) Miranda, O. R.; Chen, H. T.; You, C. C.; Mortenson, D. E.; Yang, X. C.; Bunz, U. H. F.; Rotello, V. M. *J. Am. Chem. Soc.* **2010**, *132*, 5285.

[12] Scrimin, P.; Prins, L. J. *Chem. Soc. Rev.*, **2011**, *40*, 4488.

[13] Miranda, O. R.; Li, X.; Garcia-Gonzalez, L.; Zhu, Z.-J.; Yan, B.; Bunz, U. H. F.; Rotello, V. M. *J. Am. Chem. Soc.* **2011**, *133*, 9650.

[14] (a) Shoji, E.; Freund, M. S. *J. Am. Chem. Soc.* **2001**, *123*, 3383. (b) Wei, H.; Wang, E. *Anal. Chem.* **2008**, *80*, 2250.

[15] (a) Jv, Y.; Li, B. X.; Cao, R. *Chem. Commun.* **2010**, *46*, 8017. (b) Song, Y. J.; Qu, K. G.; Zhao, C.; Ren, J. S.; Qu, X. G. *Adv. Mater.* **2010**, *22*, 2206. (c) Guo, Y. J.; Deng, L.; Li, J.; Guo, S. J.; Wang, E. K.; Dong, S. J. *ACS Nano* **2011**, *5*, 1282. (d) Pelossof, G.; Tel-Vered, R.; Elbaz, J.; Willner, I. *Anal. Chem.* **2010**, *82*, 4396.

[16] Wiester, M. J.; Ulmann, P. A.; Mirkin, C. A. *Angew. Chem. Int. Ed.* **2011**, *50*, 114.

[17] Gao, L. Z.; Zhuang, J.; Nie, L.; Zhang, J. B.; Zhang, Y.; Gu, N.; Wang, T. H.; Feng, J.; Yang, D. L.; Perrett, S.; Yan, X. *Nat. Nanotech.* **2007**, *2*, 577.

[18] Asati, A.; Santra, S.; Kaittanis, C.; Nath, S.; Perez, J. M. *Angew. Chem. Int. Ed.* **2009**, *48*, 2308.

[19] Ornatska, M.; Sharpe, E.; Andreescu, D.; Andreescu, S. *Anal. Chem.* **2011**, *83*, 4273.

[20] Gao, L. Z.; Wu, J. M.; Lyle, S.; Zehr, K.; Cao, L. L.; Gao, D. *J. Phys. Chem. C* **2008**, *112*, 17357.

[21] Park, K. S.; Kim, M. I.; Cho, D. Y.; Park, H. G. *Small* **2011**, *7*, 1521.

[22] In our study, we found that hemoglobin had an enhancement in OD response instead of inhibition. We believe this is due to the peroxidatic activity of the heme group in hemoglobin.

Reference: (a) Bunn H.F.; Jandl J.H. *J. Biol. Chem.* **1968**, *243*, 465. (b) Karnovsky M. J. *J. Cell. Biol.* **1967**, *35*, 213.

[23] H. Qu, D. Caruntu, H. Liu, C. J. O'Connor, *Langmuir* **2011**, *27*, 2271.

[24] S. Sun, H. J. Zeng, *J. Am. Chem. Soc.* **2002**, *124*, 8204.

[25] M. J. Hostetler, A. C. Templeton, R. W. Murray, *Langmuir* **1999**, *15*, 3782.

CHAPTER 5

**DETECTION OF BACTERIA IN DRINKING WATER BY STABLE INKJET PRINTED TEST STRIPS USING
ARTIFICIAL ENZYMES**

Introduction

Clean water is the most essential need for human existence. Sadly, even as we enter the 21st century, there are places that have access to water that may be infested with bacteria, such as cholera, salmonella, and cyanobacteria that can cause gastrointestinal infections, lung infections, and, in some cases, death. According to UNICEF and the World Health Organization, an estimated 1.2 billion people worldwide are without access to safe drinking water.¹ A study done in 1996 implicates contaminated water as a cause of cholera and other diarrheal bacteria that kills about 2 million children and causes 300 million cases of illness per year.² The great majority of these deaths occur in the emerging nations of the world, where the water is contaminated with bacteria from animal and human feces that cannot be easily detected. In light of these dramatic statistics, a quantitative low cost sensor needs to be developed to determine microbial water quality.

Current research has published many methods for detecting bulk bacteria concentrations in drinking water using bioluminescence,³ chemiluminescence,⁴ and fluorescence.⁵ These methodologies fail to address the urgency need for water quality, as most are expensive, require a working laboratory, and need several hours or days for proper analysis. Microbial water quality can vary rapidly and widely, however, as short term peaks in the concentration of bacteria can lead to increased outbreaks of disease,⁶ making off-site testing that takes even a

few days quickly irrelevant. Ideally, the sensor should track overall bacterial count, more specifically the change in count, as it can be used as an indicator of overall water quality.⁷ In Chapter 3, we generated a sensing system using an enzyme amplified array to detect bulk bacteria in water samples. In brief, this strategy uses functionalized cationic gold nanoparticles (NPs) to reversibly inhibit an anionic enzyme, β -galactosidase.⁸ In the presence of bacteria, the microbes will disrupt the nanoparticle-enzyme complex through competitive binding, reactivating the enzyme. The free enzyme then catalyses the hydrolysis of a colorimetric substrate, chlorophenol red- β -D-galactopyranoside (CPRG), generating a visible response. This sensor can identify bulk bacteria at concentration on the order of 10^3 coliforms(cfu)/mL on a paper substrate. However, these sensors would denature over time due to the and only were useable for upwards of one week when kept under optimal conditions, making these strips unattractive for off-site testing.

To replace the fragile components of the previous sensor, we have developed a sensing system using synthetic enzyme mimic, iron oxide nanoparticles (Fe_3O_4 NPs) that replace enzymes as signal amplifiers to catalyze colorimetric reactions.⁹ The use of artificial enzymes addresses the issue caused by enzymes instability and activity variation, providing a way to fabricate robust biosensors. The intrinsic enzyme-like activity of Fe_3O_4 NPs is modulated by differential interactions of analytes, generating discernable patterns with color readouts provided by the Fe_3O_4 NP-catalyzed oxidation of a chromogenic substrate in the presence of hydrogen peroxide (H_2O_2) (Figure 30). As discussed in Chapter 4, the sensitivity of this approach was validated by testing with model analyte protein in solution, enabling rapid detection and identification of ten types of proteins at a 50 nM concentration. In this report, we propose here an iron oxide and mixed ferrite NP-composed test strip sensor that gives a colorimetric response to bacterial

contamination of water. This sensing system will be integrated with an inkjet printing approach provide a scalable manufacturing strategy. We will first probe the sensitivity of this sensing system with model bacteria strains. The system will then be transferred to a field-friendly strip platform by inkjet printing strategy and will be tested for bacteria detection in water.

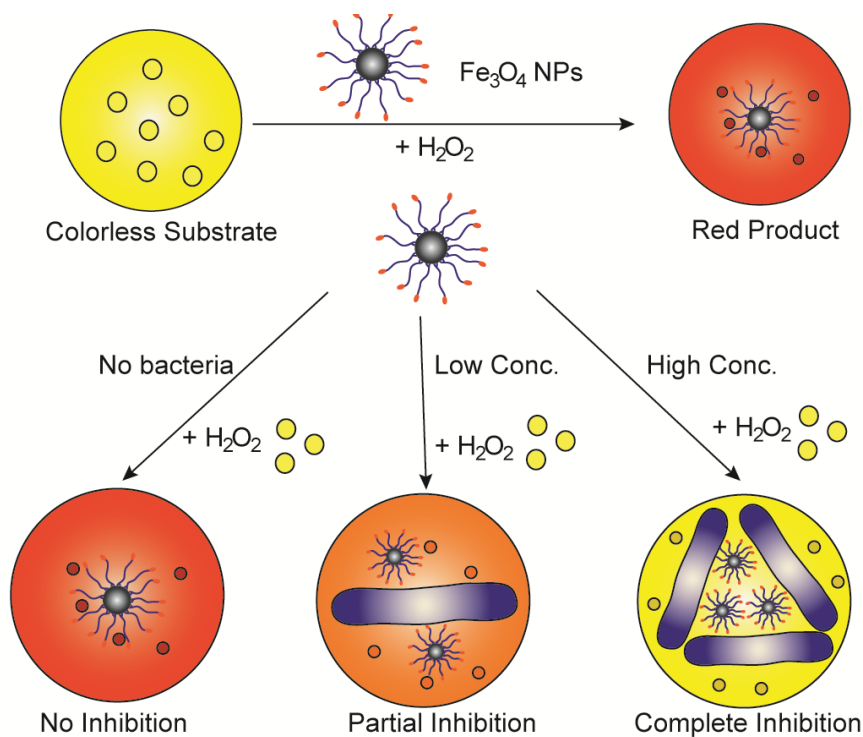


Figure 30 - Sensing strategy used for bacteria determination in this work.

Results and Discussion

To first test to see if our overall hypothesis that iron oxide particles can detect concentrations of bacteria as well as explore what surface functionalization of the particle generates the best sensitivity to the bacteria, three additional iron oxide particles were synthesized for testing against the treated dopamine particle developed in Chapter 4 (Figure 31). As shown in Figure 32, both aminobenzoic acid and trimethylammonium functionalized particles showed some

sensitivity towards bacteria. While the aminobenzoic acid particles were not as sensitive to the bacteria showing a sensitivity of 10^5 bacteria/mL, the trimethylammonium particles showed comparable results to the dopamine control. The negatively functionalized citric acid particles showed no response during testing. Given that the dopamine ligand is commercially available while the trimethylammonium ligand requires complicated synthetic steps to produce, we chose the dopamine ligand for our future work.

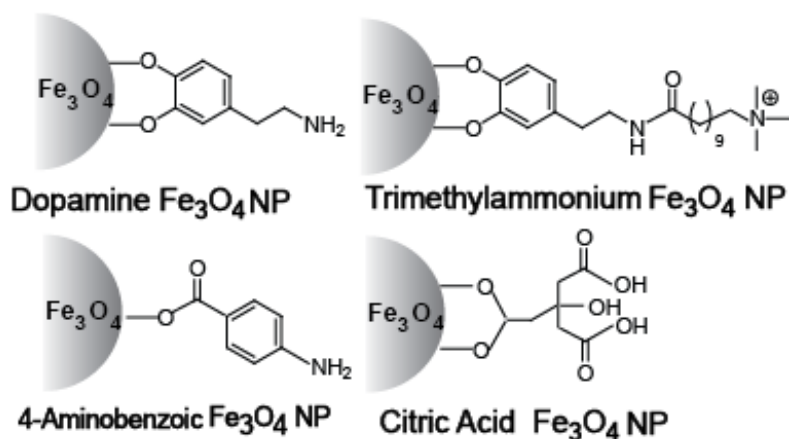


Figure 31 – Chemical Structures of the Particles used in the Study

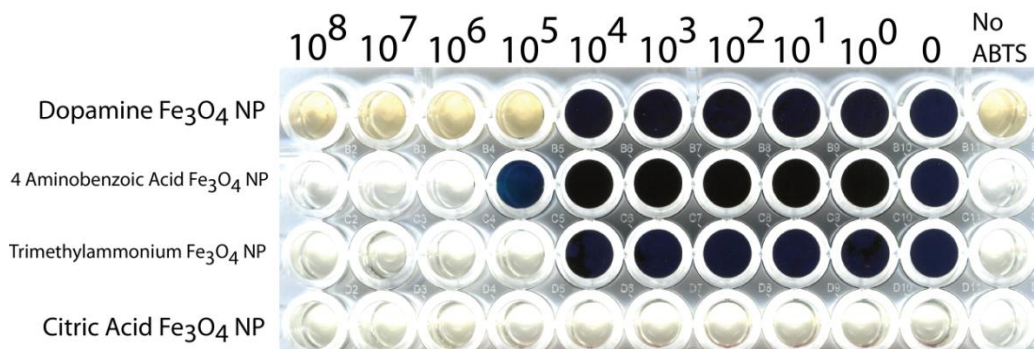


Figure 32 - Colorimetric Responses to Bacteria Based on the Chemical Functionality of the Particle

Inkjet printing is a powerful tool for patterning nanoparticles¹⁰ and proteins¹¹ as well as simple colorimetric substrates. In Chapter 2 and 3, we have demonstrated the use of inkjet printing for

direct deposition of nanoparticles similar to the Fe_3O_4 NPs in our sensor.¹² To provide the hydrogen peroxide in reaction, we explored the use of urea hydrogen peroxide (UHP, $\text{CH}_6\text{N}_2\text{O}_3$), a widely available and stable peroxide generator when stored in cool and dry conditions.¹³ In our sensor design, NPs will be spatially deposited next to the colorimetric substrate and the peroxide generator (Figure 33). This process will assure that the elements will not interact on the strip prior to use. Upon immersion into the water sample, the substrate and peroxide will diffuse to the Fe_3O_4 NPs, allowing oxidation to give a color readout. In the presence of bacteria, however, Fe_3O_4 NP-catalyzed reaction will be modulated, giving a lighter color or no color at all depending on the bacteria concentration.

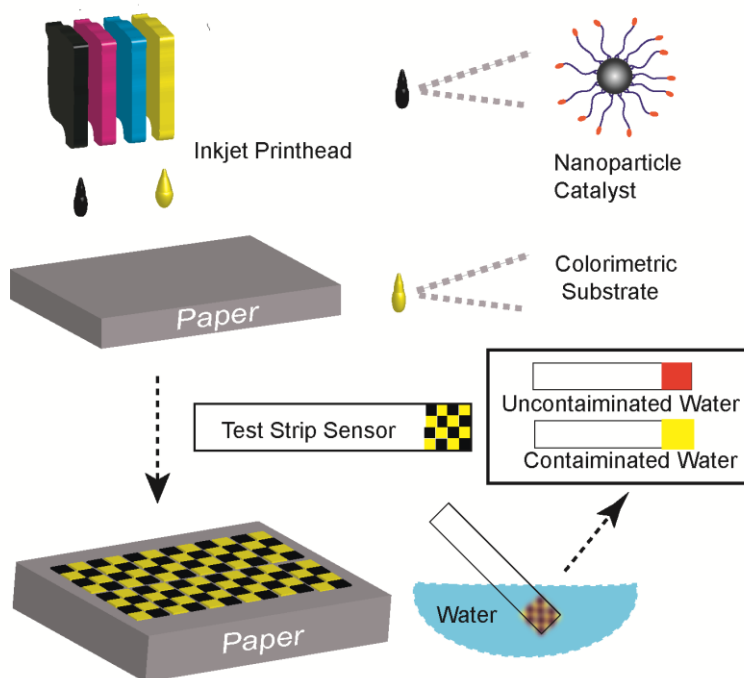


Figure 33 - Proposed Inkjet Printed Test Strip Fabrication

Our second goal is to properly depositing the sensor material onto the paper substrate, as improper ink formulation can not only provide inferior prints and therefore unusable sensors but also irreparably harm the printer. Optimizing the ink components to achieve good print

performance while not altering the sensor elements is typically done by altering the ink composition. Using water only as the printing solvent produced 1 to 2 defect-free prints from the printer, but further prints had multiple nozzle failures that could not be recovered by simple flushing of the printhead. Even if printing was recovered, cleaning the system after one or two prints would not be feasible on an industrial scale. To create a more reliable ink for our system, we investigated the use of glycerol as a humectant to retard nozzle drying, thus increasing reliability. While increasing the amount of glycerol to 20% did increase reliability somewhat, adding another humectant, 1,2 hexanediol, that also reduces water loss at the nozzle, allowed printing with no defects for upwards of 20 pages, which is the maximum amount of full page prints per cartridge, without any cleaning of the nozzle. As an example, Figure 34 shows on the left a block of the iron oxide nanoparticles printed next to a printed box of colorimetric substrate (o-phenylenediamine)(center). As both are quite colorless when they do not interact, they do produce a very distinct orange pattern when printed together. If either channel has any issues printing, bands or defects will be visible when printed together. In Figure 34, we see not only the color response, but no visible defects on printing.

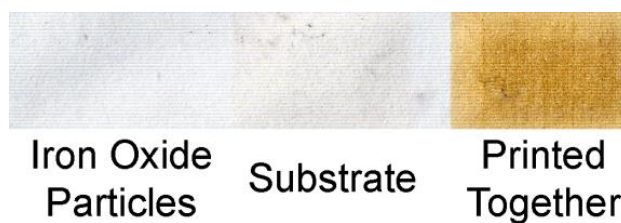


Figure 34 - The components printed separately as well as together.

To increase the sensitivity of our testing material to meet our goal as well as potentially lower production costs, we investigated the use of new synthesis strategies for iron oxide particles. In order to test these materials quickly without using large quantities of material, we screened our

particles against various concentrations of bacteria in solution with our color producing substrate. One particularly promising particle is functionalized with the same chemical as in our proposal, but created using lower temperatures. When incubated with lower concentrations of bacteria, the particles can interact with a yellow colored substrate to create in this case a strong orange/brown color. As shown in Figure 35, the color response only occurs at concentrations around 10^2 cells/mL, a concentration far lower than our original goal. However, these particles had some stability issues as their ability to cause the colorimetric reaction lessened over a period of a few days. This issue may explain the reduced sensitivity of the test strips created with these particles as shown in Figure 36.



Figure 35 - Solution-based testing using the developed particles against concentrations of E. coli DH5α bacteria

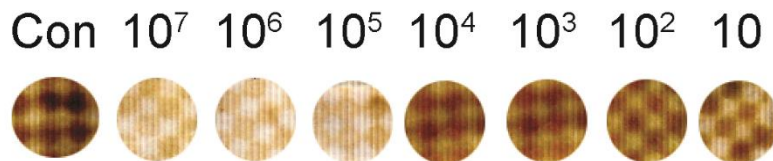


Figure 36 - Colorimetric response of our test strips to various concentrations of E. coli DH5α bacteria

While these particles showed increased sensitivity, the stability of these particles was quite poor, settling out of solution in just a few days. Mixed ferrite nanoparticles that incorporate metals such as cobalt and manganese into an iron oxide nanoparticle are known to have better stability than simple iron oxide nanoparticles while continuing to act as an artificial enzyme of horseradish peroxidase. We investigated both $MnFe_2O_4$ and $CoFe_2O_4$ nanoparticles in our system

using the low temperature synthesis method discussed earlier. While both particles showed decent sensitivity toward bacteria, the manganese particles had a lower limit of detection (Figure 37). Furthermore, the cobalt nanoparticles had a particle size of 160 nm, which is too large to be printable by inkjet printing while the manganese particles had a size of only 80 nm. Therefore, only the manganese particles were tested on a test strip format. As shown in Figure 37b, these particles produced viable test strips that could sense *E. coli* bacteria down to 10^3 cfu/ml.

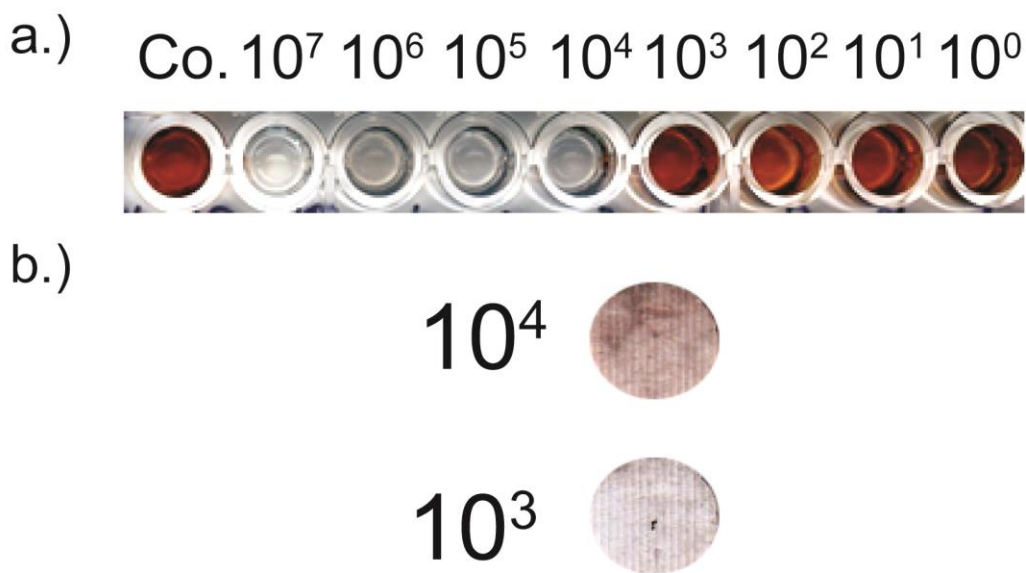


Figure 37 - Colorimetric response in both solution (a) and on a test strip (b) using various concentrations of *E. coli* XL1 bacteria

As this sensor is based on electrostatics, differentiation between live and dead bacteria is impossible. In developing nations, the treatment of water with bleach to eliminate any residual bacteria left in the water stream is common. In our sensor scheme, high concentrations of these bacteria would illicit a response from our sensor scheme that would indicate hazardous drinking water when in fact the water has been properly treated. To elevate this issue, we incorporated a chlorine sensor into our test strip design that would indicate that the water has

been properly treated even if there is a signal for high levels of bacteria in the water source. DPD (N,N-dimethyl-p-phenylenediamine sulfate) is a colorimetric substrate that is readily oxidized by the presence of chlorine in solution to produce a vivid magenta color when detected.¹⁴ To incorporate this chlorine sensor, we simply inkjet printed a solution of this chemical onto the same paper substrate used for our bacteria strips and processed the print to generate circular test strips. After optimizing the color response by increasing the amount of sensor material to 10 times the solution amount, we were able to generate a visual readout showing detection around .5 to 5 ppm of chlorine which is in the range that most chlorinators operate to disinfect water streams.¹⁵ It is important to note that the 5 ppm strip produced a magenta color initially but faded before the scanned image could be taken. While the color response could be optimized for this proof-of-concept system, commercially available testing strips for chlorine exist and could also be readily incorporated into our bacteria testing platform.

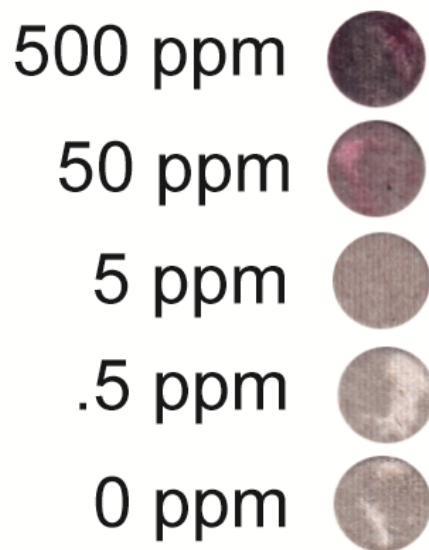


Figure 38 – Chlorine Sensor on a Test Strip Format

Materials and Methods

All ligands and colorimetric substrates were purchased from Sigma Aldrich and used without further purification except for the TMA ligand that was created according to our published work (See Chapter 4).¹⁶

High Temperature Iron Oxide Nanoparticle Creation

Water-dispersible Fe₃O₄ nanoparticles (NPs) with the stated capping ligands were synthesized and purified according to literature.¹⁷ In general, FeCl₂•4H₂O (99.4 mg, 0.5 mmol), FeCl₃•6H₂O (270.3 mg, 1mmol), and 20 g of diethylene glycol (DEG) were added to a nitrogen-protected three necked round bottom flask. A solution of NaOH (160 mg, 4 mmol) in 20 g DEG was then added to the flask. The mixture was heated for 2 h at 220 °C. At the end of heating, a mixture of 1mmol of the capping ligand in 400 µL of H₂O and 5 g of DEG was injected into the flask. After cooling to room temperature, the solid product was isolated by centrifugation and washed five times with ethanol and finally redispersed in water.

Low Temperature Fe₃O₄, MnFe₂O₄, and CoFe₂O₄ Nanoparticles Synthesis

Fe₃O₄ nanoparticles were synthesized under alkaline conditions, while maintaining a molar ratio of Fe²⁺ : Fe³⁺ = 1 : 2 in argon. 0.29 mmol FeCl₂•4 H₂O and 0.58 mmol FeCl₃•6 H₂O were dissolved in 5 mL of deionized water with vigorous stirring. To create the MnFe₂O₄ or CoFe₂O₄, we simply substituted MnCl₂ or CoCl₂ for the FeCl₂ mole to mole. In a separate vial, 2.32 mmol of NaOH and 0.14 mmol dopamine were dissolved in 5 mL of deionized water. Fe₃O₄ nanoparticles were formed immediately after the addition of the base solution to the precursor solution. The pH of the reaction mixture was maintained at 12. The TEM micrograph showed Fe₃O₄ nanoparticle

core was 3-4 nm in diameter. The concentration in water was 33 mg/mL, equivalent of 0.65 % volume fraction.

Bacteria Creation

Bacteria were grown according to a standard procedure in Luria–Bertani (LB) medium. Cultures were incubated aerobically overnight at 37 °C, during which time they were shaken at 275 rpm. They were harvested after a total of 24 h during logarithmic growth. Centrifugation at 100g and resuspension in phosphate buffer was conducted 5 times to remove protein and other impurities that might potentially contaminate the surfaces. All bacteria were studied within 72 h of preparation and stored in a refrigerator near 4 °C.

Solution Testing

After creation, the NPs were dried and redispersed in MilliQ water to a concentration of 1 mg/ml. Separate aqueous solutions of 1mM 2,2'-azino-bis(3-ethylbenzothiazoline-6-sulphonic acid) (ABTS) and 2.5mM hydrogen peroxide (H₂O₂) were also created in the case of ABTS sensing. All other colorimetric substrates were used with the same molar ratio. In this procedure, each bacteria solution was first mixed with 50µL of NP and incubated at room temperature for 30 minutes followed by the addition of 50 µL of H₂O₂ and 50µL of ABTS. The colorimetric results were obtained by using an Epson scanner after 5 minutes of incubation. For o-phenylenediamine and pyrogallol testing, the ABTS solution was replaced with a 5mM o-phenylenediamine or pyrogallol solution and the amount of H₂O₂ was increased to 5mM. Also, the o-phenylenediamine solution was made right before usage as the solution gradually oxidizes producing a faint orange color. Pyrogallol did not show the same degradation when stored under dark and refrigerated conditions.

Inkjet Printing

Aqueous solutions of 10mg/mL Fe₃O₄ NPs, 10mM colorimetric substrate (ABTS, pyrogallol, or o-phenylenediamine) , and 25mM urea hydrogen peroxide were created and filtered through a .22 μm syringe filter and into a virgin aftermarket Epson cartridge. Please note that we use urea hydrogen peroxide as it is stable in a dried printed form. Inkjet printing was done using an Epson Artisan 50 inkjet printer (Long Beach, CA USA) that was used as packaged. The substrate was loaded by placing standard copy paper into the paper feed slot. Patterning was done by using Microsoft Powerpoint. After printing, the paper was removed from the paper and cut into circles with a hole punch. These circles were then pasted onto thin 3 inch by .5 inch card stock strips. Once the glue had dried, the strips could then be used for sensing. Test strip analysis of water was done by immersing the strip into the water for 1 minute then drying the strip in air for 5 minutes. Images were obtained by scanning using an Epson desktop scanner.

Inkjet Printing of the Chlorine Sensor

The chlorine sensor was created by printed by loading an Epson cartridge with the solution described in literature¹⁴ but multiplying the amount of DPD by 10 times. Printing and fabrication was done similar to the bacteria test strip, but the strips were stored in a dark area as the DPD is light sensitive. Chlorine detection was done by diluting standard household bleach

Conclusions

We have developed sensor elements that can meet our low limit of bacteria detection using both solution experiments and printed strips. Given our recent success in generating viable materials, we will in the near future investigate stability sensor testing. This work will be done with our collaborators in Pakistan using locally sourced water. For our future work, we plan to

continue developing this sensor platform for possible commercialization. Currently, we are still optimizing our particle synthesis methods to hopefully drive the limit of detection to 100 cells/mL, where the sensor would be clinically relevant. Finally, we are investigating image processing methods to allow quantification of the test strip response by smartphones and other mobile devices.

Notes

[1] UNICEF and World Health Organization “Joint Monitoring Programme for Water Supply and Sanitation, Progress on Drinking Water and Sanitation” Geneva: UNICEF, New York and WHO, 2008.

[2] Ford, T.E.; Colwell, R.R. “A Global Decline in Microbiological Safety: A Call for Action” A report from The American Academy of Microbiology, Washington, D.C., 1996.

[3] Frischer, M.E.; Danforth, J.M.; Foy, T.F.; Juraske, R. *J. Environ. Qual.*, **2005**, *34*, 1328.

[4] Oleniaz, W.S.; Pisano, M.A.; Rosenfeld, M.H.; Elgart, R.L. *Environ. Sci. Technol.*, **1968**, *2*, 1030.

[5] Disney, M.D.; Zheng, J.; Swager, T.M.; Seeberger, P.H. *J. Am. Chem. Soc.*, **2004**, *126*, 13343.

[6] Halkos, G.E.; Tzeremes, N.G. *Annu. Rev. Microbiol.*, **2001**, *55*, 201.

[7] Rompré, A.; Servais, P.; Baudart, J.; de-Roubin M.R.; Laurent, P. *Microbiol. Methods.*, **2002**, *49*, 31.

[8] Miranda, O. R.; Li, X.; Garcia-Gonzalez, L.; Zhu, Z.-J., Yan, B.; Bunz, U. H. F., Rotello, V. M. *J. Am. Chem. Soc.*, **2011**, *133*, 9650.

[9] Li, X.; Wen, F.; Creran, B.; Jeong, Y.; Zhang, X.; Rotello, V. M. *Small*, **2012**, *8*, 3589.

- [10] Ko, S.H.; Pan, H.; Grigoropoulos, C.P.; Luscombe, C.K.; Frechet, J.M.J.; Poulidakos, D. *Nanotechnology*, **2007**, *18*, 345202.
- [11] Cook, C.C.; Wang, T.; Derby, B. *Chem Commun.*, **2010**, *46*, 5452.
- [12] Creran, B.; Yan, B.; Moyano, D. F.; Gilbert, M. M.; Vachet, R. W.; Rotello, V. M. "Laser Desorption Ionization Mass Spectrometric Imaging of Mass Barcoded Gold Nanoparticles For Security Applications" *Chem. Commun.*, **2012**, *48*, 4543.
- [13] Jakob H.; Leininger, S.; Lehmann, T.; Jacobi, S.; Gutewort, S. "Peroxo compounds, inorganic" *Ullmann's Encyclopedia of Industrial Chemistry*, 6th ed., Wiley-VCH:Weinheim, 2003.
- [14] Best, D. G.; deCasseres, K. E.; *Analyst*, **1985**, *110*, 221.
- [15] <http://www.lamotte.com/en/blog/test-factors/72-measuring-chlorine> (Accessed 5/14/15).
- [16] Li, X.; Wen, F.; Creran, B.; Jeong, Y.; Zhang, X.; Rotello, V. M. *Small*, 2012, *8*, 3589.
- [17] Qu, H.; Caruntu, D.; Liu, H.; O'Connor, C. J. *Langmuir*, 2011, *27*, 2271.

APPENDIX

SCIENTIFIC OPERATION OF AN ARTISAN 50 PRINTER FOR A LABORATORY ENVIRONMENT

Introduction

It is important that any person wanting to use inkjet printing should read the few chapters of this guide before printing. These chapters will give a baseline knowledge of how to print and safely handle the printer. Later portions are for more advanced users and contain information that may not pertain to certain projects. The final chapter on troubleshooting is best read by responsible persons when a particular issue arises. Finally, the Appendix contains historical information as well as inkjet terminology.

For work done in the Rotello Labs, we have used an Epson Artisan 50 Inkjet Printer to put our nanoparticle and colorimetric substrate onto paper for our small scale research. In addition to the printer's low cost and ability to print on hard substrates such as silicon wafers, we selected the Artisan 50 as it is relatively easy to clean and maintain. Furthermore, Epson printers use a piezoelectric print head as opposed to the thermal print head used by Canon/HP printers. In our experience, the heat generated by Canon/HP printers affected the materials printed. We are aware that printer models rapidly evolve and we will inform you if and when we do change printers. Do not use unapproved printers and expect similar results to the ones shown in this guide. Print head technologies are not visible to the common consumer, but affect how materials are printed. Use only the Artisan 50 printer or the Asian/European equivalent unless instructed otherwise.

Setting Up Your Printer

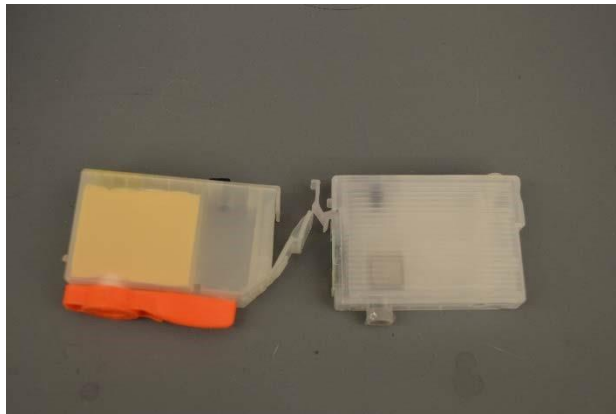
Unpack the printer as indicated by the manufacturer. Read the enclosed manual that comes with the printer to understand the hazards associated with printing.

DO NOT put the OEM cartridges into the printer. (For definitions of OEM as well as any other inkjet printer specific terminology, please see the Definitions section). Once the ink from the OEM cartridges gets into the printer system, it is very difficult to flush the colorant out (4-5 head cleanings). However, keep the cartridges in case you need to check the quality of the print head if and when it is clogged.

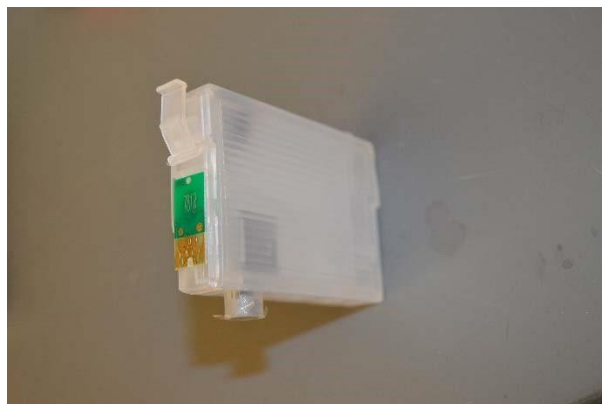
Cartridge Selection

Currently, we use virgin aftermarket inkjet cartridges for the Artisan printer. These cartridges have NOT been filled with printer ink and therefore will not have any interfering materials that could impact our research. Given the current patent disputes between Epson and the manufacturers of these cartridges, it can be difficult to find these types of cartridges and even harder to find good quality ones. We currently purchase them from Cobra Ink Systems (<http://cobraink.com/cartridges/cartridges%2046%20color%20empty%20.htm>) but it may be able to find cartridges elsewhere especially if you are not in the United States. All high quality ink cartridges do NOT contain sponges as the sponge can preferentially hold our experimental materials giving inconsistent prints (Appendix Figure 39). If possible, use a new cartridge for each new experiment unless it was used for something similar. For example, an ABTS cartridge may be refilled with more ABTS solution, but should not be used for iron oxide nanoparticles. Finally, a word on choosing cartridges as there is a computer chip on the side of the cartridge that indicates to the printer both the identity and ink level of the material (Appendix Figure 40).

This prevents you from using a yellow ink in the black nozzle (a good thing for the consumer) but also non-genuine Epson products from being used (bad for experimental use). Auto resettable cartridges get around the second problem by faking the electronic signature allowing you to fool the printer into printing your solution. These cartridges also reset the level of ink from empty to full when removed from the printer. This type of chip is highly desirable for flushing fluid cartridges that can be simply refilled with fluid each time they are empty, instead of requiring a new cartridge each time. Therefore, when buying cartridges, be sure to get auto resettable cartridges.



Appendix Figure 39 - A comparison of a cartridge containing a sponge (left) versus a high quality spongeless cartridge (right). Note that the left cartridge is not for an Epson Artisan 50 cartridge and is used as a demonstration only.



Appendix Figure 40 - Computer chip located on the cartridge.

Cartridge Preparation and Ink Formulation

This section is an extremely short overview of the potential ink formulations that can be used in inkjet printer. We use these formulations as they work well in our system. Ink formulations consist of surfactants, humectants, biocides, and polymers that are added to the ink to reduce the surface tension, increase the viscosity, or sterilize the ink for proper printing performance. For example, water alone has a surface tension of 72 dynes/cm at room temperature, which is out of the normal range for efficient inkjet printing. By adding glycerol and ethanol, we can lower the surface tension to ~30 dynes/cm making it ideal for printing. The attached recipes have been used in our lab to ensure that we are operating at optimal conditions for printing.

In these recipes, I assume that whatever you are attempting to print is dispersable/soluble in water. If you are attempting to print something that is not soluble in water, see the section on non-water formulations. In my experience, these water-based formulations are good imitations of what the actual OEM uses for their ink vehicle. However, some performance issues can be present and they are noted below the formulation. All percentages refer to weight percent and are not by volume. For example, to make 10 grams of the Generation 1 formulation, you would mix 7 grams of water with 2 grams of glycerol and 1 gram of diethylene glycol along with whatever you are attempting to print.

To begin exploration, start with the Generation 2 Formulation and work down the recipes until you find the optimal formulation for you and your sample. If you are trying to print something down onto the paper that you have previously done in solution, multiply the concentration you

used by 10 fold for printing purposes. For example, a 2.5 mM dye solution used in solution reactions might need 25mM in the cartridge for visible detection on a paper substrate. This multiplication is needed as so little material is actually printed out onto the substrate.

When you set up and maintain an inkjet printer, it is imperative that you make a decent amount of cleaning solution (or more commonly referred to as flushing fluid) as your printer needs to be constantly filled with fluid to keep the printhead wet. A highly colorimetric dye is added so that print tests can show if clogs exist using known good ink formulations. Rhodamine is used as it is relatively inexpensive, colorimetric, and requires very small amounts of material to produce vibrant colored solutions. As an alternative, one could also use methylene blue that produces a blue ink. However, the solubility of methylene blue is not as good, producing faded blue prints even with high concentrations of the dye. One could use OEM cartridges instead of flushing fluids but that would be quite expensive and require multiple flushings each time you switched to the cartridge of interest.

Proven Recipes for General Printing

Generation 2 Formulation

- 69% Water (MilliQ purified water is preferable), 20% glycerol, 10% 1,2 hexanediol, and 1% triethanolamine (optional – for pH stability. May be replaced with 1% water)
- Pros – Good ink stability, proven ink formulation in our labs.
- Cons – May require a small amount of BYK 347/348 surfactant for spreading. These surfactants are not necessary for most small scale experiments and the BYK surfactants may be hard to obtain.

Generation 1 Formulation

- 70% Water (MilliQ purified water is preferable), 20% glycerol (glycerin), and 10% diethylene glycol
- Pros – Unpatented formulation, inexpensive, preferred by some colleagues to Generation 2
- Cons – Not specifically formulated to the Artisan 50 printer, Sometimes leads to banding issues, slight solubility issues

Unproven Recipes for General Printing

These recipes have some issues that do not allow for use as an everyday formulation. Some of these recipes include exotic surfactants that may be very difficult to obtain. Other recipes may be used for flushing stubborn clogs and are unstable over long periods of time.

Generation 1 Formulation with Surfanol 465

- 70% Water (MilliQ purified water is preferable), 19.5% glycerol (glycerin), 10% diethylene glycol, and .5% Surfanol 465
- Pros – Inexpensive, can potentially print very stable biomolecules, reduces banding
- Cons – Slight solubility issues, unsure if this formulation is patented, obtaining Surfanol 465 is challenging as you have to request a free sample from Air Products.

Generation 1 Formulation with Ethanol

- 50% Water (MilliQ purified water is preferable), 20% ethanol, 20% glycerol (glycerin), and 10% diethylene glycol

- Pros – Inexpensive, can clear most clogs in the print head.
- Cons – Not at all good for biomolecules, tends to be on the lower side of tolerable surface tension and viscosity. Tends to lead to a more unstable ink.

Generation 1 Formulation with Ethanol and Surfanol 465

- 50% Water (MilliQ purified water is preferable), 20% ethanol, 19.5% glycerol (glycerin), 10% diethylene glycol, and .5% Surfanol 465.
- Pros – Inexpensive, can clear most clogs in the print head, reduces banding
- Cons – Slight solubility issues, unsure if this formulation is patented, obtaining Surfanol 465 is challenging as you have to request a free sample from Air Products.

Water Formulation

- 100% Water (MilliQ water is preferred)
- Pros – Extremely Simple, no left over surfactants to affect performance after printing.
Can work in some instances
- Cons – Water is a difficult formulation for the printer to handle. It CAN be useful for small prints (page or two at most) but you will need to do head cleanings frequently. The surface tension and viscosity is far outside the proper parameters for printing, BUT it can be used as a last resort if need be. Be sure that the liquid levels in your cartridges are full.

Non-Water Formulations

First, see if you can solvate your compound in a little bit of a water-miscible solvent such as acetonitrile or DMF and then add it to one of the previous formulations. If that doesn't work, you can feel free to use alcohols such as methanol, ethanol, or 2-propanol (Isopropyl alcohol). In fact, we routinely use straight ethanol for solar cell applications. However, drying becomes a significant issue if the cartridge is left in the printhead. If you do decide to use alcohol-based solvent instead of water, be sure to flush after printing with a water-based cartridge.

Known Good Flushing Fluid Recipes

Generation 2 Rhodamine Flushing Fluid Formulation

- 69% water, 20% glycerol, 10% 1,2 hexanediol, 1% triethanolamine and 10mg/mL rhodamine B.
- Pros – Good ink stability, proven ink formulation in our labs. Strong Red/Pink Color.
- Cons – Some slight issues on paper (poor spreading)

Generation 1 Rhodamine Flushing Fluid Formulation

- 70% Water (MilliQ purified water is preferable), 20% glycerol (glycerin), 10% diethylene glycol and 10mg/mL rhodamine B.
- Pros – Unpatented formulation, inexpensive, preferred by some colleagues to Generation 2. Strong Red/Pink Color.
- Cons – Not specifically formulated to the Artisan 50 printer, Sometimes leads to banding issues, slight solubility issues

Note – Methylene blue (blue color) and flavin mononucleotide (yellow color) can be used instead of rhodamine.

Sample Preparation

You will need:

- Your sample. The particle size must be <150nm and generally should be <100nm in size.
- At least 10mL of ink to put into the cartridge. Lower amounts will not allow proper filling and allow air to be trapped in the cartridge. Lack of fluid will cause line outs/banding on the paper. If you have not made your sample into an ink, please see Cartridge Preparation.
- 2 22 gauge or lower needle (18 is ideal) per sample. If possible, use a rounded tip (rather than a sharp injecting needle) so that you do not pierce the plastic in the cartridge.
- 1 .45 micron syringe filter per sample (Fisher Cat # 6780-2504 are ideal). .22 micron syringe filters also work (and get rid of more contaminate!)
- 1 10 or 20ml Luer-lock syringe per sample
- An extra vial to filter your ink into.

Before you place your ink into the cartridge, you must filter your ink by syringe filtration. Failure to do so will damage the printer. Even if you are sure that no constituent is above the 200nm cutoff, dirt and other particulates can easily get into your ink.

First, load the ink into the syringe.

Carefully remove the needle, attach the syringe filter and a new needle.

Firmly push the ink out of the syringe and into your extra vial. Please note that if the filter clogs (will not allow liquid to pass through), your ink is full of particulates. Consider rechecking the size of your sample and by all means reconsider printing this material.

Your ink is ready to be put in the cartridge.

Cartridge Filling

You need:

- Filtered ink from previous step
- A flat tipped (preferred) or a sharp tipped needle (18 gauge is best).
- Appropriate cartridge
- Paper towels

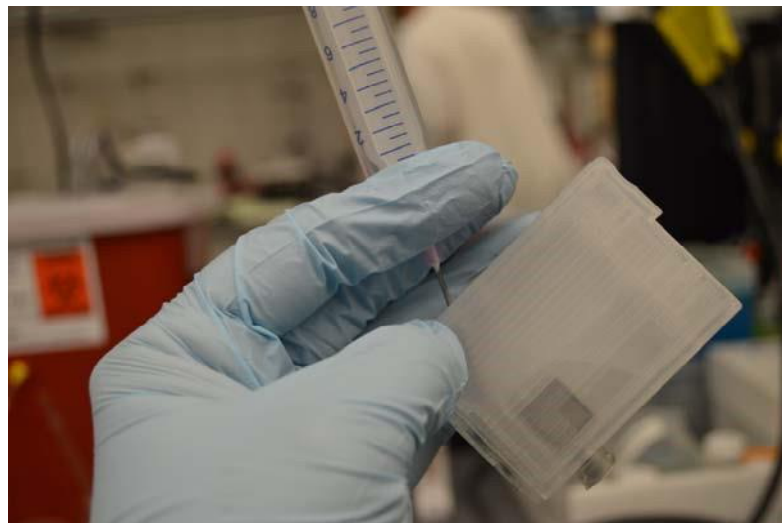
Note: there is a small bag/lining in the cartridge to keep liquid from spilling. Be careful when filling the cartridge to not pierce this liner and cause holes.

Instructions:

1. First, open the air vent on the cartridge. Discard the plug or tape.

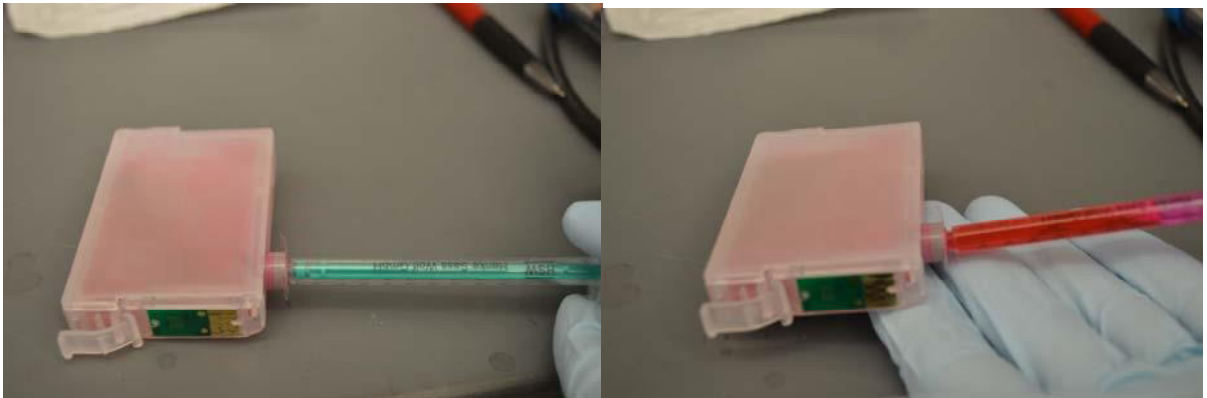


2. Open the fluid cap of the cartridge and place the cartridge on a bench (with a paper towel underneath in case of a spill).
3. Syringe fluid into the cartridge at a 45 degree angle. A medium flow is all that is required as to minimize spilling material as well as air bubbles. As you inject more into the cartridge, gradually tilt the cartridge down to the floor until the fluid line is at the top.



4. Replace the fluid cap.

5. Using a 1mL syringe or any syringe that can be pushed into the bottom of the cartridge, slowly pull out liquid out of the cartridge. This procedure eliminates any air that is stuck in the cartridge as well as reduces the amount of times a head cleaning is needed as material is now in the channel. Keep pulling out air until liquid freely comes out into the syringe. Be careful as pressure might build here causing material to spurt out. Once liquid comes out, slowly pull out the syringe and syringe any material that came out of the cartridge back in by way of opening the fluid cap. Wipe any liquid that spilled. In the case of rhodamine-based inks, ethyl acetate does a great job cleaning any spill.



6. After printing, extract out any leftover material by syringing out through the fluid port. Do not leave any experimental material in cartridges for long periods as these inks might settle or corrode the printer or cartridge.

Cleaning Cartridges

Given the low cost of replacement cartridges and the relative difficulty of cleaning them, one should consider cleaning cartridges as a bad idea. However, if funds are tight, there is a procedure for cleaning aftermarket Artisan 50 cartridges.

You will need:

- A flat tipped (preferred) or a sharp tipped needle (18 gauge is best).
- A 10mL syringe
- A 1mL syringe or a syringe that can attach or be pushed into the bottom port of the inkjet cartridge.
- Appropriate cartridge
- Squirt bottle with the main component of the ink (e.g. water or ethanol)
- Paper towels

Instructions:

1. First, extract out the leftover ink from the cartridge with the syringe.
2. Inject liquid into the cartridge through the fluid cap. Replace the cap on the cartridge.
3. Shake the cartridge.
4. Syringe out the liquid in the cartridge and squirt into a proper waste stream.
5. Using the 1mL syringe, extract all of the liquid out of the bottom port. This may require multiple pulls on the cartridge.
6. Repeat Steps 2-5 until clean.

General Printer Handling

This section covers the general handling of the printer including how to do a head cleaning.

Day to Day Printer Storage

First, the printer should at all times contain 6 cartridges filled with flushing fluid. Usually, this is done by designating a full set of cartridges with a filtered rhodamine containing flushing fluid (See Chapter 3).

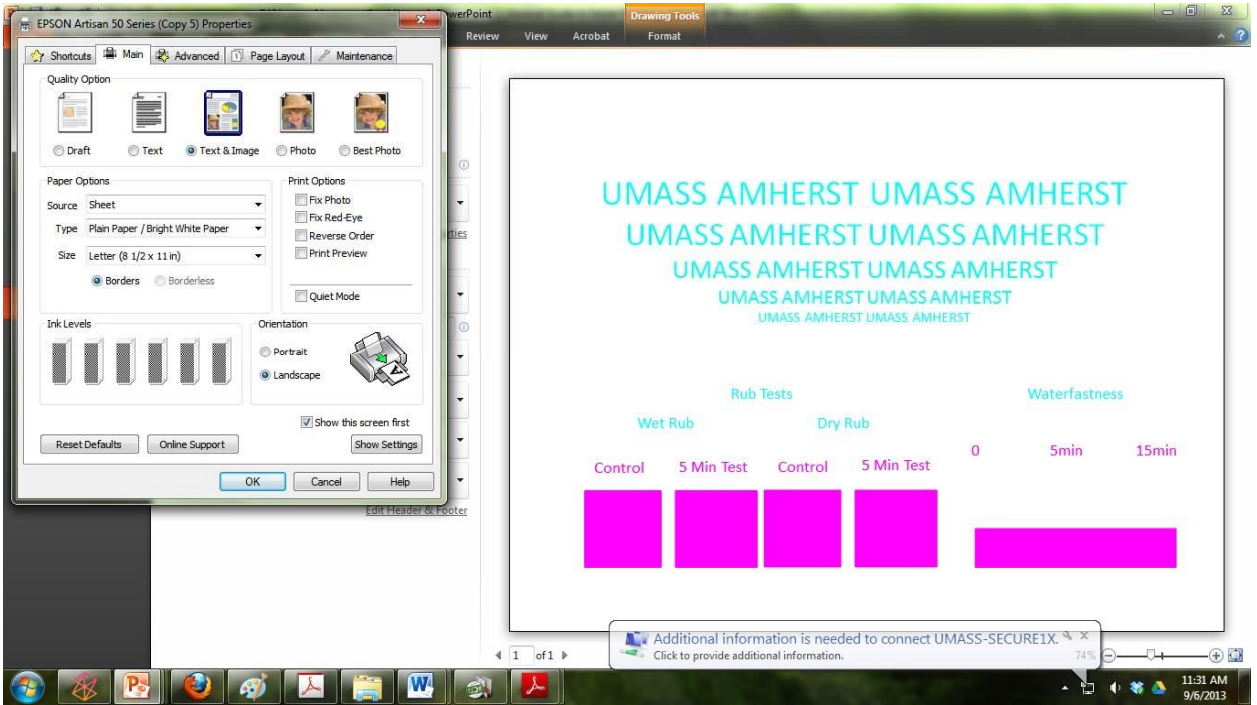
Never leave a cartridge slot empty or with an empty cartridge.

After printing with your analyte of interest, the flushing fluid cartridges are replaced into the printer and a flushing cycle is performed (see below). If you are using the printer on a semi-regular basis, leave the printer plugged in as the printer will clean itself regularly.

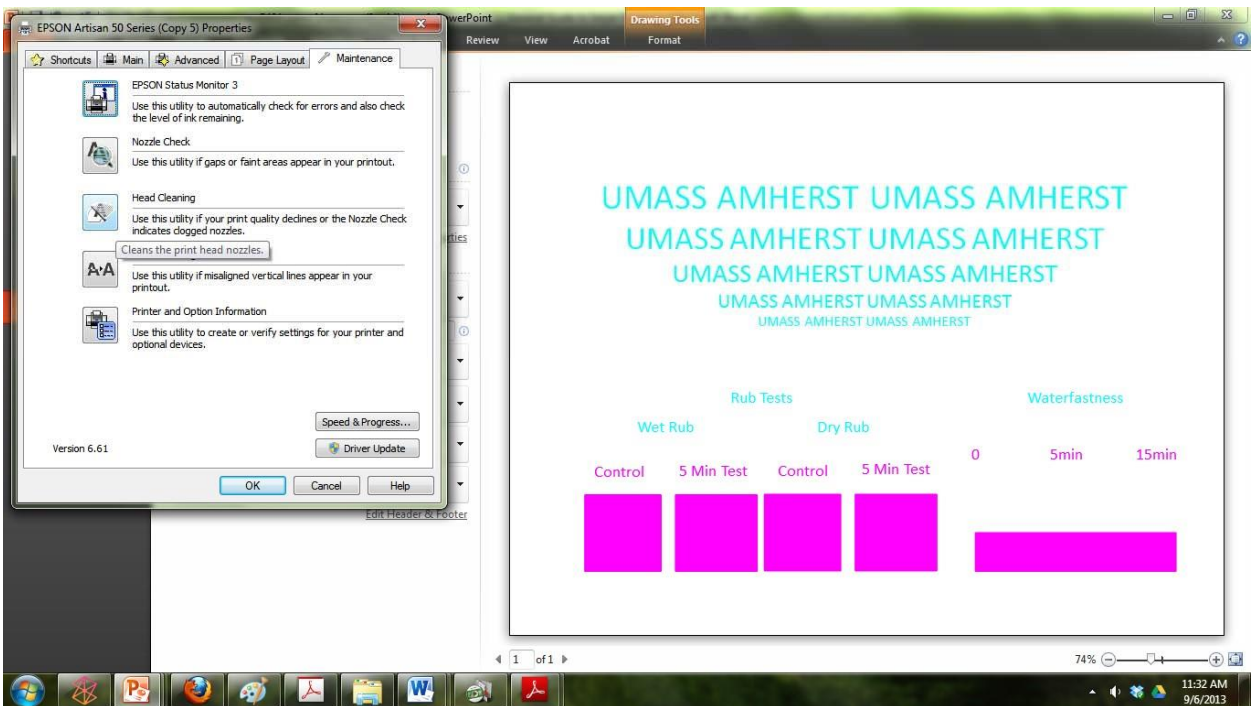
Head Cleaning

To start a head cleaning, access the printer options (usually done by clicking print in your imaging software (or Microsoft Office) and then Printer Options).

In this example, we are using Microsoft PowerPoint:

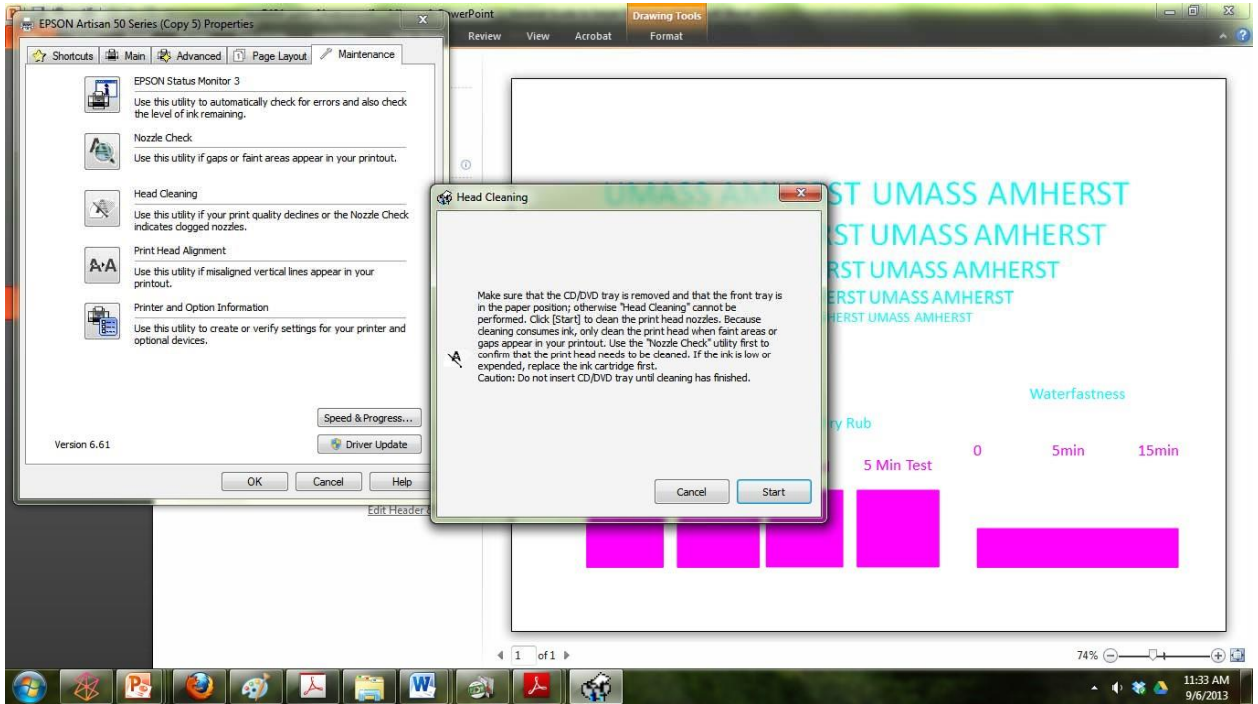


Select Maintenance.



Select Head Cleaning.

Go through the prompts and wait ~2-3 minutes. Ignore the nozzle check pattern at the end of the head cleaning unless you are trying to get rid of a clog. Click Finish at the end.



You have now cleaned the print head.

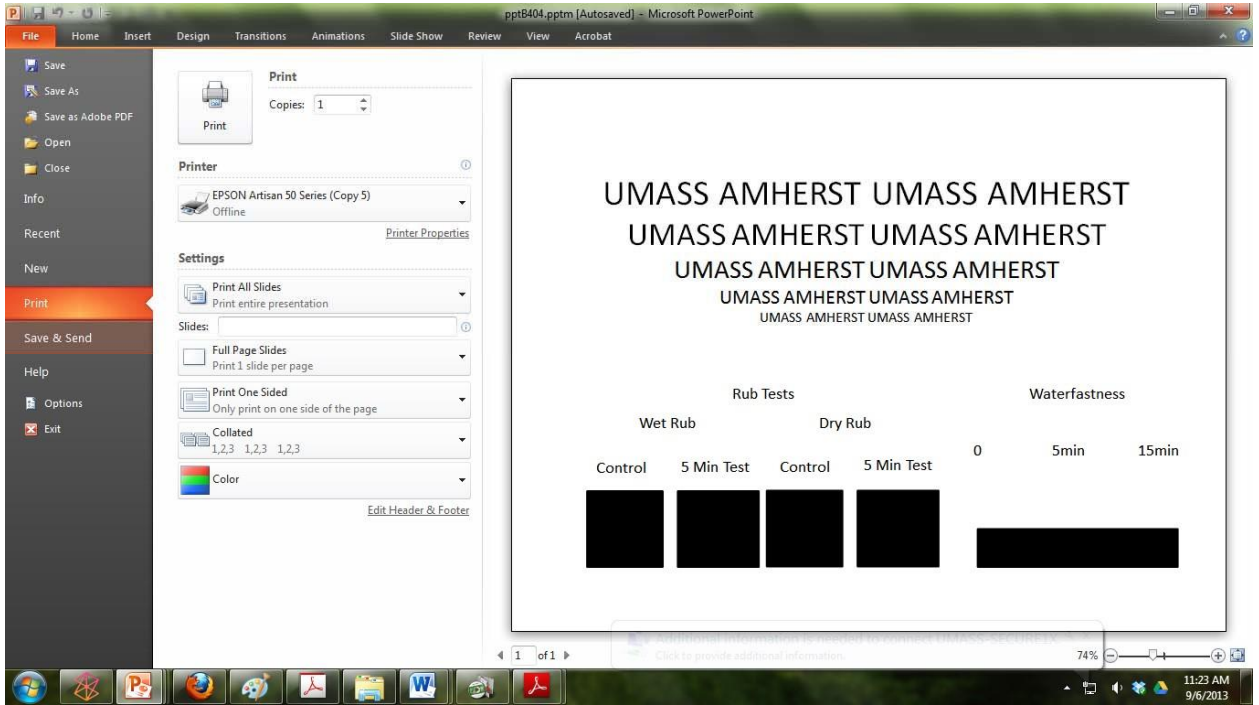
Black and Multichannel Printing

Black Channel Printing

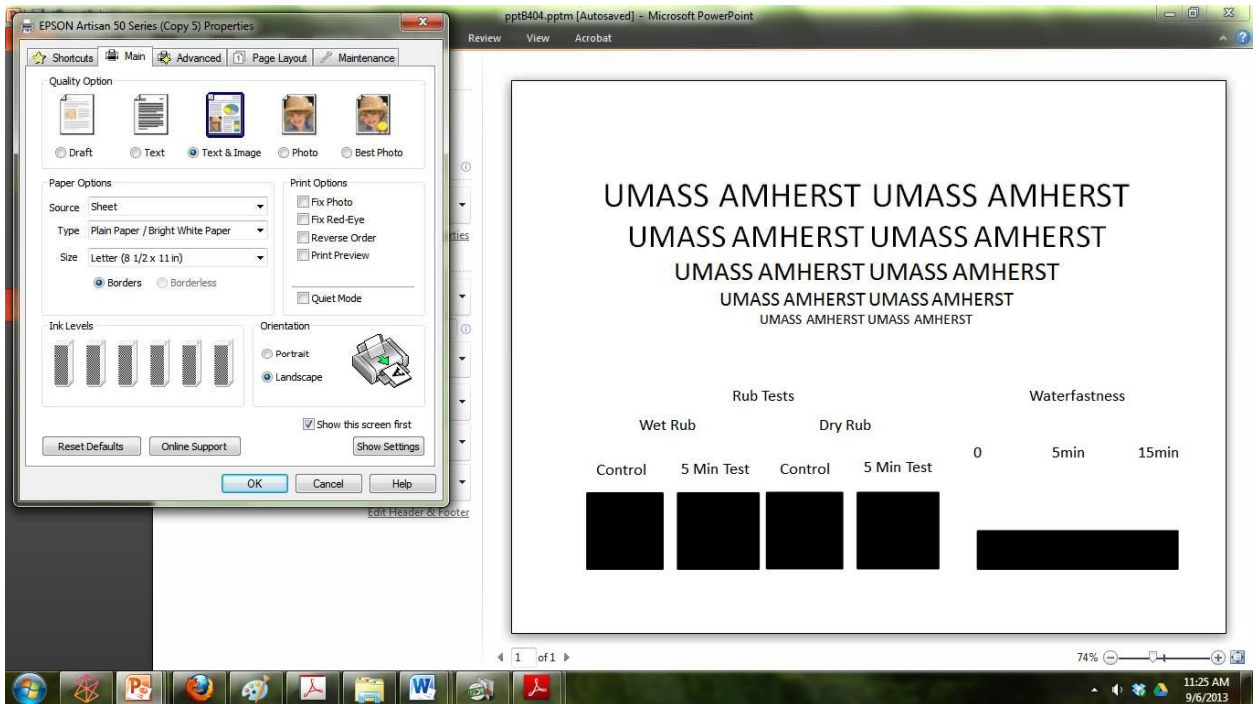
In most instances, you will only need to print one type of material at a time. In general, this is much easier to do using our Artisan system. Why is printing out of the black channel easier than the other color channels? The reason is simple – all 4 channels are not manufactured

equally. In fact, most printers print dye based inks out of the color channels and pigment only out of the black channel. As pigments are dispersed and not dissolved in water, materials coming out of the black channel have significant size (~120nm) that must be taken into account when manufacturing the print head. This same care does not usually need to be taken in creating the dye based channels. This means the color channels tend to be more intolerant of experimental materials and clog easier. A good rule to have is to never print something out of a color channel that you have not already printed out of the black channel. This check will ensure that any misprinting when you print is due only to the color channel and not your ink formulation or material.

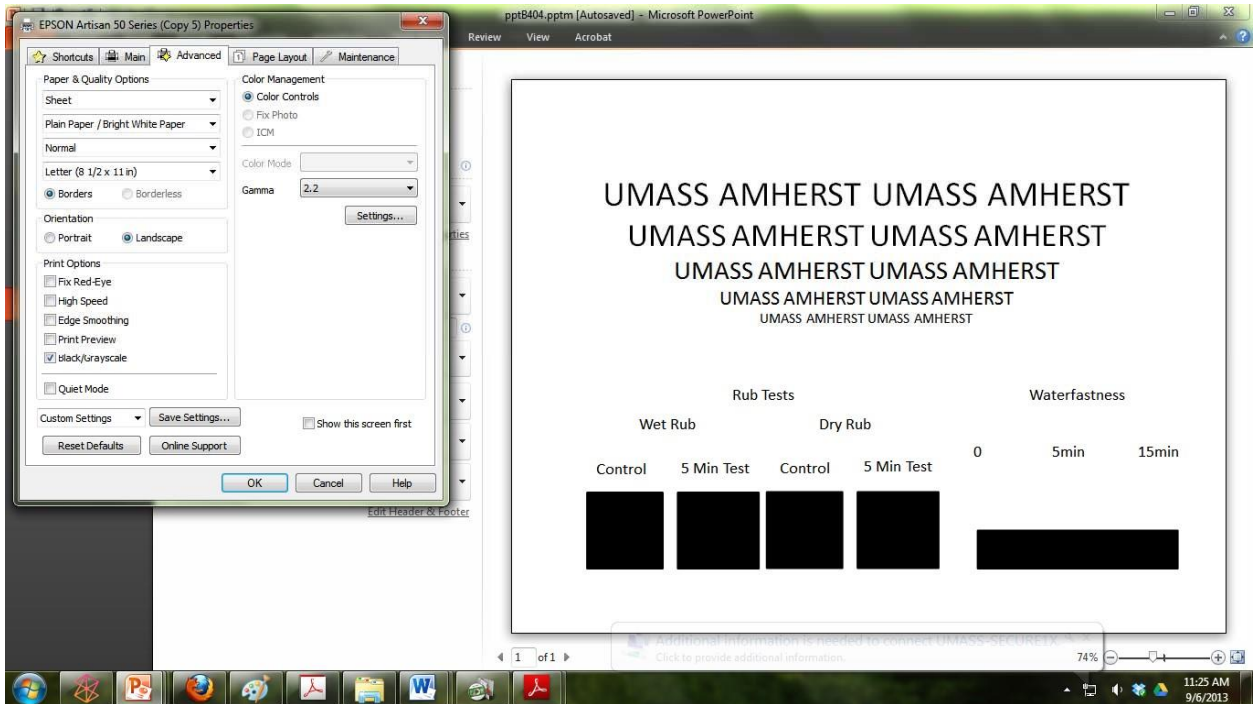
To start, create a pattern of interest and go to the print menu. Be sure to draw in black to ensure coverage in the areas of interest. For this demonstration, we will use Microsoft PowerPoint 2010. However, you may use other programs for printing if you so desire. At this point, ensure that the printer (Epson Artisan 50) is selected and is ready for use. One final note – be sure you are printing using the correct printer especially if you have multiple Artisan printers.



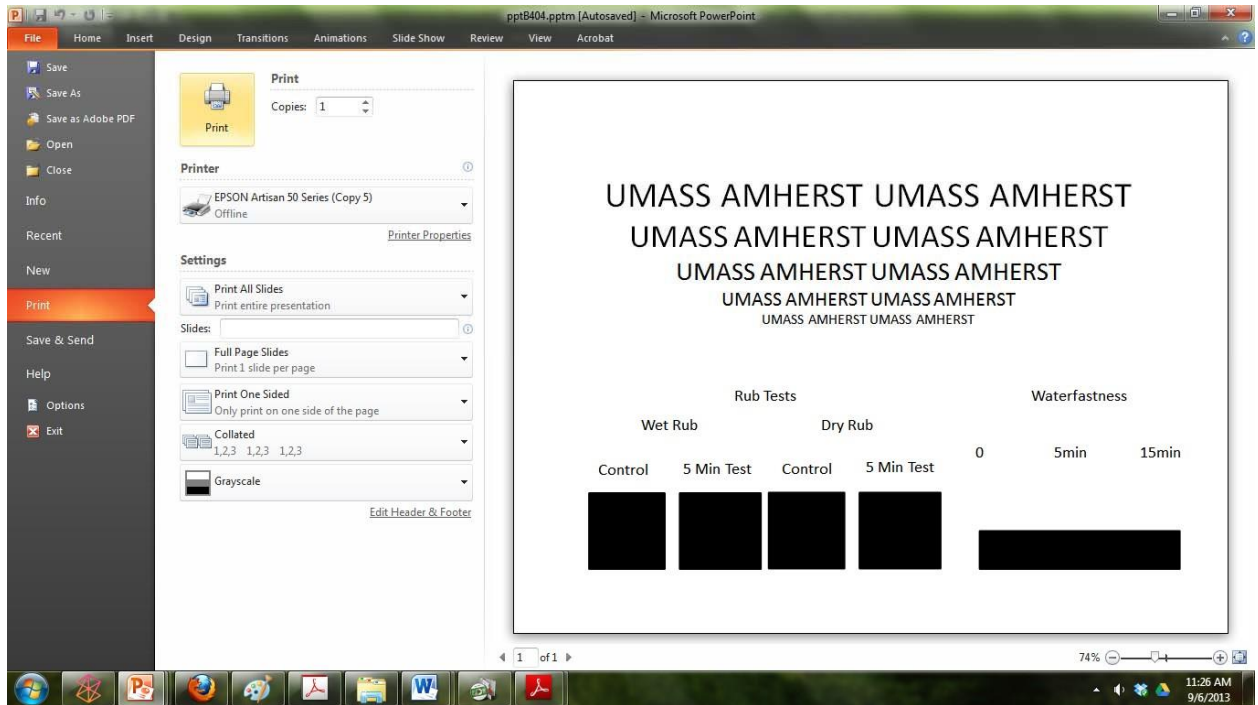
Select Properties.



Select the Advanced Settings tab



Deselect “High Speed” and Select “Black/Gray Scale”



Select OK at the bottom and select “Print”

The patterned paper will be generated for you.

4 Color Printing

If you need to print more than one material at the same time, you need set up the pattern for 4 channel printing. First, you must force the computer to print only the channel you want at that position on the substrate. This is done through the CMYK color pallet. If you want to print out of the yellow channel, you would set the color in CMYK to [255,255,0] where 255 is the highest value possible. However, most major imaging software programs define colors in RGB coordinates instead of CMYK. Therefore we must convert our values from CMYK to RGB, which is done in the table below.

To print just using the magenta channel, set the RGB value to 255, 0, 255.

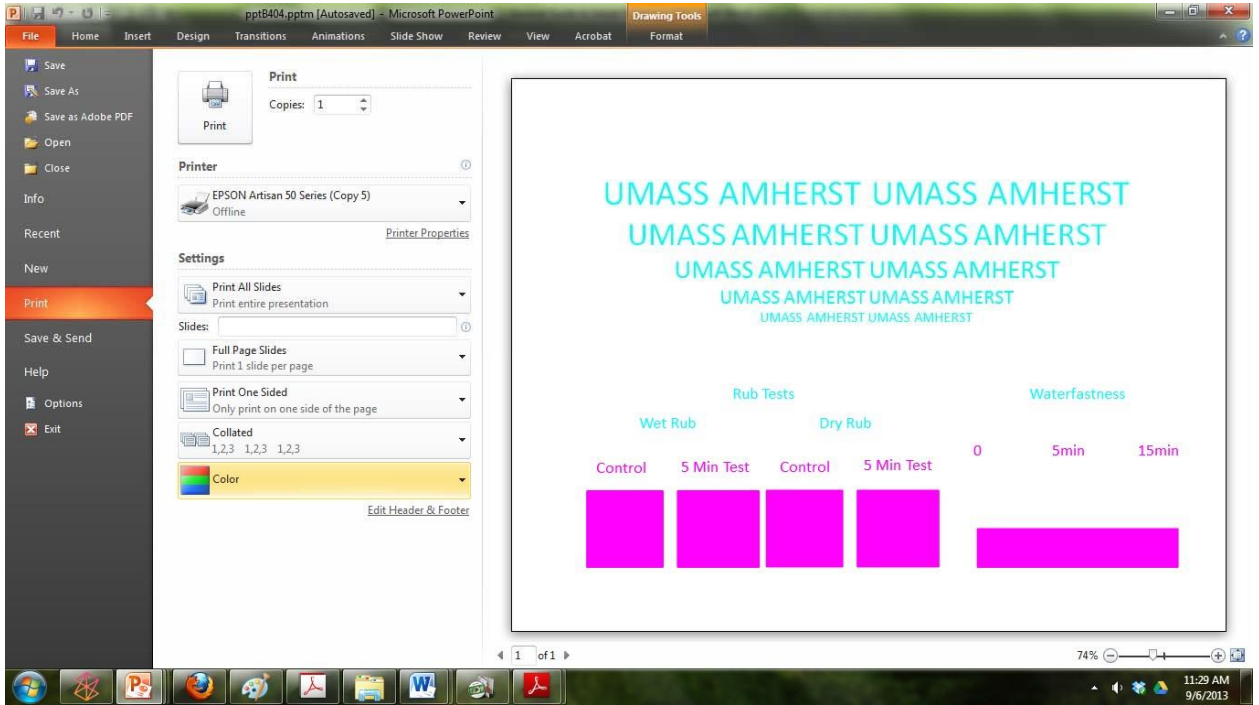
To print just using the cyan channel, set the RGB value to 0, 255, 255.

To print just using the yellow channel, set the RGB value to 255, 255, 0.

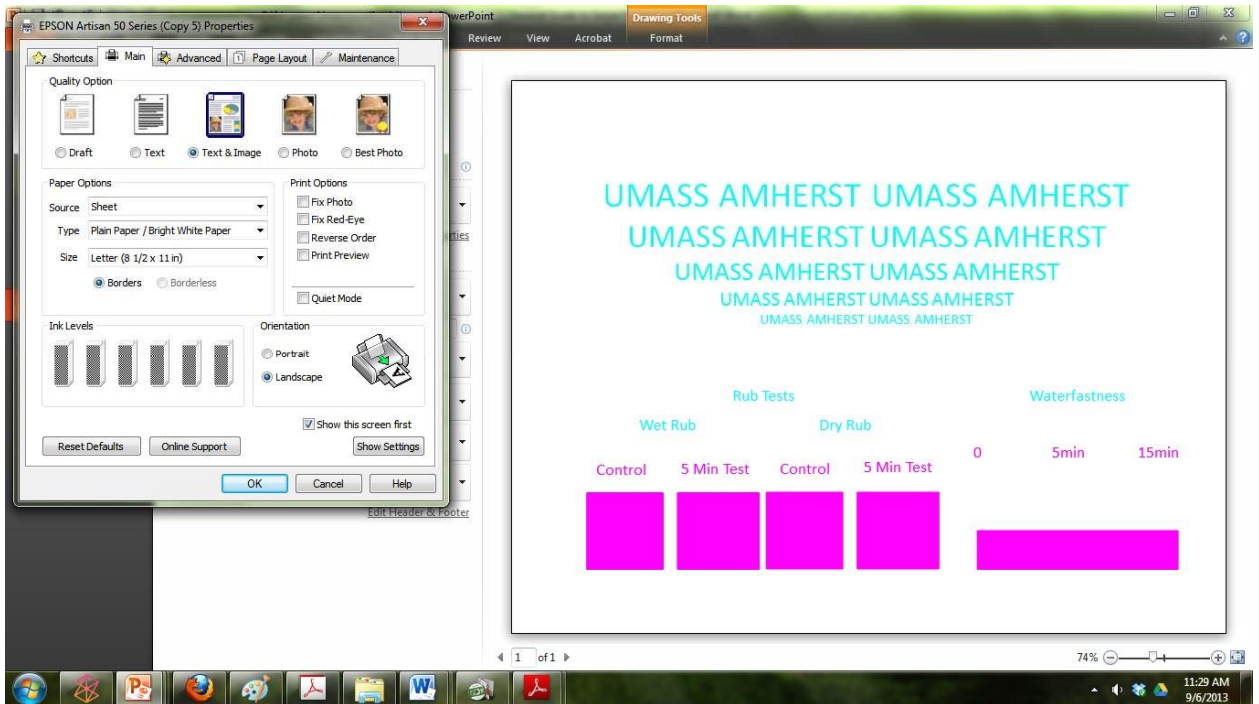
If you want to mix two channels together at the same spot on the substrate, see Advanced Inkjet Printing.

Using these colors, draw the pattern using the software. I will demonstrate using Microsoft Power Point 2010 for ease of use.

Once you have finalized your pattern, click Print and select Printer Properties.

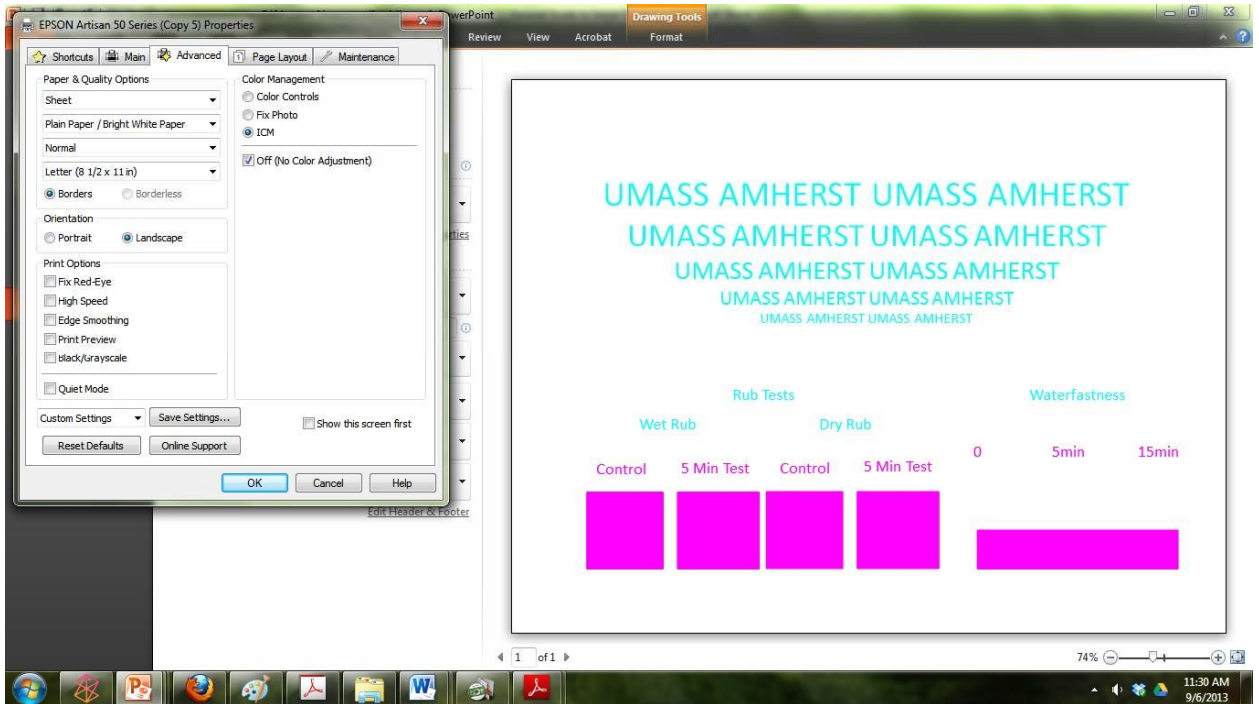


Select the Advanced Settings tab

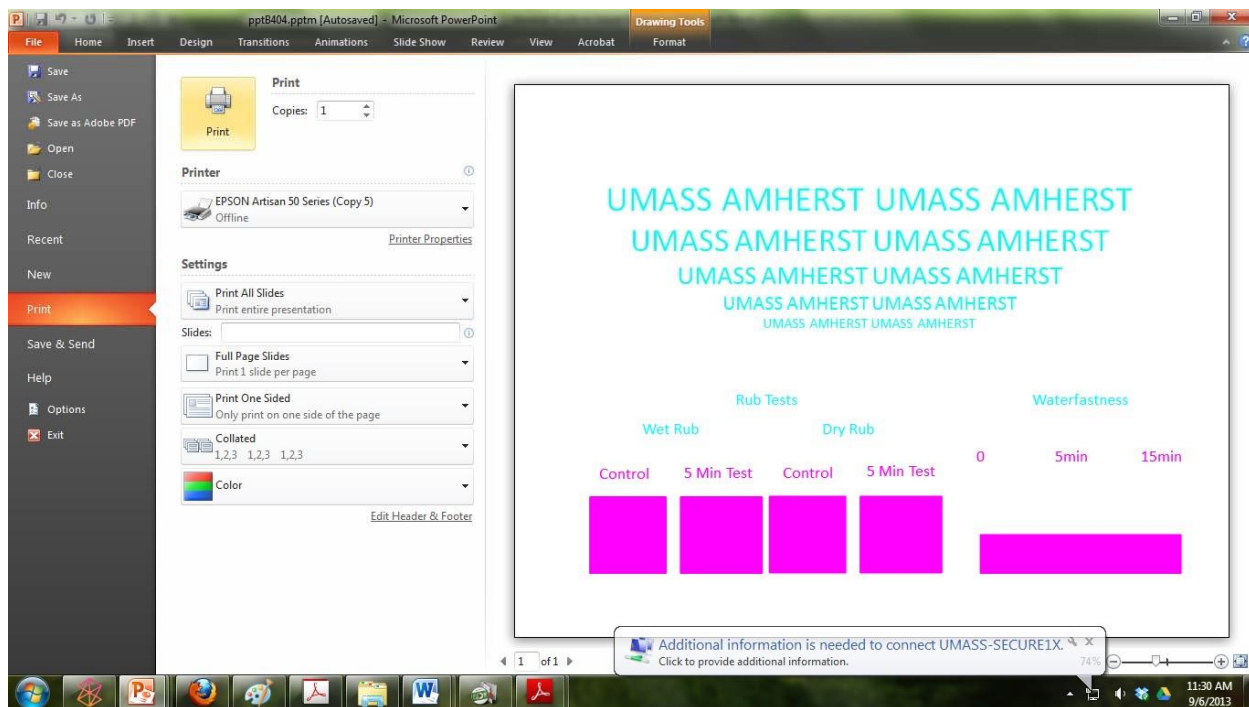


Deselect “High Speed” and “Edge Smoothing” on the left panel

Select “ICM” on the right panel followed by “Off”



Select OK at the bottom



Select "Print"

Mixed Channel Printing

Of this entire guide, this section is the least researched as we are just starting to do mixed channel printing. Furthermore, we will only cover mixing 2 channels at a time as mixing 3 is quite challenging.

Mixed channel printing, as opposed to 4 channel printing, has more than one channel printing onto a given point on the substrate. For instance, if you wanted to print an area with 80% of the cyan channel (Protein A) and 20% of the yellow channel (Protein B) you would use mixed channel printing. 4 channel printing would only put down the contents of one channel. Mixed channel printing is excellent for combinatorial chemical studies where you can easily vary the

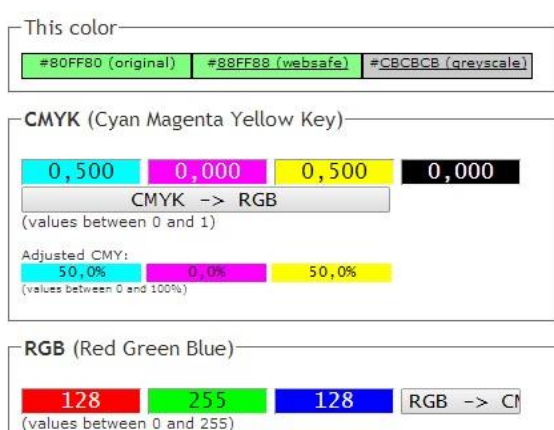
amount of components on a surface, creating different areas on the same substrate. In this work, we will show you how to mix 2 channels (cyan, magenta, or yellow only) using CMY to RGB conversion.

Converting Mix to a Color – CMYK to RGB Conversion

First, consider how we instructed the computer to print the channel of interest using 4 channel printing. Earlier in the guide, we used RGB values to tell the printer (along with shutting off the ICM function) to print only the cyan, yellow, or magenta channel. In mixed channel printing, how much of each component is done in a similar fashion by calculating the RGB value that corresponds to the correct ratio amount of material we want on the surface. This can easily be done through the use of a CMYK to RGB converter. RGB color values can also be expressed as CMYK values that take into account the amount of Cyan, Magenta, Yellow, and Black in a specific color. For instance, a (1,0,0,0) CMYK value which would render as purely Cyan can be converted to a RGB value of 0,255,255. This value remind you of what you inputted earlier in 4 channel printing to get only cyan to print. By converting CMYK values to RGB values that can be entered into your software, we can control the percentage of each channel on a specific area. While you can mathematically convert CMYK values by hand, converters found online such as <http://web.forret.com/tools/color.asp> but feel free to use another. For all of the mixing work, the K value should always remain 0 as you do not want any black intermixing with our sample. The printer will overcompensate for the black portion of the color and not give us the correct proportion of the channels. Therefore, we only need to concern ourselves with the CMY portion.

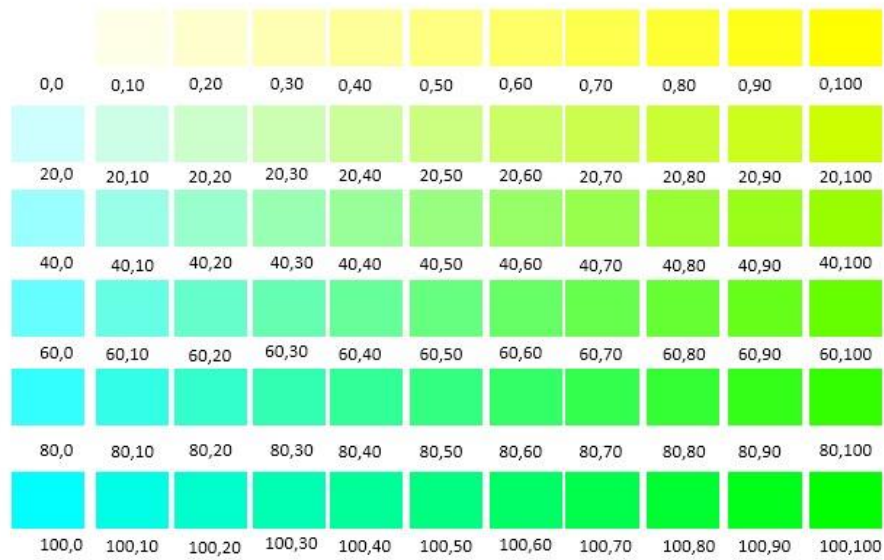
To best show how this mixed channel printing works, consider this example of producing a 50%/50% mix of the cyan and yellow channels respectively. Using our online software

(Appendix Figure 41), we type in that we want .5,0,.5,0 as our CMYK output (this website likes CMKY from 0 to 1). As seen in the Figure, we are easily given an RGB value that can be entered into any software that handles RGB values. You may note that the example assumes your CMYK value adds up to 1, which is important if you are trying to keep the amount of liquid printed the same. This normalization is critical for combinatorial chemical studies. We are relatively sure that this is true, but we will let you know if later studies prove this wrong.



Appendix Figure 41 - A 50%/50% mix of the cyan and yellow channels.

We have generated Powerpoint slides that change the concentrations stepwise on one sheet using Cyan/Yellow and Magenta/Yellow (Example shown as Appendix Figure 42).



Appendix Figure 42- A Powerpoint sheet that has the different combinations of cyan and yellow channels

Non-Paper Printing Using the CD Tray

You will need:

- A computer with the Epson Print CD software installed
- Your substrate cleaned and ready for printing
- CD Tray that was included with the printer
- White Paper (heavy card stock is ideal)
- A CD for tracing
- Double Sided tape
- To read the Manual on how to print onto a CD (not covered here)

First, some notes. The Epson Print CD is not user friendly at all. It can only print basic shapes and lines on the substrate. Furthermore, it is difficult to manipulate these shapes in the software to get them to be where you would like on the actual substrate. Have patience while printing.

Setting up the CD Tray

In order to print onto the CD tray, you have to first trick the printer that there is in fact a CD in the tray and not wafers for instance. In order to do this, one must trace a CD onto paper then cut it out to be taped onto the tray. Tape the cut out paper to the CD tray using double sided tape ensuring that the cut out paper fits exactly like a CD would fit (Appendix Figure 43). Over time, the paper will get damaged and printed on which may require the paper to be changed occasionally.



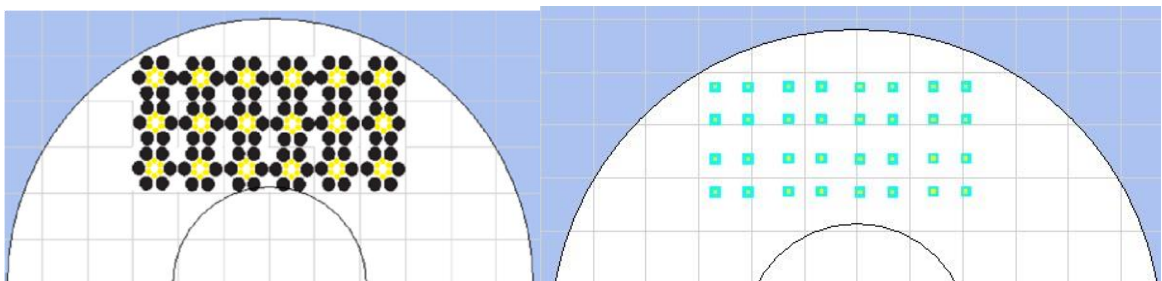
Appendix Figure 43 - Proper paper lining on the CD tray

Substrate Attachment to the Tray

Attaching substrates to the CD tray is usually done by adhering double sided tape to the paper and then attaching the substrate to it. Please note that you should put substrate only on the top half of the tray as anything below the halfway point will generate an error that the CD tray is improperly loaded. Scotch double sided tape (yellow packaging) seems to work the best for adhesion. Press the substrate onto the tray and ensure the substrate does not fall off. As the printer passes over the substrate, sometimes the printhead will impact the substrate. If the substrate is not secured, the impact of the printhead will often cause the substrate (a silicon wafer for instance) to fly throughout the printer potentially falling into the printer.

Using the Epson CD Software

First load the Epson CD Software on your computer. Since you will be editing on the CD tray, select new CD label if the software asks. If it helps mentally, the top half of where you would manipulate what you want on the CD label is where the substrates are located. The CD software is a standard design program so I will not go into gross detail of how to make a box for example. However, Appendix Figure 44 a and b show some standard patterns I have made for group projects.



Appendix Figure 44 - Some pattern examples from our work.

Notes for using the software

- Print color correction should always be set to +0. Otherwise, the color amount will be inconsistent.
- As always, manual print should be done as directed earlier.
- To better align the patterns, be sure to turn on the grid system and zoom in as much as possible using the buttons at the top (Control and the plus key does not work)
- When you make a shape, you can change the color by right clicking on the rectangle and selecting properties.

Troubleshooting Your Artisan 50 Printer

Empty Cartridge Errors

It is very common for the printer to inform you that the ink in certain cartridges is running low especially after multiple printings. While these notices can be helpful, it is more important to visually inspect the levels every time you change a cartridge. This is also why using a rhodamine dye in your flushing fluid is helpful. As our cartridges have the ability to auto reset (changing the chip from an empty to full state), any empty cartridge can be refilled simply by adding liquid and waiting 5 seconds before being put back into the printer. If the cartridge is full of liquid already, the error can be reset by removing the cartridge from the printer and replacing it 5 seconds afterward. Be sure that the cartridge clips into the printer making a clicking sound. If removing the affected cartridge does not solve the issue (after a few tries), the chip on the exterior of the cartridge may be damaged. Use another cartridge.

Cleaning the Printer

One of the biggest challenges in inkjet printing is keeping your printer clean, especially in a research and development environment. Here are some general tips for cleanliness when you eventually get a clog (or see banding in the print), see the troubleshooting portion of this document.

General Tips:

- Never let a channel go dry. Always have fluid in the cartridge sitting in the printer and ensure that you do not forget to put a cartridge in the slot when changing cartridges. This usually happens late in the day.
- Filter every ink.
- Ensure the particle size is below 200nm if not below 140nm. Anything larger will clog the channels. Also, be aware of unstable solutions especially experimental nanoparticles, biomolecules, or complexes. What is under 50nm in particle size one day can increase to over 300nm overnight.
- If you accidentally leave an experimental sample in the cartridge (especially one that may have a volatile size/stability), do not use the cartridge in the printer again. Settling may occur and since the nozzle portion is at the bottom, the aggregates will end up in the print head clogging the printer.
- After you are done with an experimental cartridge, replace the cartridge with a flushing fluid cartridge and do a head cleaning. This will ensure full cleaning of the head.

- Leave the printer plugged in at all times if you are not using it for a long period of time. It will self clean the print head once every few days.

Specific Error Troubleshooting

Please also see the official Printer troubleshooting guide for any issues. The following list contains errors commonly found when using the printer for experimental use or errors that are not commonly addressed.

The ink will not print.

- Did you remove the vent plug? If no, do a head cleaning and retry.
- Is there ink in the cartridge (~1/2 way full)? If no, refill.
- Are you printing more than 1 channel and have grayscale checked? If yes, turn off grayscale and then turn ICM off.
- Did you ensure that the particle size of your material is lower than 200nm? If no, you may have damaged the printer. Unless you are sure that they are indeed below the 200nm threshold, you will run the risk of irreversibly clogging the print head with large aggregates. Be sure to also filter your inks before putting in the printer.
- Was the printer left dry (no full cartridge left in the printer)? You may need to flush the printer with cleaning solution multiple times before you can reuse it. See Cleaning the Printer for more information.
- It is possible that it did print but it may be too low of a concentration for you to visualize. Try printing on transparency film. This will allow you to better see the print. If you are

printing on hard surfaces, use a microscope slide as a substrate. After printing, breathe on the glass. If it printed, you will see the outline of the pattern.

The printer prints, but the outputted print has banding.

- Is there ink in the cartridge (~1/2 way full)? If no, refill.
- Did you ensure that the particle size of your material is lower than 200nm? If no, you may have damaged the printer. Unless you are sure that they are indeed below the 200nm threshold, you will run the risk of irreversibly clogging the print head with large aggregates. Be sure to also filter your inks before putting in the printer.
- Was the ink based on a known good formulation? Surface tension and viscosity play a huge role in whether a solution will print. Try a ink formulation lower down the list (See Ink Formulation)
- If the ink is non-valuable, do multiple head cleanings to dislodge the air or particulate in the print head. If the ink is valuable, remove the valuable ink cartridge, replace it with a flushing fluid cartridge, and then do multiple head cleanings.
- Try another cartridge. Again, the quality of the cartridge can vary. Remove the ink from the affected cartridge and use another new cartridge. While a new cartridge might be an expensive fix, it usually fixes the issue if the previous tips did not work.

The cartridge leaks!

- Did you pierce the side of the cartridge when filling? If yes, remove your ink quickly to a vial and throw out the cartridge. Carefully fill a new cartridge with your ink and print.

- If the cartridge is not compromised (check again), the surface tension of your ink may be too low. Use a known good ink formulation (See Ink Formulation)
- Try another cartridge. Again, the quality of the cartridge can vary. Remove the ink from the affected cartridge and use another new cartridge. .

The printer has an error message (red flashing lights)

On your computer, there is an Epson Status Monitor 3 program. It will usually tell you what the error message is. If this program does NOT appear with the error message, go to the Maintenance tab in the printer settings and click on the Epson Status Monitor 3. The instruction manual that came with the printer has quite a bit of information on these types of issues.

The CD tray is not accepted by the printer

- First, ensure that the CD tray is lined up with the line on the tray.
- Are the substrates above the middle of the tray? If not, put them above the line.
- Has it ever worked before? If not, remake the paper covering (Chapter 7 – Setting up the CD Tray). If it has, is the paper in good condition? If not, remake it.
- If it still does not work after a few attempts, cancel the job and restart. Sometimes the printer gets stuck in a loop and cannot get past the error.

It has an End of Life (Waste Pad) error that will not go away.

The printer has waste pads in the machine that soak up the liquid that you flush through the system. At a certain point, these pads will become saturated and potentially overflow into the

printer. Therefore, Epson enforces a printer shutoff after 100,000 cycles. Epson allows you to reset this error within 1 year of purchase (afterwards it costs ~\$USD 15). If it is under a year, go to <https://ipr.ebz.epson.net/ipr/maintenance.do> and get a key to remove the error.

Opening the Printer

This section, by all means, should be your last resort. We have much experience in repairing Artisan 50 printers and we still have issues resuscitating printers that have been opened for cleaning. However, some clogs cannot be cleansed without taking the printhead out. Furthermore, some parts of the printer can be quickly fixed such as the cartridge pin connector. This tutorial will show you how to open up the printer to remove the printhead.

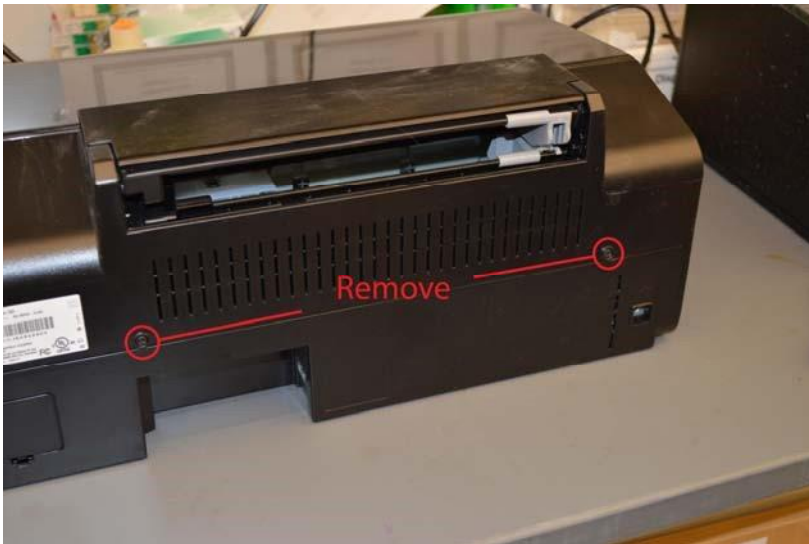
You will need:

- A flat head screwdriver
- A medium sized Phillips screwdriver
- A very small tipped screwdriver or a flat tipped needle on a syringe Or
- A multi-tipped screwdriver set

Instructions

1. Click the ink button on the printer to get the cartridge carriage to come out on a plugged in printer.
2. Unplug the printer.
3. Remove the paper feed at the top

4. Remove the two back screws on the printer (see next page for image)



5. Open the top flap of the printer and remove the left screw



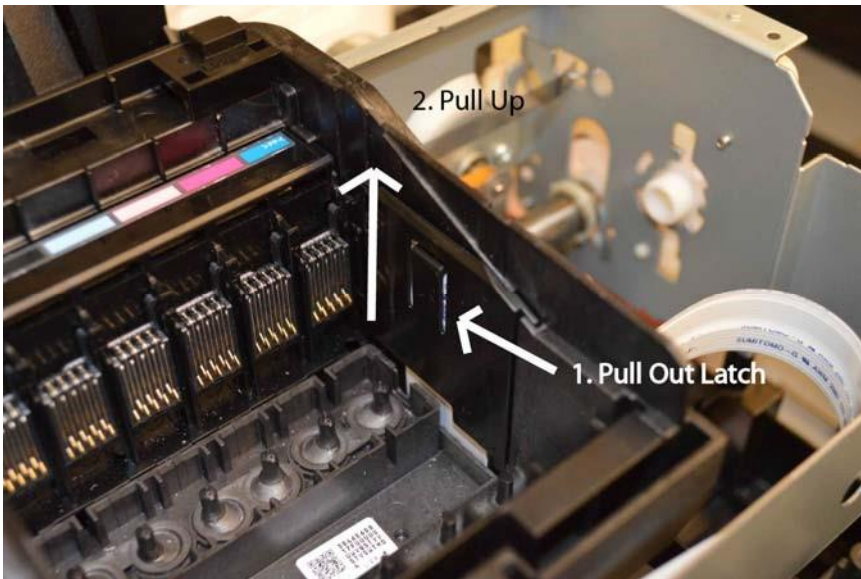
6. Towards the front right, there is a recessed screw towards the bottom. Take it out.



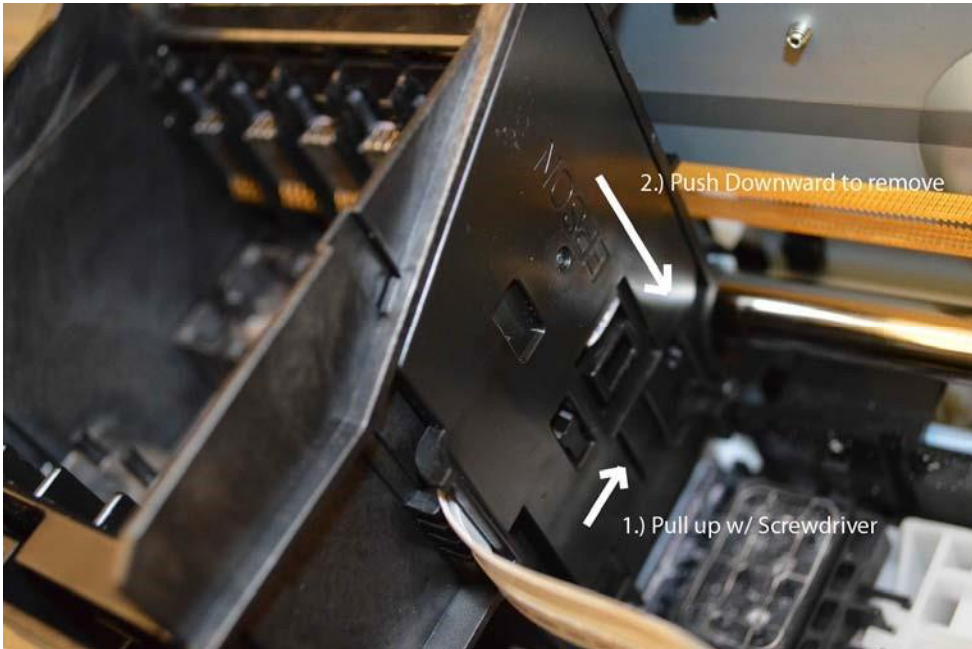
7. Take off the top.

8. Open the cartridge container and remove any cartridges that you left in there.

9. On the right inside of the container, there is a sliding plastic divider. Using a flat head screwdriver, slide it up and out. You should see white plastic cabling.



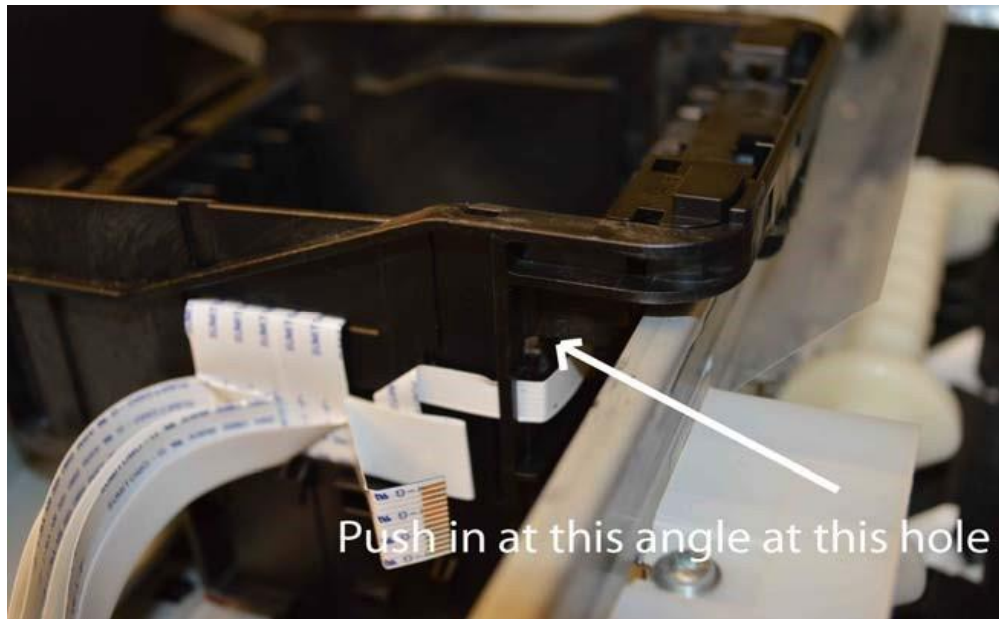
10. On the right outside of the container, remove another sliding panel with the flat head screwdriver.



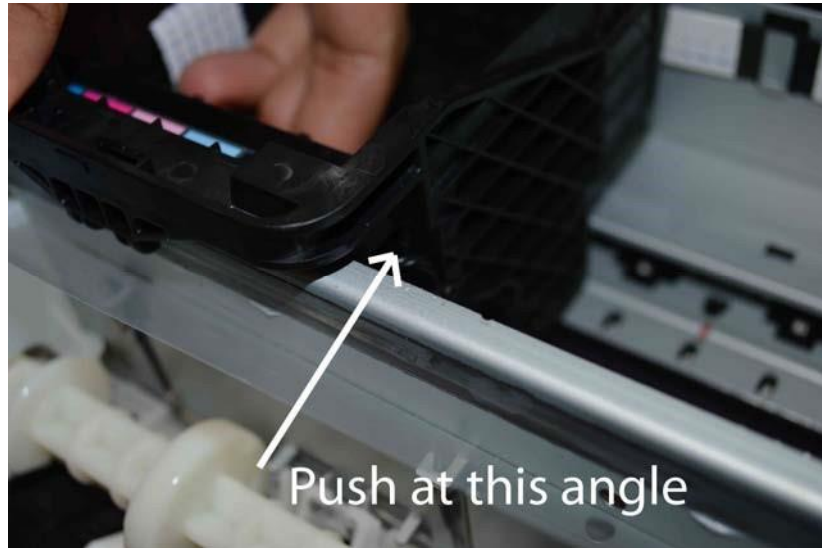
11. There are two ribbons that attach to the back. Loosen the bigger ribbon on the bottom.



12. You need to remove the pin connector. Using the small tipped screwdriver, press on the hole shown below. While you are pressing on this hole, pull firmly up on the pin connector. The pin connector will eventually loosen if you hit the spot correctly. You will eventually get it but it will require a lot of patience.



Then do the same to the hole shown on the other side of the container.



13. If you just needed to replace the pin connector, go ahead and do so by reversing the directions after installing the new one. If there is only one pin connector that needs to be changed, use fin-tipped tweezers to do it. If you need the printhead, continue on.

14. Unscrew the three screws at the bottom of the container and carefully pull out the printhead. Be careful – ribbons are attached. Slowly pull the ribbons out and the printhead is yours. Feel free to wash the printhead (see below) or attach a new one by doing the directions in reverse.

Washing the Printhead Manually

You will need:

- A printhead taken out of the printer
- A small sonicator
- Solvents – ethanol works well for most clogs as well as ethyl acetate.

- A beaker that houses the bottom of the printhead but not the entire top. Recommended – Kimble 60x35 dish Part # 23000

Instructions:

1. Fill the beaker with ethanol (first) up to 1 cm above the bottom of the printhead
2. Put the beaker with the printhead in the sonicator that has a water level equal or slightly below the water level of the beaker.



3. Place beaker into the sonicator. Turn on the sonicator for a few minutes depending on how much impurity comes out.
4. Repeat as needed.
5. Dry the printhead for at least 1 day.
6. If needed, try using ethyl acetate especially if you are using a rhodamine-based dye in your system.

BIBLIOGRAPHY

- Aili, D.; Selegard, R.; Baltzer, L.; Enander, K.; Liedberg B. *Small*, **2009**, *5*, 2445.
- Albert, K. J.; Lewis, N. S; Schauer, C. L.; Sotzing, G.A.; Stitzel, S. E.; Vaid, T. P.; Walt, D. R. *Chem. Rev.* **2000**, *100*, 2595.
- Aldhous, P. *Nature*, **2005**, *434*, 132.
- Anderson, N. L.; Anderson, N. G. *Mol. Cell. Proteomics* **2002**, *1*, 845.
- Antohe, B. V.; Wallace, D. B. *J. Imaging Sci. Technol.*, **2002**, *46*, 409.
- Asati, A.; Santra, S.; Kaittanis, C.; Nath, S.; Perez, J. M. *Angew. Chem. Int. Ed.* **2009**, *48*, 2308.
- Bajaj, A.; Miranda, O. R.; Kim, I. B.; Phillips, R. L.; Jerry, D. J.; Bunz, U. H. F.; Rotello, V. M. *Proc. Natl. Acad. Sci. U. S. A.* **2009**, *106*, 10912.
- Baldrich, E.; Vignes, N.; Mas, J.; Munoz, F. X. *Anal. Biochem.* **2008**, *383*, 68.
- Bermel, A. D.; Bugner, D. E. *J. Imaging Sci. Technol.*, **1999**, *43*, 320.
- Best, D. G.; deCasseres, K. E.; Analyst, **1985**, *110*, 221.
- Brust, M.; Walker, Bethell, D.; Schiffrin, D. J.; Whyman, R. *J. Chem. Soc., Chem.*, **1994**, 801.
- Bügler, J. H.; Buchner, H.; Dallmayer A. *J. Forensic Sci.*, **2008**, *53*, 982.
- Bunn H.F.; Jandl J.H. *J. Biol. Chem.* **1968**, *243*, 465.
- Calvert, P. *Chem. Mater.*, **2001**, *13*, 3299.
- Cao, X. D.; Ye, Y. K.; Liu, S. Q. *Anal. Biochem.* **2011**, *417*, 1.

Causin, V.; Casamassima, R.; Marega, C.; Maida, P.; Schiavone, S.; Marigo, A.; Villari, A. *J. Forensic Sci.*, **2008**, *53*, 1468.

Charych, D. H.; Nagy, J. O.; Spevak, W.; Bednarski, M. D. *Science* **1993**, *261*, 585.

Chughtai, K.; Heeren, R. M. *Chem. Rev.*, **2010**, *110*, 3237.

Chung, H. J.; Castro, C. M.; Im, H.; Lee, H.; Weissleder, R. *Nat. Nanotechnol.* **2013**, *8*, 369.

Cook, C.C.; Wang, T.; Derby, B. *Chem Commun.*, **2010**, *46*, 5452.

Cornett, D. S.; Reyzer, M. L.; Chaurand, P.; Caprioli, R. M. *Nat. Methods*, **2007**, *4*, 828.

Creran, B.; Li, X.; Duncan, B.; Kim, C. S.; Moyano, D. F.; Rotello, V. M. *ACS Appl. Mater. Interfaces* **2014**, *6*, 19525.

Creran, B.; Yan, B.; Moyano, D. F.; Gilbert, M. M.; Vachet, R. W.; Rotello, V. M. *Chem. Commun.* **2012**, *48*, 4543.

de Gans, B. J.; Duineveld, P. C.; Schubert, U. S. *Adv. Mater.* **2004**, *16*, 203.

de Gans, B.-J.; Kazancioglu, E.; Meyer, W.; Schubert, U. S. *Macromol. Rapid Commun.*, **2004**, *25*, 292.

De, M.; Rana, S.; Akpinar, H.; Miranda, O. R.; Arvizo, R. R.; Bunz, U. H. F.; Rotello, V. M. *Nat. Chem.* **2009**, *1*, 461.

Delehanty, J. B.; Ligler, F. S. *Anal. Chem.*, **2002**, *74*, 5681.

Derby, B. *J. Mater. Chem.* **2008**, *18*, 5717-5721.

Dijksman, J. F. J. *Fluid Mech.*, **1984**, *139*, 173.

Disney, M.D.; Zheng, J.; Swager, T.M.; Seeberger, P.H. *J.Am.Chem.Soc.*, **2004**, *126*, 13343.

Drinking Water Contaminates <http://water.epa.gov/drink/contaminants/> (Accessed 6/24/14).

Elghanian, R.; Storhoff, J. J.; Mucic, R. C.; Letsinger, R. L.; Mirkin, C. A. *Science* **1997**, *277*, 1078.

Fernandez, F. M.; Green, M. D.; Newton, P. N. *Ind. Eng. Chem. Res.*, **2008**, *47*, 585.

Folmer-Andersen, J. F.; Kitamura, M.; Anslyn, E. V. *J. Am. Chem. Soc.* **2006**, *128*, 5652.

Ford, T.E.; Colwell, R.R. "A Global Decline in Microbiological Safety: A Call for Action" A report from The American Academy of Microbiology, Washington, D.C., 1996.

Frischer, M. E.; Danforth, J. M.; Foy, T. F.; Juraske, R. *J. Environ. Qual.* **2005**, *34*, 1328.

Fromm, J. E. *IBM J. Res. Dev.*, **1984**, *28*, 322.

Gao, L. Z.; Zhuang, J.; Nie, L.; Zhang, J. B.; Zhang, Y.; Gu, N.; Wang, T. H.; Feng, J.; Yang, D. L.; Perrett, S.; Yan, X. *Nat. Nanotech.* **2007**, *2*, 577.

Gao, L. Z.; Wu, J. M.; Lyle, S.; Zehr, K.; Cao, L. L.; Gao, D. *J. Phys. Chem. C* **2008**, *112*, 17357.

Geiman, I.; Leona, M.; Lombardi, J. R. *J. Forensic Sci.*, **2009**, *54*, 947.

Greene, N. T. and Shimizu, K. D. *J. Am. Chem. Soc.* **2005**, *15*, 5695.

Griffith, K. L.; Wolf, R.E. *Biochem. Biophys. Res. Commun.* **2002**, *290*, 397.

Guo, Y. J.; Deng, L.; Li, J.; Guo, S. J.; Wang, E. K.; Dong, S. J. *ACS Nano* **2011**, *5*, 1282.

- H. Qu, D. Caruntu, H. Liu, C. J. O'Connor, *Langmuir* **2011**, *27*, 2271.
- Halkos, G. E.; Tzeremes, N. G. *Annu. Rev. Microbiol.* **2001**, *55*, 201.
- Hartwell, L.; Mankoff, D.; Paulovich, A.; Ramsey, S.; Swisher, E. *Nat. Biotechnol.* **2006**, *24*, 905.
- Hayes, D. J.; Wallace, D. B.; Boldman, M. T. *Proc. SPIE-Int. Soc. Opt. Eng.*, **1992**, *1847*, 316.
- Ho, H. A.; Najari, A.; Leclerc, M. *Acc. Chem. Res.* **2008**, *41*, 168.
- Hossain, S. M. Z.; Luckham, R. E.; McFadden, M. J.; Brennan, J. D. *Anal. Chem.* **2009**, *81*, 9055.
- Hossain, S. M. Z.; Luckham, R. E.; Smith, A. M.; Lebert, J. M.; Davies, L. M.; Pelton, R. H.; Filipe, C.D.M.; Brennan, J.D. *Anal. Chem.* **2009**, *81*, 5474.
- Hostetler, M. J.; Templeton, A. C.; Murray, R. W. *Langmuir*, **1999**, *15*, 3782.
- Huang, C. C.; Huang, Y. F.; Cao, Z. H.; Tan, W. H.; Chang, H. T. *Anal. Chem.* **2005**, *77*, 5735.
- Ifa, D. R.; Gumaelius, L. M.; Eberlin, L. S.; Manicke, N. E.; Cooks, R. G. *Analyst*, **2007**, *132*, 461.
- Jakob H.; Leininger, S.; Lehmann, T.; Jacobi, S.; Gutewort, S. "Peroxo compounds, inorganic"
Ullmann's Encyclopedia of Industrial Chemistry, 6th ed., Wiley-VCH:Weinheim, 2003.
- Jv, Y.; Li, B. X.; Cao, R. *Chem. Commun.* **2010**, *46*, 8017.
- Karnovsky M. J. *J. Cell. Biol.* **1967**, *35*, 213.
- Kim, J. H.; Grant, S. B. *Environ. Sci. Technol.* **2004**, *38*, 2497.
- Kimura, Y. K. T. K. J. *Biosensors*, **1988**, *4*, 41.

Kindhauser, M. K. Communicable Diseases 2002. World Health Organization, Geneva, **2003**.

Kingsmore, S. F.; Patel, D. D. *Curr. Opin. Biotechnol.* **2003**, *14*, 74.

Ko, S.H.; Pan, H.; Grigoropoulos, C.P.; Luscombe, C.K.; Frechet, J.M.J.; Poulidakos, D.
Nanotechnology, **2007**, *18*, 345202.

Komuro, N.; Takaki, S.; Suzuki, K.; Citterio, D. *Anal. Bioanal. Chem.* **2013**, *405*, 5785.

Lancaster, I. M.; Mitchell, A. *Proceedings of SPIE 5310*, **2004**, *5310*, 34.

Larsson, A.; Johansson, M. E.; Wangefjord, S.; Gaber, A.; Nodin, B.; Kucharzewska, P.;
Welinder, C.; Belting, M.; Eberhard, J.; Johnsson A.; Uhlen, M.; Jirstrom K. *Br. J. Cancer* **2011**,
105, 666.

Lavigne, J. J.; Savoy, S. M.; Clevenger, M. B.; Ritchie, J. E.; McDoniel, B.; Yoo, S. J.; Anslyn, E. V.;
McDevitt, J. T.; Shear, J. B.; Neikirk, D. P. *J. Am. Chem. Soc.* **1998**, *120*, 6429.

Li, X.; Wen, F.; Creran, B.; Jeong, Y.; Zhang, X.; Rotello, V. M. *Small* **2012**, *8*, 3589.

Liu, Y.-Z.; Yu, J.; Xie, M.-X.; Liu, Y.; Han, J.; Jing, T.-T. *J. Chromatogr. A*, **2006**, *1135*, 57.

M. J. Hostetler, A. C. Templeton, R. W. Murray, *Langmuir* **1999**, *15*, 3782.

Mcdonnell, L. A.; Heeren, R. M. A. *Mass Spectrom. Rev.*, **2007**, 606.

Miranda, O. R.; Chen, H. T.; You, C. C.; Mortenson, D. E.; Yang, X. C.; Bunz, U. H. F.; Rotello, V.
M. J. Am. Chem. Soc. **2010**, *132*, 5285.

Miranda, O. R.; Creran, B.; Rotello, V. M. *Curr. Opin. Chem. Biol.*, **2010**, *14*, 728.

Miranda, O. R.; Li, X.; Garcia-Gonzalez, L.; Zhu, Z.-J., Yan, B.; Bunz, U. H. F., Rotello, V. M. *J.*

Am. Chem. Soc., **2011**, *133*, 9650.

Mullenix, M. C.; Wiltshire, S.; Shao, W. P.; Kitos, G.; Schweitzer, B. *Clin. Chem.* **2001**, *47*, 1926.

Neufeld, T.; Schwartz-Mittelmann, A.; Biran, D.; Ron, E. Z.; Rishpon, J. *Anal. Chem.*, **2003**, *75*, 580.

Neumann, C.; Ramotowski, R.; Genessay, T. *J. Chromatogr. A*, **2011**, *1218*, 2793.

Newman, J. D.; White, S. F.; Tothill, I. E.; Turner, A. P. F. *Anal. Chem.*, **1995**, *67*, 4594.

Nishioka, G. M.; Markey, A. A.; Holloway, C. K. *J. Chem. Soc., Chem.* **2004**, *126*, 16320-16321.

Northen, T. R.; Yanes, O.; Northen, M. T.; Marrinucci, D.; Uritboonthai, W.; Apon, J.; Golledge, S. L.; Nordström, A.; Siuzdak, G. *Nature*, **2007**, *449*, 1033.

Okuno, J.; Maehashi, K.; Kerman, K.; Takamura, Y.; Matsumoto, K.; Tamiya, E. *Biosens. Bioelectron.* **2007**, *22*, 2377.

Oleniaz, W. S.; Pisano, M. A.; Rosenfeld, M. H.; Elgart, R. L. *Environ. Sci. Technol.* **1968**, *2*, 1030.

Ornatska, M.; Sharpe, E.; Andreescu, D.; Andreescu, S. *Anal. Chem.* **2011**, *83*, 4273.

Park, K. S.; Kim, M. I.; Cho, D. Y.; Park, H. G. *Small* **2011**, *7*, 1521.

Parolo, C.; de la Escosura-Muniz, C. A.; Merkoci, A. *Biosens. Bioelectron.* **2012**, *40*, 412.

Pelossof, G.; Tel-Vered, R.; Elbaz, J.; Willner, I. *Anal. Chem.* **2010**, *82*, 4396.

Phillips, R. L.; Miranda, O. R.; You, C. C.; Rotello, V. M.; Bunz, U. H. F. *Angew. Chem.* **2008**, *120*,

2628.

Pineda, F. J.; Lin, J. S.; Fenselau, C.; Demirev, P. A. *Anal. Chem.* **2000**, *72*, 3739.

Rabin, M.; Poli de Figueiredo, C. E.; Wagner, M. B.; Antonello, I. C. *Appetite* **2009**, *52*, 609.

Rakow, N. A.; Suslick, K. S. *Nature* **2000**, *406*, 710.

Reis, N.; Ainsley, C.; Derby, B. J. *Appl. Phys.*, **2005**, *97*, 094903

Rompré, A.; Servais, P.; Baudart, J.; de-Roubin M.R.; Laurent, P. *Microbiol. Methods.*, **2002**, *49*, 31.

Sanitation, Progress on Drinking Water and Sanitation” Geneva: UNICEF, New York and WHO, 2008.

Sastry, M.; Lala, N.; Patil, V.; Chavan, S. P.; Chittiboyina, A. G. *Langmuir* **1998**, *14*, 4138.

Scrimin, P.; Prins, L. J. *Chem. Soc. Rev.*, **2011**, *40*, 4488.

Setti, L.; Fraleoni-Morgera, A.; Ballarin, B.; Filippini, A.; Frascaro, D.; Piana, C. *Biosens. Bioelectron.* **2005**, *20*, 2019.

Setti, L.; Fraleoni-Morgera, A.; Mencarelli, I.; Filippini, A.; Ballarin, B.; Di Biase, M. *Sens Actuators B* **2007**, *126*, 252.

Shawky, S. M.; Bald, D.; Azzazy, H. M. E. *Clin. Biochem.* **2010**, *43*, 1163.

Shoji, E.; Freund, M. S. *J. Am. Chem. Soc.* **2001**, *123*, 3383.

Singh, M.; Haverinen, H. M.; Dhagat, P.; Jabbour, G. E. *Adv. Mater.*, **2010**, *22*, 673.

Sirringhaus, H.; Shimoda, T. *MRS Bulletin*, **2003**, *28*, 802.

Song, H., Spencer, J., Jander, A., Nielsen, J., Stasiak, J., Kasperchik, V., & Dhagat, P. *J. Appl. Phys.*, **2014**, *115*(17), 17E308.

Song, Y. J.; Qu, K. G.; Zhao, C.; Ren, J. S.; Qu, X. G. *Adv. Mater.* **2010**, *22*, 2206.

Staake, T.; Thiesse, F. Fleisch, E. *Eur J Market*, **2009**, *43*, 320.

Storhoff, J. J.; Elghanian, R.; Mucic, R. C.; Mirkin, C. A.; Letsinger, R. L. *J. Am. Chem. Soc.* **1998**, *120*, 1959.

Taira, S.; Sugiura, Y.; Moritake, S.; Shimma, S.; Ichiyonagi, Y.; Setou, M.; *Anal. Chem.*, **2008**, *80*, 4761.

Tang, H.-W.; Wong, M. Y.-M.; Chan, S. L.-F.; Che, C.-M.; Ng, K.-M. *Anal. Chem.*, **2011**, *83*, 453.

Tenkin, E.; Smith, P.J.; Shubert, U.S. *Soft Matter*, **2008**, *4*, 703.

Thanh, N. T. K.; Rosenzweig, Z. *Anal. Chem.* **2002**, *74*, 1624.

Then, W. L.; Garnier, G. *Rev. Anal. Chem.*, **2013**, *32*, 269.

Trafela, T.; Strlic, M.; Kolar, J.; Lichtblau, D. A.; Anders, M.; Mencigar, D. P.; Pihlar, B. *Anal. Chem.*, **2007**, *79*, 6319.

UNICEF and World Health Organization "Joint Monitoring Programme for Water Supply and

Vest, R. W.; Tweedell, E. P.; Buchanan, R. C. *Int. J. Hybrid Microelectron.*, **1983**, *6*, 261.

Wei, H.; Wang, E. *Anal. Chem.* **2008**, *80*, 2250.

Wiestner, M. J.; Ulmann, P. A.; Mirkin, C. A. *Angew. Chem. Int. Ed.* **2011**, *50*, 114.

Wu, W.; He, Q.; Jiang, C. *Nanoscale Res. Lett.*, **2008**, *3*, 397.

Yan, B.; Zhu, Z.-J.; Miranda, O. R.; Chompoosor, A.; Rotello, V. M.; Vachet, R. W. *Anal. Bioanal. Chem.*, **2010**, *396*, 1025.

Yeh, Y.-C.; Creran, B.; Rotello, V. M. *Nanoscale*, **2012**, *4*, 1871.

Yetisen, A. K.; Akram, M. S.; Lowe, C. R. *Lab Chip*, **2013**, *13*, 2210.

You, C. C.; Miranda, O. R.; Gider, B.; Ghosh, P. S.; Kim, I. B.; Erdogan, B.; Krovi, S. A.; Bunz, U. H. F.; Rotello, V. M. *Nat. Nanotech.* **2007**, *2*, 318.

Zhang, C.; Suslick, K. S. *J. Am. Chem. Soc.* **2005**, *127*, 11548.

Zhao, W.; Brook, M. A.; Li, Y. F. *ChemBioChem* **2008**, *9*, 2363.

Zhu, Z.-J.; Ghosh, P. S.; Miranda, O. R.; Vachet, R. W.; Rotello, V. M. *J. Am. Chem. Soc.*, **2008**, *130*, 14139.